

University of New Hampshire

University of New Hampshire Scholars' Repository

Doctoral Dissertations

Student Scholarship

Spring 2015

DEVELOPMENT OF AN ISOTOPIC APPROACH FOR DETAILING HEPARIN SEQUENCES

Qing Guo

University of New Hampshire, Durham

Follow this and additional works at: <https://scholars.unh.edu/dissertation>

Recommended Citation

Guo, Qing, "DEVELOPMENT OF AN ISOTOPIC APPROACH FOR DETAILING HEPARIN SEQUENCES" (2015).
Doctoral Dissertations. 2201.

<https://scholars.unh.edu/dissertation/2201>

This Dissertation is brought to you for free and open access by the Student Scholarship at University of New Hampshire Scholars' Repository. It has been accepted for inclusion in Doctoral Dissertations by an authorized administrator of University of New Hampshire Scholars' Repository. For more information, please contact Scholarly.Communication@unh.edu.

**DEVELOPMENT OF AN ISOTOPIC APPROACH FOR
DETAILING HEPARIN SEQUENCES**

BY

QING GUO

B.S., Beijing University of Aeronautics and Astronautics, Beijing, China, 2009

DISSERTATION

Submitted to the University of New Hampshire

in Partial Fulfillment of

the Requirements for the Degree of

Doctor of Philosophy

in

Chemistry

May, 2015

ALL RIGHTS RESERVED

© 2015

QING GUO

This thesis/dissertation has been examined and approved in partial fulfillment of the requirements for the degree of Doctor of Philosophy in Chemistry by:

Dissertation Director, Dr. Vernon N. Reinhold,
Research Professor in Molecular, Cellular, and Biomedical Sciences

Dr. W. Rudolf Seitz, Professor in Chemistry

Dr. Gonghu Li, Assistant Professor in Chemistry

Dr. Erik Berda, Assistant Professor in Chemistry

Dr. Feixia Chu,
Assistant Professor in Molecular, Cellular, and Biomedical Sciences

On April 20th, 2015

Table of Contents

DEDICATION	ix
ACKNOWLEDGMENTS	x
LIST of FIGURES	xi
LIST of TABLES	xiv
LIST OF ABBREVIATIONS	xv
ABSTRACT	xvii

CHAPTER	PAGE
1 INTRODUCTION	1
1.1 Proteoglycans	1
1.2 Glycosaminoglycans	2
1.2.1 Overview of glycosaminoglycan structures	2
1.2.2 Biological significance	4
1.3 Heparin (highly sulfated form of HS) and heparan sulfate (HS)	7
1.3.1 A brief history	7
1.3.2 Biosynthesis	8
1.3.3 Chemistry of heparin	9
1.3.3.1 Methylation	9
1.3.3.2 Desulfation	10
1.3.3.3 Acetylation	16

1.3.4 Commercial production process for heparin and heparin-like polysaccharides	16
1.4 The antithrombin binding site, a unique pentasaccharide sequence	18
1.5 Current GAG characterization protocols and analytical limitations	19
1.5.1 Liquid chromatographic approaches	19
1.5.1.1 Size exclusion chromatography	20
1.5.1.2 Strong anion exchange chromatography	21
1.5.1.3 Hydrophilic interaction chromatography	23
1.5.1.4 Ion-pair reversed-phase (IP-RP) high-performance liquid chromatography	25
1.5.1.5 IP-RP liquid chromatography coupling with mass spectrometry (MS)	30
1.5.1.6 Graphitized carbon chromatography (GCC)	33
1.5.2 Mass spectrometric approaches	34
1.5.2.1 Matrix assisted time-of-flight mass spectrometry	35
1.5.2.2 Electrospray ionization mass spectrometry	38
1.5.3 Alternative approaches	39
1.5.3.1 Capillary electrophoresis mass spectrometry	39
1.5.3.2 Fluorophore-assisted carbohydrate electrophoresis	40
1.5.3.3 Nuclear magnetic resonance spectroscopy	41
2 RESEARCH OBJECTIVES AND SPECIFIC AIMS	42
2.1 Motivation for understanding GAG structures	42
2.1.1 Limitations of current structural characterization protocols	43
2.1.2 MS ⁿ introducing a new sequencing strategy	44
2.1.3 Research strategies	45

2.2 Specific Aims	48
Aim 1: Dual permethylation of heparin/heparan sulfate disaccharide standards	48
Aim 2: Dual permethylation of Arixtra [®]	49
Aim 3: MS ⁿ analysis for confirmation of chemical structure of Arixtra [®]	51
Aim 4: An MS ⁿ spectral library of dual permethylated Arixtra [®]	51
3 DUAL METHYLATION OF HEPARIN/HEPARAN SULFATE DISSACHARIDES	52
3.1 EXPERIMENTAL SECTION	52
3.1.1 Materials	52
3.1.2 Chemical derivatizations of heparin/heparan sulfate disaccharide standards	54
3.1.3 Glycan analysis	59
3.2 RESULTS AND DISCUSSIONS	60
3.2.1 Permethylated non-sulfated heparin/heparan sulfate disaccharide standard	60
3.2.2 Permethylated sulfated heparin/heparan sulfate disaccharide standards	61
3.2.2.1 Dual permethylation of mono-O-sulfated heparin/heparan sulfate disaccharides	61
3.2.2.2 Dual permethylation of di-O-sulfated heparin/heparan sulfate disaccharide	72
3.2.2.3 Dual permethylation of O-, N-disulfated heparin/heparan sulfate disaccharide	77
3.2.3 Sulfation site identification of reduced dual-permethylated heparin/heparan sulfate disaccharides	84
3.2.4 Investigation of desulfation conditions	87
3.3 Summary	91

4 DUAL PERMETHYLATION OF ARIXTRA®	92
4.1 EXPERIMENTAL SECTION	92
4.1.1 Materials	92
4.1.2 Chemical derivatizations of Arixtra	93
4.1.3 Glycan analysis	100
4.2 RESULTS AND DISCUSSIONS	102
4.2.1 MS analysis of native Arixtra	102
4.2.2 Recovery of desalting and ion exchange	107
4.2.3 Investigation of permethylation conditions	110
4.2.3.1 Variations of sample amounts	112
4.2.3.2 Multiple times of permethylation	116
4.2.3.3 Quenching solutions	118
4.2.3.4 Concentration of sodium hydroxide in DMSO	120
4.2.3.5 Reaction time	122
4.2.3.6 Microwave assisted permethylation	123
4.2.3.7 Underpermethylation at 3-O-sulfated N-sulfoglucosamine (GlcNS) moiety	124
4.2.4 Solvolytic desulfation of Arixtra	125
4.2.4.1 Time study of solvolytic desulfation with permethylated Arixtra	125
4.2.4.2 Influence of methanol concentration on incomplete desulfation of permethylated Arixtra	128
4.2.4.3 Influence of temperature on incomplete desulfation of native Arixtra	129
4.2.5 MS ⁿ analysis of desulfated Arixtra	131
4.2.6 MS ⁿ analysis of permethylated-desulfated Arixtra following N-acetylation	139

4.2.7 MS ⁿ analysis of fully derivatized Arixtra	142
4.3 Summary	154
5 CONCLUSIONS AND PERSPECTIVES	155
REFERENCES	158
APPENDICES	170
APPENDIX A: LC/MS profiles of permethylated Arixtra.	171
APPENDIX B: Spectra ion assignments of derivatized Arixtra following N-acetylation step.	172

DEDICATION

To my parents, Lin Xue and Guangshun Guo,
with deepest love and gratitude.

Their support and encouragement have inspired me always.

ACKNOWLEDGMENTS

First, I would like to express my sincere gratitude to my advisor Dr. Vernon N. Reinhold, for his guidance and support throughout my years at UNH. I admire his academic enthusiasm and greatly respect the person that he is. His professional expertise has been invaluable to me. I couldn't have done this work without him.

I would like to thank my co-advisor Dr. W. Rudolf Seitz for his support and encouragement. It's a great pleasure to be one side of Seitz.

I must thank my committee, Dr. Gonghu Li, Dr. Erik Berda and Dr. Feixia Chu, for their time and advice.

I am grateful to my fellow group members, David J. Ashline, Hailong Zhang and Thuy Tran for their friendship, collaboration and help. Also, I would like to thank my former group member, Andy J. Hanneman for his support of my project in early phases.

This research was supported by NIH P01 grant HL107146 Program of Excellence in Glycosciences.

Many thanks to Julia Chan, Chao Liu, Hao Geng, Jianyu Zhao, Jinyu Yang, Tong Jin, Rui Zhu, Cindi Rohwer and Peggy Torch for their assistance and friendship.

Finally, I thank all my professors, colleagues and friends at UNH.

LIST of FIGURES

Figure 1-1 Proposed mechanism of solvolytic desulfation.	13
Figure 2-1 Chemical derivatization with/without N-acetylation.	46
Figure 2-2 Experimental workflow of dual permethylation.	47
Figure 3-1 Chemical structures of heparin/heparan sulfate disaccharides.	52
Figure 3-2 SAX chromatogram of underivatized heparin/HS disaccharides mixture.	54
Figure 3-3 Experimental workflow of dual permethylation.	58
Figure 3-4 Permethylation of non-sulfated disaccharide D0A0.	61
Figure 3-5 Dual permethylation of D2A0 at different stages of chemical derivatization.	63
Figure 3-6 Dual permethylation of D0A6 at different stages of chemical derivatization.	64
Figure 3-7 Positive ion MS ⁿ spectra of permethylated mono-O-sulfated disaccharides.	67
Figure 3-8 MS ⁿ spectra of PM desulfated mono-O-sulfated heparin disaccharides.	69
Figure 3-9 MS ⁿ spectra of dual permethylated mono-O-sulfated heparin disaccharides.	71
Figure 3-10 Dual PM of reduced D2A6 at different stages of chemical derivatization.	73
Figure 3-11 MS ⁿ spectra of reduced dual permethylated D2A6.	76
Figure 3-12 Dual permethylation of D2S0 at different stages of chemical derivatization.	78
Figure 3-13 Positive ion MS and MS ² spectra of reduced permethylated D2S0.	79
Figure 3-14 Positive ion MS ⁿ spectra of reduced PM desulfated D2S0.	80
Figure 3-15 MS ² spectra of reduced PM DESUL acetylated D2S0.	81
Figure 3-16 Positive ion MS ² spectra of reduced dual permethylated D2S0.	82
Figure 3-17 Positive ion MS profile of reduced dual PM D2S0 without N-acetylation.	83

Figure 3-18 Sulfation sites identification of reduced dual-permethylated heparin/heparan sulfate disaccharides.	86
Figure 3-19 Comparison between solvolytic desulfation and methanolic desulfation.	87
Figure 3-20 Time study of solvolytic desulfation.	89
Figure 3-21 Time study of D2S6 in positive and negative ion MS.	90
Figure 3-22 Time study of solvolytic desulfation using negative ion MS.	90
Figure 4-1 Chemical structure of Fondaparinux.	93
Figure 4-2 Experimental workflow of dual permethylated Arixtra.	99
Figure 4-3 Negative ion MS profile of native Arixtra.	104
Figure 4-4 Negative ion MS profile of native Arixtra after desalting.	105
Figure 4-5 Negative ion IP-RP-LC/MS profile of native Arixtra.	106
Figure 4-6 Comparison of different sample amounts for permethylation.	115
Figure 4-7 Comparisons of multiple permethylation.	117
Figure 4-8 Comparisons of different quenching solutions.	119
Figure 4-9 Comparisons of different NaOH/DMSO concentrations.	121
Figure 4-10 Comparison of different reaction times.	122
Figure 4-11 Comparison between permethylation and microwave-assisted permethylation.	123
Figure 4-12 Desulfation time study of permethylated Arixtra.	127
Figure 4-13 Investigation of methanol concentration on incomplete desulfation.	129
Figure 4-14 Investigation of temperature on incomplete desulfation.	130
Figure 4-15 Positive ion MS profile of desulfated PM-Arixtra.	131
Figure 4-16 Positive ion MS ² spectrum of m/z 1030.	132

Figure 4-17 Positive ion MS ² spectrum of m/z 1132.	133
Figure 4-18 Annotation of chemical structure for precursor ion m/z 1030.	134
Figure 4-19 MS ³ analysis of complete desulfated Arixtra.	135
Figure 4-20 Sequential MS ⁿ disassembly of Z ₁ -ion, pathway I.	136
Figure 4-21 Sequential MS ⁿ disassembly of Z ₁ -ion, pathway II.	138
Figure 4-22 Positive MS profile of desulfated PM-Arixtra after acetylation.	140
Figure 4-23 MS ⁿ analysis of derivatized Arixtra after acetylation.	141
Figure 4-24 Chemical structures of Arixtra before and after dual permethylation.	143
Figure 4-25 Chemical structures of fully derivatized Arixtra with different isotopic labels.	144
Figure 4-26 Positive ion MS profiles of fully derivatized Arixtra.	145
Figure 4-27 Comparisons of MS ² spectra of fully derivatized Arixtra.	147
Figure 4-28 MS ⁿ analysis of fully derivatized Arixtra, m/z 1273.	148
Figure 4-29 MS ⁿ analysis of fully derivatized Arixtra, m/z 1264.	150
Figure 4-30 MS ⁿ comparisons of fully derivatized Arixtra, Z-ions.	152

LIST of TABLES

Table 4-1 Gradient profile of RP-IP-LC.	100
Table 4-2 Recovery of desalting columns.	109
Table 4-3 Recovery of IE columns.	109
Table 4-4 Compositions and their corresponding m/z values in IP-RP-LCMS profile.	111
Table 4-5 Variations of sample amounts in Figure 4-6.	113

LIST OF ABBREVIATIONS

PGs	Proteoglycans
GAGs	Glycosaminoglycans
UA	Uronic acid
Δ UA	Unsaturated uronic acid
GluA	Glucuronic acid
IdoA	Iduronic acid
GlcN	Glucosamine
GlcNAc	N-Acetylglucosamine
GlcNS	N-sulfoglucosamine
D0A0	Δ UA-GlcNAc
D2A0	Δ UA2S-GlcNAc
D0A6	Δ UA-GlcNAc6S
D2A6	Δ UA2S-GlcNAc6S
D2S0	Δ UA2S-GlcNS
D2S6	Δ UA2S-GlcNS6S
ESI	Electrospray ionization
IT	Ion trap
MS	Mass spectrometry
MS ⁿ	Sequential mass spectrometry
CID	Collision induced dissociation
MALDI-TOF	Matrix assisted laser desorption/ionization time-of-flight
IE	Ion exchange
PM	Permethylation

DMSO	Dimethyl sulfoxide
HA	Hyaluronan
HS	Heparan sulfate
LMWHs	Low molecular weight heparins
AT	Antithrombin
CS/DS	Chondroitin/Dermatan sulfate
OSCS	Oversulfated chondroitin sulfate
KS	Keratan sulfate
SEC	Size exclusion chromatography
SAX	Strong anion exchange
IP-RP-LC	Ion-pair reversed-phase liquid chromatography
IP	Ion pairing
PTA	Pentylamine
HILIC	Hydrophilic interaction chromatography
GCC	Graphitized carbon chromatography
FACE	Fluorophore-assisted carbohydrate electrophoresis
CEMS	Capillary electrophoresis mass spectrometry

ABSTRACT

DEVELOPMENT OF AN ISOTOPIC APPROACH FOR DETAILING HEPARIN SEQUENCES

By

Qing Guo

University of New Hampshire, May 2015

Heparin/heparin sulfates are carbohydrate polyionic polymers that participate in a host of critically important biological processes such as blood anticoagulation, pathogen infection, cell differentiation, growth, migration and inflammation, to mention a few. A century has passed since heparin's initial discovery with a fair understanding of its overall composition. Unfortunately, there has been no structural work at the detailed chemical level that might support a synthetic effort. In this study, I utilize a chemical derivatization strategy (dual permethylation) that imparts isotopic structural specificity, which can be followed by step-wise disassembly in an ion trap mass spectrometer, (MS^n). A set of analytical protocols is described that introduces a probable sequencing strategy for heparin analogs. Following derivatization, the O-sulfo groups are converted to deuterio methyl esters and the N-sulfo groups are converted to N-deutero acetyl groups. Mass shifts among derivatized products

with differential isotopic labeling verified the numbers of N-sulfo groups and O-sulfo groups, while sulfo group positions were characterized by MSⁿ analysis on selected precursor ions. Documentation has been studied with simple heparin/heparin sulfates disaccharides and a synthetic octasulfated pentasaccharide (Arixtra[®]). Determination of this analogous composition, sequence and sulfonation patterns were accomplished by MSⁿ. The protocols provide unique insights into monomer sequence with monomer structural detail observed by cross-ring fragments often resolved by deuterated isotopic labeling.

CHAPTER 1

INTRODUCTION

1.1 Proteoglycans

Proteoglycans (PGs) are comprised of a protein core and one or more covalently attached glycosaminoglycan chains. They are widespread components of most tissues and organs. Given that the number of glycosaminoglycans (GAGs) types are rather few, PGs fall into major families, including the hyaluronan (HA) binding proteoglycans, small leucine-rich proteoglycan (SLRPs), lecticans, syndecans, glypicans and others (Couchman and Pataki 2012).

The lecticans are a family of chondroitin sulfate PGs and consist of four members; aggrecan, versican, neurocan, and brevican. Aggrecan is the major PG of cartilage, while versican is enriched in large blood vessels. Neurocan and brevican are concentrated particularly in the extracellular matrices of the brain. It should be pointed out that syndecan and glypican contain heparan sulfate chains. Syndecans are single transmembrane domain PGs that carry three to five glycosaminoglycans chains. Glypicans are heparan sulfate proteoglycans that are bound to the external surface of the plasma membrane by a glycosyl-phosphatidylinositol linkage.

Not all the PGs can be assigned to families; there are single examples such as agrin and prelecan. Agrin is a heparan sulfate PG that is highly concentrated in the synaptic basal lamina at the neuromuscular junction. Perlecan is a large multidomain heparan sulfate PG of the extracellular matrix.

Proteoglycans are found ubiquitously throughout the extracellular matrix. Moreover, PGs are found on virtually every cell surfaces as well as within basement membranes of different tissues. Proteoglycans are known to mediate many biological processes including cell-cell and cell-matrix interactions, and control of some enzymatic activities, growth factors, chemokines, cytokines and morphogens in the development and repair of tissues (Capila and Linhardt 2002, Cattaruzza and Perris 2006, Ly, Laremore et al. 2010, Aspberg 2012, Roennberg, Melo et al. 2012). Their roles are many but their structures are poorly understood.

1.2 Glycosaminoglycans

1.2.1 Overview of glycosaminoglycan structures

As the major group of PGs, glycosaminoglycans (GAGs) are noted to be linear polysaccharide chains and are classified into diverse types according to the unique repeating disaccharide building blocks. The main types are listed as hyaluronan, (the simplest GAG); keratan sulfate, (a sulfated polyglactosamine); and chondroitin /dermatan sulfate and heparin/heparan sulfate, (both linked by xylose to serine). Glycosaminoglycans are the major structural components of many organisms within tissues on their cell surfaces, extracellular matrix and basement membranes.

Hyaluronan (HA) is the simplest GAGs. The HA is a repeating unsulfated disaccharide consisting of N-acetylglucosamine and glucuronic acid (GlcNAc β 1-3GlcA β 1-4). In each chain, the disaccharide building block is repeated many times forming chains that can exceed 106 Da or more. Hyaluronan is distributed widely in nature, as capsules of streptococcus bacilli and tissues of invertebrate and vertebrate organisms. Hyaluronan is also abundant in skin and skeletal tissues, the vitreous humour of the eye, the umbilical cord, and synovial fluid in mammals.

Chondroitin/dermatan sulfate (CS/DS) both consist of a repeating disaccharide of N-acetylgalatosamine and glucuronic acid (GalNAc-GlcA). This disaccharide may be sulfated on the 4- and/or 6-positions of GalNAc. Dermatan sulfate is a CS variant that has some of the uronic acid epimerized to iduronic acid (IdoA) by the enzyme epimerase. This IdoA may be sulfated at the 2-position.

Keratan sulfate (KS) is a sulfated polylactosamine chain of repeating disaccharides (galactose and N-acetylglucosamine), both of which can be 6-O sulfated. Their structures are identical to the N- and O-linked glycans found on glycoproteins and mucins. Their linkage to proteins distinguishes two types of KS (KS I and KS II); KS I is linked to the protein through an N-linked core glycan structure originally found in the cornea. KS II (skeletal KS) is an O-glycan linked through GalNAc to Ser/Thr, like the linkage found in mucins. Keratan sulfate consists of approximately 50 disaccharide repeating units (20–25 kDa) and contains a mixture of nonsulfated, monosulfated (Gal-GlcNAc6S), and disulfated (Gal6S-GlcNAc6S) disaccharides.

Heparin/heparan sulfate consists of the disaccharide unit of N-acetylglucosamine and glucuronic acid (GlcNAc α 1-4GlcA β 1-4). It is modified by N-deacetylase/N-sulfotransferase enzymes leaving selective N-acetylglucosamines deacetylated and N-sulfated; these sulfated domains undergo uronic acid epimerization, converting the glucuronic acid to iduronic acid which is followed by 2-O-sulfation. Further modifications include 6-O-sulfation and rarely 3-O-sulfation of the hexoamine residues. Consequently, mature chains have a pattern of N-acetylated domains with a low degree of O-sulfation and N-sulfated domains and a high degree of O-sulfation.

Heparin is a naturally occurred polysaccharide with a major trisulfated disaccharide repeating unit and a minor amount of undersulfated disaccharide repeating units. In addition, heparin also contains a unique pentasaccharide sequence within the chain; it's known as the antithrombin III binding site that binds to the serine protease inhibitor ATIII. In HS, these modifications do not go to completion, thus, HS chains are composed primarily of the undersulfated or non-sulfated repeating disaccharide domains. The exacting details remain unidentified.

1.2.2 Biological significance

Hyaluronan (HA) is a linear polysaccharide with diverse biological functions. It has been found in the extracellular matrix and even within cells. The structure is known to maintain tissue hydration and provides a structural framework for cell development. As a result of its distinct biophysical and biomechanical properties, HA contributes to various biological processes including protein interactions, morphogenesis, wound healing and role in disease processes, notably cancer (Dicker, Gurski et al. 2014).

Keratan sulfate (KS) is found in the cornea (KS I) of eyes and cartilage (KS II). The high abundance of KS in cornea is responsible for maintenance of tissue hydration which is critical for cornea transparency. Moreover, it is involved in many biological processes, such as embryonic development, and various roles in wound healing (Funderburgh 2000).

Chondroitin/dermatan sulfate (CS/DS) chains act as cell surface receptors, modulators and signaling molecules (Mikami and Kitagawa 2013). As the major GAGs of lecticans, the biological functions of CS/DS are manifested through their interactions with a large number of binding proteins.

The structural diversity of heparin/heparan sulfate contributes to a variety of biological functions. Generally speaking, heparin/heparan sulfate carry out their functions in two ways. Either they interact with proteins through the sulfo groups that involve electrostatic interaction, or through hydrogen bonding with basic amino acids of the target protein.

Heparin is expressed in connective-tissue mast cells, and these chains are attached to serglycin (an important PG in the formation of several inflammatory mediators). Endogenous heparin is a major component of mast cell secretory granules. Accordingly, mast cell heparin has a role in the storage of histamine and specific granule proteases (Forsberg, Pejler et al. 1999, Humphries, Wong et al. 1999). Exogenous heparin is mainly used clinically as an anticoagulant; and has many other biological activities such as release of lipoprotein lipase and hepatic lipase (Liu, Hultin et al. 1992), inhibition of complement activation (Kazatchkine, Fearon et al. 1981, Sharath, Merchant et al. 1985), inhibition of angiogenesis and tumor growth (Folkman, Langer et al. 1983, Crum, Szabo et al. 1985).

In the coagulation cascade, one factor activates the next until prothrombin (factor II) is converted to thrombin (factor IIa). Thrombin and factor Xa which is inhibited by antithrombin III (ATIII) are coagulation factors, and ATIII is the serine protease inhibitor. Heparin can simultaneously bind to thrombin and ATIII. Upon binding, it undergoes a conformational change resulting in the inhibition of thrombin and other coagulation cascade proteases. Only a third of the chains of pharmaceutical grade heparin contain the ATIII binding site. Heparin can also interact with thrombin using its higher negative charge density to inhibit coagulation.

Heparan sulfate is expressed ubiquitously in animal tissues and owing to its diverse structures, HS also has a wide range of biological activities and functions. Importantly, HS helps protect protein from protease degradation and regulates protein transport through basement membranes (Dowd, Cooney et al. 1999) and mediates internalization of proteins (Reiland and Rapraeger 1993). In addition, HS facilitates cell adhesion (Lindholt, Lidholt et al. 1994), regulation of cellular growth and proliferation (Castellot, Hoover et al. 1985, Perrimon and Bernfield 2000), developmental processes (Perrimon and Bernfield 2000), blood coagulation (Marcum, McKenney et al. 1986) as well as cell surface binding of various proteins (Cheng, Oosta et al. 1981, Shimada, Gill et al. 1981, Taipale and Keski-Oja 1997, Tumova, Woods et al. 2000).

Significantly, as diverse as yet specific as these functions are, the details of their structural makeup remains elusive.

1.3 Heparin (highly sulfated form of HS) and heparan sulfate (HS)

1.3.1 A brief history

Heparin is a naturally occurring GAG and is widely used as a clinical blood anticoagulant. Almost a centenary has passed since its initial discovery in 1916 (Barrowcliffe 2012), when Jay McLean, isolated heparin by accident from canine liver. Its commercial production started in the early 1920s soon after its discovery. The first marketed heparin in the USA was extracted from beef lung tissues in 1939. Beef lung continued as a source material until the mid-to-late 1950s. At this time, porcine intestinal mucosa was found to be a cleaner tissue. Unfractionated heparin was the dominated product in the market until the late 1970s. With the development of improved analytical methods, the chemical structure of heparin was increasingly evaluated. Heparin could be depolymerized into low molecular weight heparins (LMWHs) using a variety of techniques, such as peroxide oxidation, deaminative degradation and β -elimination. In 1976, teams led by Lindahl and Rosenberg were able to fractionate heparin into high-affinity and low affinity components for the first time. There was little difference between these components in terms of chemical composition (Cheng, Oosta et al. 1981, Atha, Lormeau et al. 1985). This finding indicated that there must be a specific sequence responsible for binding to antithrombin. The unique pentasaccharide sequence was unraveled by Lindahl's group in 1982. One year later, this unique pentasaccharide was first synthesized by Petitou and his colleagues. This was one of the most remarkable contributions to heparin chemistry.

1.3.2 Biosynthesis

Heparin and HS share the same polysaccharide backbone and the same general biosynthesis pathway, but the details of monomer structure have yet to be confirmed. Functional differences strongly suggest attractions in structural details. This is not a template driven process. The biosynthesis of heparin and HS is a rapid process with a large number of different enzymes taking part in the process. The principle steps include initiation, elongation and modification (Carlsson and Kjellen 2012).

The initiation starts with the formation of a tetrasaccharide linkage region (-GlcA-Gal-Gal-Xyl-), followed by the attachment of the terminal xylose residue to one or more serines within the core protein (Roden 1980). Only certain serines that share acidic amino acid residues (on one or both sides) are selected for GAG attachment (Esko and Zhang 1996). Xylosyltransferase initiates this linkage from UDP-xylose to the hydroxyl group of serine on the core protein. After xylosylation, a stepwise transfer of two galactose moieties is catalyzed by Gal-transferase I and II followed by a glucuronic acid and galactose to complete the linkage region.

After synthesis of the linkage region, the heparin/heparan sulfate chains are elongated by polymerase enzymes (EXT1 and EXT 2) (Zak 2005). The polymerization is carried out by the addition of alternating glucuronate and N-acetyl-glucosamine residues from their respective UDP-sugars donors to the nonreducing end of the chain. A series of metabolic steps occur in the presence of the sulfate donor 3'-phosphoadenosine 5'-phosphosulfate (PAPS) (Esko and Lindahl 2001). The modification starts with N-deacetylation and N-sulfation of the original N-acetylglucosamine units. After N-sulfation, a C5-epimerase

catalyzes the epimerization of glucuronic acid to iduronic acid. 2-O-sulfation of the uronic acid is closely associated with epimerization, followed by 6-O-sulfation and/or a rare 3-O-sulfation of the glucosamine. This 3-O-sulfate group is a crucial functional component of the antithrombin-binding pentasaccharide of heparin. Although the basic mechanisms of the biosynthetic process have been elucidated, the overall organization and regulation of the enzymes that catalyze the process remain poorly understood.

1.3.3 Chemistry of heparin

For effective MS spectral understanding of GAGs sequences, indigenous molecular charges must be blocked or removed. In this section 1.3.3, I review the chemical reactions served for this purpose. Methylation, desulfation and acetylation are the key steps of this chemistry coupled with specific marker replacement.

1.3.3.1 Methylation

These GAGs structures, either sulfate esters or sulfated amines (or both) represent the targets. Growth of the disaccharide chain greatly increases the polarity. Methylation of most glycans easily obtained by performing methylation (Ciucanu and Kerek 1984) with sodium hydroxide and iodomethane in dimethyl sulfoxide (DMSO). However, the Ciucanu and Kerek method has been reported to be unsuitable for permethylation of GAG oligosaccharides because of the sodium salt contamination (Dell, Rogers et al. 1988). By applying an ion change pre-step to the glycans, they have been converted from sodium salt to triethylammonium salt. The glycans are more soluble in DMSO thereby increasing the yield of methylated sulfated glycans (Stevenson and Furneaux 1991).

Successful permethylation protocols for heparin disaccharides were introduced by Heiss et al. (Heiss, Wang et al. 2011). Permethylation is carried out by first adding an anhydrous suspension of NaOH in DMSO (Anumula and Taylor 1992), followed by iodomethane. The permethylated heparin disaccharides can be isolated by elution with 50% methanol through a C₁₈ Sep-Pak cartridge. For trisulfated heparin disaccharides, the reaction mixture was desalted with a C₁₈ Sep-Pak cartridge in ion-pairing mode.

1.3.3.2 Desulfation

In chemically resolving sulfate positions, two matters had to be considered; could they be removed quantitatively and secondly, could the N- and O-sulfates be differentiated. The pK_a of a sulfate group is around 3, thus, the GAGs are highly acidic and labile. Mass spectral analysis can only be approached using a soft ionization technique (Reinhold, Carr et al. 1987). In many cases, removal of sulfate groups prior to structural analysis with mass spectrometry has proven more successful. Various methods for desulfation have been developed for this approach, such as acid-catalyzed desulfation, solvolytic desulfation, alkali-catalyzed desulfation and desulfation mediated by silylating reagents.

1.3.3.2.1 Acid-catalyzed desulfation

Sulfate groups can be hydrolyzed in aqueous acid solution (Rees 1963) or using methanolic hydrogen chloride (Kantor and Schubert 1957, Wolfrom, Vercellotti et al. 1964). Acid-catalysis was frequently used with 0.25 M hydrochloric acid in a boiling-water bath (Rees 1963). Progress was followed using a chloroaminodiphenyl reagent with spectrophotometric determination. The study showed that acid hydrolysis rates can be useful for characterization of single sulfate ester but not multiple sulfates. Methanolic desulfation is

capable for liberating both O- and N-sulfo groups. This is a convenient method, because it only requires a suspension of dried sample in methanolic hydrogen chloride at room temperature.

In a study of chondroitin sulfate, dried sample was treated with 0.06 M hydrochloric acid in methanol at room temperature for a day and yielded a product with no ester sulfate and with methylated carboxyl groups (Kantor and Schubert 1957). In this report, they pointed out that the acid-methanol would be expected to methylate the carboxylate groups but not the sulfate ester groups.

In the case of heparin sulfate, desulfation failed to go to completion (Danishefsky, Eiber et al. 1960). The difference in the ease of sulfate removal between heparin and chondroitin sulfate is due to N-sulfates and monosaccharide spatial position. Sulfoamino groups are more acid-labile than O-sulfate esters and thus liberated more quickly to produce free amino groups (Nagasawa and Yoshidome 1969). According to the generally accepted mechanism for acidic hydrolysis of esters, the reaction likely involves an initial step of protonation to the comparatively negative oxygen (Usov, Adamyants et al. 1971, Guo and Gaiki 2005, Usov 2011). The explanation was that since the liberated free amino groups can be considered as stronger proton acceptors, they could inhibit hydrolysis of sulfate esters (Nagasawa, Inoue et al. 1977). Acetylation of the amino groups facilitates the removal of additional sulfates from heparin, but still, the desulfation was incomplete (Nagasawa, Inoue et al. 1977). However, this approach requires a prolonged period to enable solid phase (dried sample) and liquid phase (methanolic HCl) to react heterogeneously. Moreover, degradation of the polysaccharide chain accompanies the sulfate liberation process (Wolf from, Vercellotti

et al. 1964). It is worth noting that selective N-desulfation with acid-methanol is inevitably, leading to liberation of O-sulfo groups (Foster, Martlew et al. 1961).

1.3.3.2.2 Solvolytic desulfation

Since the acid-catalyzed desulfation causes cleavage of glycosidic linkages, researchers have looked into alternative approaches. The solvolytic desulfation is one of the most frequently employed. It has been shown that pyridine accelerates the desulfation of N-substituted sulfamic acid with (Nagasawa and Yoshidome 1969). Pyridine seems to act as a catalyst to decompose N-substituted sulfamic acid. A similar catalytic activity was shown by dimethyl sulfoxide (Whistler, King et al. 1967) as well. It is believed that this type of degradation involves an intermediate step resulting in formation of "solvent-SO₃ adduct." Conversely, the reversibility of this reaction leads to generation of acid sulfates (Nagasawa and Yoshidome 1969).

In 1972, Usov, et al. found that pyridinium salts of sulfated glycans undergo desulfation when heated in relatively polar aprotic solvents such as *p*-dioxane, pyridine, dimethyl sulfoxide or *N,N*-dimethyl formamide (Usov, Adamyants et al. 1971). With this understanding, it was found that the sulfated galactans were successfully desulfated by heating the pyridium salts in 2 % pyridine-dimethyl sulfoxide. These conditions were found to give higher yields and less degradation than methanolic desulfation (Usov, Adamyants et al. 1971). The addition of a small amount of water or methanol to this system accelerates the desulfation process when applied to glycosaminoglycans (Nagasawa, Inoue et al. 1977, Nagasawa, Inoue et al. 1979) such as heparin and chondroitin sulfates. It should be kept in mind that the process of solvolysis has not yet been fully understood. The possible mechanism of this reaction may be concluded as following:

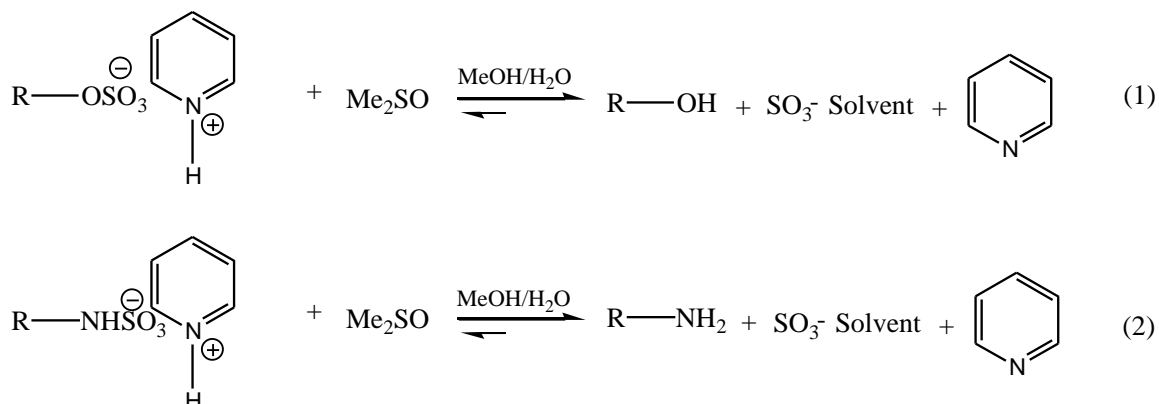


Figure 1-1 Proposed mechanism of solvolytic desulfation.

Sulfated polysaccharides are first converted to their pyridinium salts before solvolysis. Decomposition rate of 2-deoxy-2-sulfoamino-D-glucose pyridinium salts (Nagasawa and Inoue 1974) in a couple of aprotic polar solvents was studied, and the rate was found to decrease in the order: pyridine > *N,N*-dimethylformamide > dimethyl sulfoxide > hexamethyltriamide phosphate > acetonitrile. Although the decomposition rate was higher in pyridine and *N,N*-dimethylformamide, decomposition of 2-deoxy-2-amino-D-glucose was found in these solvents. In dimethyl sulfoxide decomposition, the rate was fairly rapid and the product stable, hence, dimethyl sulfoxide seems to be the best suited solvent.

Heating in the reaction process, pyridinium salts were decomposed when using dimethyl sulfoxide as a solvent (Nagasawa and Inoue 1974). The liberated sulfates formed sulfur trioxide-dimethyl sulfoxide complexes and released pyridine. Methanol or water may act as acceptors of the sulfur trioxide to complete the reaction, thus accelerating the solvolysis process. In Figure 1-1, the solvent could be dimethyl sulfoxide, methanol, water or pyridine.

Solvolytic desulfation of heparin was occurred when treating pyridinium salts with dimethyl sulfoxide containing 10% water or methanol at 80-100 °C (Nagasawa, Inoue et al. 1977). Completely desulfation was achieved with N-desulfated, acetylated heparin under similar condition. These results suggested that the free amino groups liberated by prior N-desulfation may be combined with sulfate ester groups to stabilize the polysaccharide against further desulfation. Acetylation converts the free amino groups to N-acetyl groups, thus inhibiting this process.

This solvolytic desulfation method allows for selective removal of certain sulfate groups and selective N-desulfation was achieved with their pyridinium salts in dimethyl sulfoxide containing 5% of water or methanol without any liberation of O-sulfates (Nagasawa and Inoue 1974, Inoue and Nagasawa 1976). Moreover, selective 6-O-desulfated product of heparin was obtained under controlled conditions (Baumann, Scheen et al. 1998).

Solvolytic desulfation of sulfated polysaccharides can be greatly accelerated by heating the pyridinium salts when dissolved in dimethyl sulfoxide in a microwave oven (Navarro, Flores et al. 2007). The desulfation can be completed efficiently by microwave heating in just one minute, although some depolymerization occurs. It should be kept in mind that this method was not applied to any N-sulfates in this report.

In connection with solvolytic desulfation, Miller and Blunt reported an improved method that remove all sulfate esters in good yield (Miller and Blunt 1998). They treated the pyridinium salts of sulfated polysaccharides with pyromellitic acid and a small amount of pyridine in completely dried dimethyl sulfoxide. Arsenous oxide (As_2O_3) or antimony trioxide (Sb_2O_3) was used as acceptors for sulfur trioxide. It is worth noting that when

sodium fluoride was the sulfate acceptor, selective desulfation of nonaxial sulfate esters was achieved.

1.3.3.2.3 Alternative approaches

It has been previously demonstrated that desulfation can be carried out by alkaline treatment, however, this desulfation often leads to ether bond formation within the sugar ring (Rees 1961, Rees and Conway 1962). Alkali catalyzed 2-O-desulfation resulted in an ether bond between the C-2 and C-3 positions while 6-O-desulfation introduced an ether bond between the C-3 and C-6 positions. In other words, this type of desulfation appeared to occur when a sulfoxyl group and a free hydroxyl group are combined in a sterically favorable configuration. Hence, this process can be described as alkaline sulfate elimination, in which the sulfate group severing as a leaving group. This method has been successfully applied for desulfation of heparin specific to 2-O-sulfo groups (Rej, Jaseja et al. 1989).

Another alternative approach for sulfate removal can be assisted with silylation reagents in pyridine (Takano, Kanda et al. 1995). It has been shown that silylating with *N,O*-bis(trimethylsilyl)acetamide (BTSA) and *N,O*-bis(trimethylsilyl)trifluoroacetamide (BTSTFA) can greatly enhance the rate of 6-O-desulfation but completely suppress desulfation at 3-O and other positions. The reagent (BTAS) was effective for complete desulfation of chondroitin sulfates having 6-O-sulfates without any extraneous degradation of polysaccharide chain (Matsuo, Takano et al. 1993). But for heparin, it only removed two-thirds of the 6-O-sulfo group under similar conditions and higher reaction temperature leads to side reactions (Matsuo, Takano et al. 1993). In contrast, specific 6-O-desulfated products of heparin were obtained by using *N*-methyl-*N*-(trimethylsilyl)trifluoroacetamide (MTSTFA) (Takano, Ye et al. 1998). In summary, these alternative desulfation approaches are more

valuable when at specific position is desired. For non-specific desulfation, acid-methanol or solvolysis may be a better choice.

1.3.3.3 Acetylation

Acetylation is another commonly used chemical derivatization method for glycan linkage analysis. However, methylation is often favorable because it results in a smaller mass with a greater stability and volatility. In general, acetylated products are generated by treatment with acetic anhydride in presence of pyridine (Bourne, Stacey et al. 1949). In the case of heparin, N-acetylation is usually performed after desulfation to avoid formation of quaternary ammonium salts when methylation is the goal. Moreover, N-acetylation facilitates the removal of additional sulfate from heparin (Danishefsky, Eiber et al. 1960).

1.3.4 Commercial production process for heparin and heparin-like polysaccharides

Heparin is used primarily as a clinical anticoagulant drug and pharmaceutical grade heparin is a purified tissue extract from animals. Porcine intestines and bovine lungs are the prime source, but like all naturally occurring polysaccharides, they are a polydisperse mixture. Heparin chains range in molecular weights from 5000 to over 40,000 Da providing disaccharides with significant sequence heterogeneity.

Commercial preparations of heparin generally involve multiple steps (Cheng, Oosta et al. 1981, Linhardt and Gunay 1999). Isolated intestines are salted with sodium metabisulfite or sodium chloride to protect the tissue from degradation and assist dehydration (Mozen and Evans 1962, Vidic 1978, Bhaskar, Sterner et al. 2011). The tissues are then depolymerized by alkaline pH and protease treatment. The protease is removed by heat

deactivation (Panasyuk 2007) and crude heparin is recovered in one of two ways: a resin based chromatographic step using a strong anion exchange resin, or a precipitation step using a hydrophobic quaternary ammonium salt. The steps appear to be carried out without current good manufacturing practices (cGMP) facilities that may result in impurities.

Further purification is typically performed under good manufacturing practices conditions. Depending on the purification method the final step differs as well. The final preparations are water-insoluble and can be re-dissolved in highly concentrated sodium chloride solution or higher alcohols (Nomine, Penasse et al. 1961). The quaternary ammonium salts flocculate easily at low pH thus allowing for filtration (Hyamine 1622). This filtrated precipitate can be re-solubilized in butanol followed by solvent exchange to end up with an aqueous solution. This solution can be treated with ethanol or salt to a purified heparin. Preparation uses ion exchange where raw heparin is adsorbed onto the resin according to the differences of charge-density. The resin is then washed and subsequently eluted under basic or high salt conditions depending upon the resin.

The raw heparin is filtered next at low pH to remove residual amounts of protein followed by alkali to obtain a purified product. All the unwanted cations are then removed by passing the solution through a cation exchange resin and ethanol precipitation for removal of nucleotides. Finally, the purified heparin is recovered through membrane filtration to remove all other remaining salts.

Low molecular weight heparins (LMWHs) are defined as salts of sulfated GAGs with enhanced anti-factor Xa/anti-factor IIa ratio and having an average molecular weight of less than 8000 Da. In addition, at least 60% of LMWHs chains are less than 8000 Da (Linhardt

and Gunay 1999). LMWHs are prepared by fractionation or depolymerization of heparin such as oxidation, deaminative degradation, chemical β -elimination and enzymatic β -elimination (Bhaskar, Sterner et al. 2011).

1.4 The antithrombin binding site, a unique pentasaccharide sequence

The anticoagulant activity of heparin is closely related to the antithrombin (AT) binding site, which is an unique pentasaccharide sequence (GlcNAc/NS6S \rightarrow GlcA \rightarrow GlcNS3S,6S \rightarrow IdoA2S \rightarrow GlcNS6S). When this pentasaccharide sequence binds to AT, its inhibition process of factor Xa is activated through conformational change of AT's structure. Therefore, the speed of blood coagulation is accelerated. In contrast to natural heparin, this unique sequence with much simpler structure opens a door for industrial production of anticoagulant drug.

This antithrombin binding site was first synthesized in 1984 (Sinay, Jacquinet et al. 1984). The chemical structure of this synthetic pentasaccharide was characterized using fast-atom-bombardment mass spectrometry by Vernon N. Reinhold et al. in 1987 (Reinhold, Carr et al. 1987).

Fondaparinux (Arixtra[®], its generic name) is name of the chemically synthetic linear octasulfated pentasaccharide mimicking the site of heparin that binds to antithrombin III (ATIII). It is the first of a new class of antithrombotic agents distinct from low molecular weight heparins (LMWHs) and heparin. It exhibits only factor Xa inhibitor activity via binding to AT, which in turn inhibits thrombin generation. The full chemically name of Fondaparinux sodium is methyl O-2-deoxy-6-O-sulfo-2-(sulfoamino)- α -D-glucopyranosyl-

(1,4)-O-β-D-glucofuranuronosyl-(1,4)-O-2-deoxy-3,6-di-O-sulfo-2-(sulfoamino)-α-D-glucofuranosyl-(1,4)-O-2-Osulfo-α-L-idofuranuronosyl-(1,4)-2-deoxy-6-O-sulfo-2-(sulfoamino)-α-D-glucofuranoside, decasodium salt.

Fondaparinux sodium is a synthetic pentasaccharide anticoagulant. Fondaparinux sodium was first launched in the U.S. in 2002 by GlaxoSmithKline. Then its generic version Arixtra[®] developed by Alchemia is marketed within the US by Dr. Reddy's Laboratories.

1.5 Current GAG characterization protocols and analytical limitations

Various analytical techniques and methodologies have been applied for GAG characterization, in terms of molecular weight, sulfation level, linkages and sequences; such as nuclear magnetic resonance (NMR), liquid chromatography (LC), mass spectrometry (MS) and electrophoresis.

1.5.1 Liquid chromatographic approaches

Liquid chromatographic separations are achieved generally on the basis of three characteristics, molecular size, electrical charge and polarity. Either one or more characteristics are employed within one separation. Size exclusion chromatography (SEC), strong anion exchange chromatography (SAX), hydrophilic interaction chromatography (HILIC) and ion-pair reversed-phase liquid chromatography (IP-RPLC) are the most common seen separation techniques for analysis of heparin. Each approach has shown its unique advantages for characterization of heparin structures.

1.5.1.1 Size exclusion chromatography

A size exclusion chromatographic separation is established on basis of size differences. This method is fast, simple and rather cheaper comparing to other liquid chromatographic techniques. It does not require complicated equipments and it is easy to operate. It works efficiently for the separation of high molecular weight substances. Size exclusion chromatography (SEC) employs a simple mobile phase normally ammonium salts for preparative heparin separation. However, SEC is generally considered as a low resolution chromatography since it does not resolve isomeric species very well.

Size exclusion chromatography is used for determination of molecular weights and measurement of size dispersions for low molecular weight heparins (LMWHs) or heparin-derived oligosaccharide mixtures (Guo, Condra et al. 2003, Beirne, Truchan et al. 2011, Sommers, Ye et al. 2011). The molecular weight is determined either by using molecular weight standards or with multiangle light scattering detection. Usually, SEC is operated under low pressure but investigation of operating at high pressure for separation (Ziegler and Zaia 2006) of heparin oligosaccharides has been reported as well. Fractions from enzymatically digested heparin was collected from SEC and analyzed in negative mode electrospray mass spectrometry as ammonium salts (Chai, Luo et al. 1998). Another method has utilized SEC with on-line ESI mass spectrometric detection (Henriksen, Ringborg et al. 2004) to obtain informative spectra for characterization of LMWHs.

Size exclusion has been shown to be important for top-down structural analysis of low molecular weight heparins. In this top-down approach, intact heparin oligosaccharides can be directly analyzed without any depolymerization (Henriksen, Ringborg et al. 2004). A

major drawback, however, is the limited separation selectivity which is dependent on the porous particle size and pore volume (the ratio of air volume to total volume). With the development of ultra-performance SEC columns, narrower pore size column packing allows for greater separation efficiency and resolution. In that regard, a new strategy has been recently introduced using an ultra-performance SEC (UPSEC) column packed with 1.7 μm particles for the structural analysis of LMWHs (Bhaskar, Sterner et al. 2011). In this study, more than 70 molecular weight peaks of a commercial LMWHs drug were identified by electrospray quadruple time-of-flight-mass spectrometry (Q-TOF-MS) in combination with capillary zone electrophoresis (CZE). Nevertheless, it should be pointed out that UPSEC still did not resolve isomeric oligosaccharides and the identification was relied on the negative ion mode m/z values.

1.5.1.2 Strong anion exchange chromatography

Strong anion exchange chromatography (SAX) is a traditional separation method for heparin analysis. Separations are based on charge density differences and usually use high salt concentration in the mobile phase. The most common salt used for heparin separations is sodium chloride (NaCl). Columns are usually packed with the ion-exchanger covalently attached to the surface of a stationary phase, containing charge groups. Strong anion exchange columns are usually packed with quaternary ammonium groups. Retention time in SAX is governed by reversible adsorption of sample anions to oppositely charged stationary-phase ionic groups and its competition with mobile phase counterions. For instance, negatively charged sulfated heparin will bind to positively charged quaternary ammonium groups on the stationary phase surface. Mobile phase consists of water and sodium chloride with an acidic pH adjusted by adding hydrochloric acid. Sulfate group is considered as

weaker anions compared to chloride, thus chloride is more strongly attracted to the positively charged quaternary ammonium groups. Separations are performed using a linear gradient with increasing salt concentration. Ion exchange starts with releasing the species of the weakest ionic interaction from the stationary phase. These weakest ions are eluted by displacement with chloride anions. With the concentration increasing, stronger ions are released from the stationary phase.

Strong anion exchange chromatography has been applied for heparin fractionation with a wide range of molecular weight distribution from disaccharides to low molecular weight heparins (Linhardt, Rice et al. 1986, Thanawiroon and Linhardt 2003, Skidmore, Guimond et al. 2010). Unsaturated heparin disaccharides and oligosaccharides can be detected by UV absorbance at 232nm. However, more sensitive detection is frequently required for small amount of samples isolated from tissue or cultured cells. Hence, a fluorescence-labeling strategy is introduced to increase detection. Aminobenzamide (2-AB) is a widely used label by reductive amination and to label the reducing hemi acetal of heparin oligomers (Kinoshita and Sugahara 1999). Tissue extracts from small biological samples have achieved enhanced sensitivity with fluorescence detection using BODIPY (4,4-difluoro-5,7-dimethyl-4-bora-3a,4a-diaza-s-indacene-3-propionic acid) hydrazide which has also been applied for detecting disaccharide compositions from enzymatically digested heparin (Skidmore, Guimond et al. 2006, Skidmore, Atrih et al. 2009, Skidmore, Guimond et al. 2010). Alternatively, underivatized heparin disaccharides and oligosaccharides can be also analyzed by pulsed amperometric detection (PAD) with high sensitivity (Thayer, Rohrer et al. 1998, Campo, Campo et al. 2001).

Anion exchange with fluorescence detection offers improved sensitivity down into the picomole level, but this approach using a salt gradient is difficult to interface with a mass spectrometer. Hence, it may be better to consider no derivatization when coupling SAX on-line with MS. However, high performance anion exchange chromatography (HPAEC) with PAD has been successfully used for analysis of heparin oligomers in combination with on-line ESI-MS (Bruggink, Maurer et al. 2005, Bruggink, Wuhrer et al. 2005). This detector uses sodium hydroxide or sodium acetate which is not compatible for ESI, thus, a carbohydrate membrane desalter has been designed prior to the ESI interface. The function of this cation exchange membrane is converting sodium hydroxide into water and sodium acetate into acetic acid, which is compatible for ESI.

1.5.1.3 Hydrophilic interaction chromatography

Separations by hydrophilic interaction chromatography (HILIC) are carried out on the basis of the analyte polarity. The mechanism is similar to normal phase chromatography (NPC) where the stationary phase is polar while the mobile phase is non-polar or less polar organic solution. Hence, polar analytes bind strongly to the stationary phase and cannot be eluted. As a variant of normal phase chromatography, HILIC uses water in the mobile phase. The addition of water to the organic mobile phase allows for separation of polar analytes which are strongly retained on the column. Likewise, the common columns used in NPC can be adapted to HILIC separation. For examples, bare silica, amino-, diol- and cyano-bonded silica materials have been used for HILIC stationary phase packing (Regnier and Noel 1976, Rubinstein 1979, Olsen 2001, Guo and Gaiki 2005). Different HILIC stationary phases lead to different retention patterns. Typically, a HILIC separation employs a semi-aqueous mobile phase consisting of > 30% acetonitrile in water or a volatile buffer. The separation

mechanism in HILIC is very complex and depends on various types interactions among the solute, the mobile phase and the stationary phase. It's generally accepted that HILIC retention is governed by the partitioning of the analyte between stationary phase and mobile phase on the basis of its relative solubility (Alpert 1990). But this explanation still lacks of a thorough examination.

Under HILIC conditions, a water-rich layer is first formed on the surface of stationary phase. The separation process starts with partitioning of analyte from the mobile phase into this water-rich layer (McCalley and Neue 2008). The water adsorption on the stationary surface can be multilayer (Gritti, dos Santos Pereira et al. 2009) and is influenced by several interactions. Those interactions (Buszewski and Noga 2012) can be classified into chemical interactions including hydrogen bonding and donor-acceptor interactions, physical interactions, intermolecular interaction by Van der Waals forces and hydrophobic interactions. When the stationary phase is modified with charged groups, the retention is also affected by electrostatic interactions. Separation occur either in the isocratic mode or gradient mode (Alpert 1990) or both. Elution of analyte depends on the differential distribution between the water-deficient mobile phase and the water immobilized stationary phase. The more hydrophilic analyte tends to be more retained on the water immobilized stationary phase, which is hydrophilic as well.

In summary, HILIC chromatography retention mechanism is complicated and affected by various interactions, more importantly, it can be easily combined with various detection techniques, such as ultraviolet absorbance detection, fluorescence detection, refractive index, evaporative light scattering, charge aerosol, and mass spectrometry. In

addition, it is particularly useful for electrospray ionization because the more volatile mobile phase accelerates solvent evaporation.

Heparin/HS are highly sulfated, polydispersed linear polar polysaccharides. The structures of heparin/HS vary in terms of disaccharide compositions, chain length, sulfation level as well as sequence. These characteristics induce variations in polarity and HILIC-MS seems to be a promising strategy for detail characterization of heparin oligosaccharide mixtures (Hitchcock, Yates et al. 2008, Staples, Bowman et al. 2009, Staples, Naimy et al. 2010, Chang, Yang et al. 2012, Fu, Li et al. 2014, Li, Steppich et al. 2014). Both bottom-up (Li, Steppich et al. 2014) and top-down (Li, Zhang et al. 2012) approaches have been applied for elucidation of low molecular weight heparin structures using HILIC-MS. In the bottom-up approach, LMWHs were digested with heparin lyase II and analyzed with fourier transform mass spectrometry. In the top-down approach, HILIC-FT-MS was able to identify ion compositions of LWMHs from tetrasaccharides (dp4) to polysaccharides (dp26) without depolymerization. However, no further structural detail was available.

1.5.1.4 Ion-pair reversed-phase (IP-RP) high-performance liquid chromatography

Ion-pair reversed-phase high-performance liquid chromatography (IP-RP-HPLC) appears to be a promising approach for analysis of heparin and heparan sulfates. The mobile phase can be modified by the addition of cationic or anionic ion-pairing agents, which can in turn interact with charged analyte molecules. Heparin with its sulfate anions, thus the ion-pairing agent will be positively charged. These interact with sulfate anions to form ion-pairs that can be retained on the column. Therefore, the hydrophilic solutes have been converted to hydrophobic ion-pairs. The basis of sample retention in IP-RP-HPLC is still controversial

but two processes have been promoted. One can be explained by the formation of an ion-pair in the mobile phase. The stationary phase then retains the ion-pair. The other explanation assumes that the ion pairing agent is first attached to the column, then, occurs by an ion-exchange process; the mobile phase counterion is replaced by charged sample ion. Although the two retention mechanisms are different, they lead to virtually equivalent retention as a function of experimental conditions in practice. Generally speaking, retention times are governed by the mobile phase and ion-pair agent for a given separation. The most important factors are; mobile phase composition; pH and ion-pairing type and agent concentration. In the case of ion-pair model, the retention time depends on how well the ion-pair is formed. The formation of ion-pair involves three steps in general. The first step is ionization of sample in the mobile phase, which is determined by its pKa value and the mobile phase pH. The second step is the interaction with the ion pairing agent and its equilibration. This step relies on the concentration of ion pairing agent and its tendency to form an ion-pair. The last step is adsorption onto the stationary phase. This process is affected by the concentration of organic modifier. At constant concentration of ion pairing agent, increasing the portion of organic modifier will hamper the ion-pair adsorption process, thus leading to a decrease in sample retention. In the case of this ion-exchange model, an increase in concentration of organic modifier will lower the amount of ion pairing agent dynamically adsorbs to the surface of stationary phase. Consequently, the ion-exchange process between the charged sample ions and mobile phase counterions is slowed down. The ion-exchange process is affected by ionization of sample solute and its tendency to exchange with mobile counterion as well. The investigation of each factor will be discussed as follows.

1.5.1.4.1 Mobile phase pH

Heparin and heparan sulfate contains O- and N-sulfo, and carboxyl groups. The pKa of a sulfate group is around 3, thus the most acidic. The pKa of the three acidic groups are <1, 1-1.5 and 3-4, respectively, and complete ionization of smaller heparin oligosaccharides might happen at pH 5.5 (Linhardt and Toida 1997). As a result of this polyelectrolyte, the pKa of carboxyl groups will increase as the length and net charge of oligosaccharides increase. To allow for complete ionization of larger oligosaccharides, the pH value should be increased as well. The effect of mobile phase pH on retention time has been investigated by Thanawiroon (Thanawiroon and Linhardt 2003). In this study, pH values from 3.5 to 7.0 were examined for the separation of heparin derived oligosaccharides. At constant concentration of ion pairing agent, higher pH provides better resolution notably for larger oligosaccharides.

1.5.1.4.2 Mobile phase composition

Acetonitrile and methanol are common organic solvents used for reversed-phase separations. Although acetonitrile seems to be the most favorable organic solvent, separation of heparin derived oligosaccharides using methanol (Bisio, Mantegazza et al. 2007) as the mobile phase has been reported as well. Both solvents were examined for separation of low molecular weight heparins (Langeslay, Urso et al. 2013) under the same condition. However, methanol showed poor resolution for oligosaccharides larger than octasaccharides.

1.5.1.4.3 Ion pairing agent type and concentration

Both linear and branched aliphatic amines have been used as ion pairing additives (Kuberan, Lech et al. 2002, Thanawiroon and Linhardt 2003, Doneanu, Chen et al. 2009, Langeslay, Urso et al. 2013). The selection of ion pairing reagents is related to properties of

the sample to be analyzed. Branched amines e.g. tetrabutylamine has shown great separation for heparin disaccharides (Thanawiroon and Linhardt 2003). Linear amines are more suitable for separation of heparin oligosaccharides (Doneanu, Chen et al. 2009, Langeslay, Urso et al. 2013, Li, Steppich et al. 2014). Those amines have been investigated as ion pairing agents and are listed as following: they are primary amines: *n*-propylamine, *n*-butylamine, *n*-pentylamine, *n*-hexylamine, *n*-octylamine; dialkylamines: dibutylamine; trialkylamines: triethylamine, tributylamine, tripropylamine; tetraalkylamines: tetrapropylamine, tetrabutylamine. These amines can also be classified as non-volatile and volatile amines as a result of its alkyl chain length. The shorter the chain length, the more volatile the amine will be.

Recently, a novel study (Galeotti and Volpi 2013) using tetrabutylammonium bisulfate as ion pairing agent was successfully applied for the separation of heparin/heparan sulfate disaccharides. In addition, this method yielded a sensitivity around four times greater than conventional strong anion exchange chromatography.

Comparisons of type and concentration of various ion pairing agents have been reported. Evaluation of the tetrabutylammonium salt with heparin oligosaccharides (Thanawiroon and Linhardt 2003) and unsaturated HS disaccharides (Kuberan, Lech et al. 2002) demonstrated that an increasing concentration led to corresponding increase in retention time with improved resolution. 10 mM tetrabutylamine showed best separation of both small and larger oligosaccharides (dp2-dp14). However, 5 mM tributylamine provides the best resolution for separation of unsaturated HS disaccharides.

Unlike the tetraalkylammonium salt, linear, di- or trialkylamines do not carry a permanent positive charge that cannot interact with negatively charged highly sulfated heparin oligosaccharides. Hence, an acid is usually added to the mobile phase to donate protons to the amine to form its salt, such as hydrochloric acid, acetic acid and 1,1,1,3,3,3-hexafluoro-2-propanol (HFIP). A comparison of column resolution ability has been investigated for the separation of heparin disaccharides and oligosaccharides using branched alkylammonium acetates (dibutylammonium acetate, tributylammonium acetate, tripentylammonium acetate and triethylammonium acetate). The results showed that among the four branched alkylammonium acetates, dibutylammonium acetate provided the better resolution and a shorter analysis time.

Another study regarding the influence of five linear amines on the retention and resolution has been performed on commercially available heparin-derived oligosaccharides. The linear amine was protonated by a special acidic additive, however, trace amounts of were difficult to be removed from the column and the LCMS systems. Among those linear amines, both pentylamine and hexylamine provided higher peak capacities than other amines. Because of increased chain length leading to longer retention time, pentylamine seems to be a better choice for separation of heparin oligosaccharides. The influence of pentylamine concentration on retention and resolution was further investigated for the separation of heparin oligosaccharides. Retention time was increasing from 5 mM to 25 mM and the best peak capacity was obtained at 15 mM. However, when the concentration reached to 40 mM, a decrease in retention time was observed. This may due to the rise of mobile phase pH which leads to incomplete protonation of pentylammonium ions.

Because it is difficult to remove trace amount HFIP, an alternative approach of using pentylamine in conjunction with acetic acid was investigated for the separation of low molecular weight heparins. This method has shown good resolution up to 22mer using a mobile phase containing 10mM pentylamine, 10mM acetic acid and acetonitrile.

In summary, ion-pair reversed-phase high-performance liquid chromatography separates sulfated heparin oligosaccharides in accordance with size, sulfation level as well as extent of isomerization. Moreover, the performance of an IP-RP HPLC separation not only relies on the selection of ion-pairing agent and mobile phase properties but also relates to size and sulfation level of the analyte.

1.5.1.5 IP-RP liquid chromatography coupling with mass spectrometry (MS)

During the past decades, mass spectrometry has shown great advantages in structural elucidation of heparin and heparan sulfates. Rapid progress in soft ionization techniques such as electrospray ionization (ESI) and matrix-assisted laser desorption/ionization (MALDI) enables characterization of heparin oligosaccharides in terms of chain length, sulfation level as well as composition of disaccharide building blocks. Nevertheless, MALDI always ends up with poor ionization due to loss of labile sulfate groups. This is observed with any matrixes commonly used in MALDI probably caused by excess energy absorbed from laser. Although sulfated heparin oligomers can be ionized readily by electrospray in negative ion mode, the MS profile is very complex owing to multiple charge states, formation of various adducts with metal cations and loss of sulfate groups. The complexity of both sample and MS profile implies that a single approach using MS for highly sulfated heparin oligosaccharides

will be difficult to reveal detail heparin structures. Apparently, a combination of a separation technique will enhance the ability of structural characterization of heparin.

Size-exclusion chromatography (Henriksen, Ringborg et al. 2004), hydrophilic interaction chromatography (Naimy, Leymarie et al. 2008) and ion-pair reversed-phase chromatography (Thanawiroon, Rice et al. 2004, Korir and Larive 2009, Langeslay, Urso et al. 2013, Li, Steppich et al. 2014) has been reported for coupling with ESI-MS for separation of heparin disaccharides and oligosaccharides or both.

A study utilizing size-exclusion chromatography with on-line MS detection has been reported for separation of low molecular weight heparins. Despite the benefit of using simple mobile phase compositions, SEC suffers from poor resolution and incapability of diminishing massive adduction of metal cations. Another study has developed a HILIC LC/MS platform for screening and quantitative analysis of a library of antithrombin III (ATIII) binding hexasaccharides derived from heparin. However, this method was not capable to resolve isomeric heparin hexasaccharides effectively.

Besides, another commonly used separation technique, strong anion exchange chromatography SAX separates analytes on the basis of charge density differences seems like a good candidate to serve for MS detection. However, SAX is very difficult to direct coupling with mass spectrometry owing to requirement of using high concentration and nonvolatile salt (sodium chloride) in the mobile phase.

Comparing to other chromatographic techniques, ion-pair reversed-phase liquid chromatography is more amendable for coupling with mass spectrometry. This technique provides several advantages: (a) it separates sulfated heparin oligosaccharides in accordance

with size, sulfation level and isomerization; (b) it removes alkali or alkaline earth metal cations from sulfate/carboxylate groups; (c) it produces ion-pairs between the sulfate groups and the alkyl amines to reduce sulfate loss during the ionization process.

The two techniques (IP-RP-LC and IP-RP-LC/MS) share the same basis on separation mechanism but a few things should be taken into consideration. First of all, when coupling to mass spectrometry, volatile amines are preferred to facilitate ionization process in mass spectrometer. Ammonium acetate is a commonly used buffer in HPLC for mass spectrometric detection, but it cannot pair with sulfated heparin oligosaccharides to obtain retention. The use of nonvolatile tetra alkyl amines has strongly suppressed MS signal intensity due to the inefficient desolvation of analyte solutes. The more volatile di- or linear alkylamines does not act as an ion pairing agent because of absence of a permanent positive charge. Therefore, acetic acid is added to donate protons to the di- or linear alkylamines resulting in alkylammonium acetate salts. The addition of acetic acid lowers solution pH and rises the concentration of alkylammonium acetates. The former effect will reduce the charge states of analytes since the more acidic solution donates more protons to analyte anions. The latter effect will improve chromatographic performance but decrease MS signal intensity.

Secondly, high concentration of ion pairing agent is not suitable for MS detection. It is analogous to the latter effect of increasing concentration of acetic acid. In addition, an increase in concentration of ion pairing agent will also result in longer retention time and the total analysis time. Hence, a compromise between chromatographic performance and mass spectrometric detection has to be found for optimum of a certain separation.

In general, IP-RP-LC/MS for heparin analysis employs negative mode ion detection due to the anionic nature of sulfate groups. But an IP-RP-LC/MS system using a special acidic additive (HFIP) has been applied for the detection of heparin oligosaccharides in positive ion mode with a better yield of signal intensity in comparison to negative ion mode. In a report of nucleic acid characterization (Huber and Krajete 2000), HFIP has been utilized in conjunction with triethylamine and methonal for removal of metal cations by on-line cation exchange. Although they were able to perform tandem MS in positive ion mode, the MS/MS spectra were not very informative with only consecutive losses of sulfate groups and pentylammonium was observed. In contrast to negative mode, the positive mode spectra contained a mixture of sodium and pentylammonium adducts but the pentylammonium adducts were predominant ions. To date, tributylamine seems to be the most suitable ion pairing agent for heparin-derived disaccharides with MS detection. Pentylamine seems most favorable for IP-RP-LC/MS of heparin-derived oligosaccharides.

1.5.1.6 Graphitized carbon chromatography (GCC)

Porous graphitized carbon (PGC) columns at the molecular level have flat surfaces. This unique property favors resolving isomeric and closely related structures. Retention of analytes on PGC columns is mainly an adsorptive process (Koizumi 1996), where planar species are generally retained than non-planar. Retention time usually increases as the chain length increases. Significantly, columns are tolerant to both strong acidic and basic and are effective throughout the entire pH range. Such techniques have been applied successfully to separate isomeric glycoaminoglycans (Karlsson, Schulz et al. 2005, Estrella, Whitelock et al. 2007, Wei, Ninonuevo et al. 2011, Gill, Wang et al. 2012). The high isomeric resolving power of porous graphitized carbon provides separation with no derivatization, which is

frequently tedious, costly, and usually leads to sample loss. The mobile phase should be free of salts ion pairing agents which makes GCC a better choice for chromatographic interfacing with mass spectrometry.

1.5.2 Mass spectrometric approaches

Many instruments have been developed for the analysis for glycan structural details and mass spectrometry (MS) has been the most successful for the characterization of glycan structures that includes sequence, branching and linkage details. The instrument has also been widely employed as a detector for many separation methods. Most frequently, MS is coupled with a liquid chromatography to resolve the diversity of structures.

Heparin contains either sulfate esters of alcohols or amides of amines or both, inside the building blocks of the disaccharides. With the growth of the disaccharide chain, the added polar residues make for a very polar glycan. The low volatility of these polar glycans makes gas phase mass spectrometric analyses most challenging goal especially for understanding the details of heparin's structures. Not only is ionization very difficult but a consequence is the loss of sulfate. The esters and amides of sulfates are more labile than the glycosidic bonds that provide sequence-informative fragmentation, hence, their positions will be lost before any knowledge of oligosaccharide sequence is known. The high degree of native heterogeneity and charge in heparin oligosaccharides makes their structural determination a very difficult task in positive or negative mode mass spectrometry. Negative ions are usually dependent on both the counter-ion adduction and the electron energy. Variations in either of these parameters can lead to remarkable changes both in the total number of ions formed and their abundances.

To resolve these structures, the most common ionization strategies are matrix-assisted laser desorption ionization (MALDI) and electrospray ionization (ESI). The two techniques are based on different physical principles and are appropriate for differing applications. For gas or liquid interfacing, ESI is simplest. For ablation from solid surfaces, MALDI works best. Both ionization techniques provide high molecular weight ions, although MALDI is more energetic and fragile samples will rupture. Multiply charged ions are acquired in ESI ionization which lowers the measured molecular weight extending the mass range. Structural detail in these molecular ions is obtained by introducing a gas (usually helium) that causes reproducible and characteristic fragmentation upon collision. Analysis of these ions provides considerable structural insight, and doing this repeatedly to develop a disassemble pathway in an ion trap instrument (IT-MSⁿ) uniquely exposes extensive structural detail. The following paragraphs will discuss each application for characterization of GAG structures.

1.5.2.1 Matrix assisted time-of-flight mass spectrometry

Matrix assisted time-of-flight mass spectrometry (MALDI-TOF-MS) is a widely used method for characterization of carbohydrates. This is a soft ionization method and it can produce intact gas-phase ions from wide dynamic molecular ranges. With the assistant of a matrix, non-volatile, thermally labile carbohydrates go through desorption and ionization with a majority of the ions singly charged. In addition, the MALDI procedure is simple by mixing the sample solution with matrix, then drying. It appears to be more tolerant to contamination by salts, buffers, detergents and this simplicity has made MALDI-TOF mass spectrometers are the most commonly used instruments that can couple with other types of mass analyzers as well.

Generally speaking, the ionization process of MALDI involves two steps. The first step is preparing the sample-matrix crystals, and following with laser ablation. The matrix contains certain organic molecules that absorbed strongly at the laser wavelength. Upon drying with the sample molecules are surrounded by matrix molecules so that each sample molecule is completely isolated from one another. The second step includes irradiation by a laser over a short time interval that causes ablation of a portion of the crystal and desolvation in the gas phase under vacuum. On the surface of the matrix crystal, the matrix molecules absorb the energy from laser irradiation, then transfer it to sample molecules. After that, they go together to the gas phase, where the desolvation happens. Protonated or cationized as well as negative ions are extracted as arranged and focused into the flight tube.

Although MALDI has been successfully used for ionization of various sample types, such as proteins, polymers and N-, O-linked glycans, it has not yet been widely applied to the analysis of highly negatively charged acidic glycans such as GAGs. The major limitations of this technology includes the low extent of desorption induced by the laser for GAGs containing many acidic groups and the facile loss of sulfate groups in the MALDI source. A few attempts to explore MALDI analysis of GAGs have emerged over the past two decades. In general, there have been two strategies. One is coupling the negatively charged GAGs with a positively charge polypeptides (Juhasz and Biemann 1994, Juhasz and Biemann 1995, Venkataraman, Shriver et al. 1999). Stronger signals have also been obtained by formation of non-covalent ionic complexes between the highly acidic heparin oligosaccharides and basic polypeptides. The heparin oligosaccharides were detected as ionic complexes in positive mode where up to hexadecasaccharides were detected at low or sub-picomole level.

The other strategy applies ionic liquid matrices (ILMs) instead of a conventional matrices (Laremore, Murugesan et al. 2006, Laremore, Zhang et al. 2007, Crank and Armstrong 2009, Przybylski, Gonnet et al. 2010). The utilization of these ionic liquids (ILs) was first introduced by Armstrong et al. (Armstrong, Zhang et al. 2001), which have shown many advantages over others commonly used. Liquid matrices produce a more homogeneous solution and better shot to shot reproducibility, but higher volatility results in uncontrolled matrix. Solid matrices usually have low vapor pressure and inherent chromophores, but lead to considerable heterogeneity and poor reproducibility. In contrast, ionic liquid matrices combine the best properties of both liquid and solid matrices exhibiting higher degree of sample homogeneity with increases in signal response and improved quantification (Li and Gross 2004). The ionic liquid matrices (Laremore, Murugesan et al. 2006) made of 1-methylimidazolium- α -cyano-4-hydroxycinnamate and butylammonium 2,5-dihydroxybenzoate has been used for detection of several relatively simple highly sulfated oligosaccharides such as sucrose sulfate and Arixtra[®] where intact molecular ions were observed in both positive and negative mode. However, sulfo group losses were observed, thus lowering the detection sensitivity. The authors then looked into alternative ionic liquid (Laremore, Zhang et al. 2007) and examining with dermatan and chondroitin sulfate oligosaccharides, an improved ionic liquid matrix was found (bis-1,1,3,3-tetramethylguanidinium- α -cyano-4-hydroxycinnamate) which has shown lower fragmentation of sulfo groups. Around the same time, another group in UK optimized the conditions for heparin/HS oligosaccharides where deca-saccharides were detected carrying from 2 to 13 sulfo groups (Tissot, Gasiunas et al. 2007).

Recently, two new ionic liquid matrices made with 2-(4-hydroxyphenylazo)benzoic acid (HABA) and 1,1,3,3-tetramethylguanidine or spermine were evaluated for analysis of heparin/HS oligosaccharides (Przybylski, Gonnet et al. 2010). The experimental results indicated that HABA-based ILMs led to a decrease of sulfo loss, cation exchange and a corresponding increase of signal-to-noise ratio.

1.5.2.2 Electrospray ionization mass spectrometry

Electrospray ionization (ESI) is a soft ionization method. Its development was awarded the Nobel Prize in chemistry to John B. Fenn. Electrospray ionization can transfer ions in solution into the gas phase in a small vacuum chamber that charges analytes as they pass from a charged needle tip and desolvated at the reduced pressure. Ions produced can be multiply charged especially for large biomolecules like proteins or peptides which have several ionizable sites. These large supramolecules are polar, non-volatile and thermally labile. The multiple charging characteristic of ESI makes the resulting mass-to-charge ratios fall in the mass ranges of all common mass analyzers. Improved sensitivity has been achieved by nano electrospray using a much lower flow rate (20–50 nL/min) compared to normal ESI (typically 1–20 μ L/min) (Banerjee and Mazumdar 2012).

Electrospray ionization has proven to be the most effective for MS analysis of GAGs with little or no in-source fragmentation of the labile sulfate groups. And negative mode ESI is commonly used owing to the high acidic nature of GAGs. ESI produces multiply charged precursor ions which allow tandem mass spectra to be acquired for compositional analysis (Naggar, Costello et al. 2004, Kailemia, Li et al. 2012).

Another Nobel Prize in physics was awarded to Hans Dehmelt and Wolfgang Paul for the development of principles leading to the ion trap technique. This instrument allows for repeated isolation of fragmentation by activation and re-analyses of product ions. Collision induced dissociation (CID) is the activation process that produces fragment ions and then scans the products to generate mass spectra sequentially (MS^n). Detailed structural information can be acquired by interpretation of fragment pathway of disassembly. This is a most effective technique for obtaining structural detail so critically important in glycans. The electrospray produces mainly molecular ions with little structural detail, however, the introduction of a collision gas induces a way to fragment a gas phase ion over multiple stages (MS^n) providing an opportunity to disassemble precursor structures to smaller known components.

1.5.3 Alternative approaches

1.5.3.1 Capillary electrophoresis mass spectrometry

Capillary electrophoresis is a useful analytical tool for the characterization of carbohydrates. When CE is used in combination with MS detection, the most common mode is capillary zone electrophoresis (CZE). This instrument combines the high separation efficiency of CE with the selectivity of MS. Hence, it has great potential as a supporting platform for structural analysis of heparin, structural detail must be left to MS^n . In a CZE separation, the capillary is generally filled with a background electrolyte and the separation is based on the electrophoretic mobility differences. The inner surface of a capillary is smooth, nonporous and lined up with silanol groups. It is generally agreed that there are 4-5 silanol groups/nm² on the capillary surface (Iler 1979). There are at least three types of ionizing

silanol groups present at the capillary wall: isolated, vicinal and geminal silanols. The pKa of ionizing silanol groups ranges between 2 and 9. When the pH is above 2, the silanol groups tend to dissociate protons and form a negatively charged surface and it is highly negatively charged at pH or above 5 (Chiari 1996). An electric double layer is formed between negatively charged capillary inner surface and buffer. Under an applied potential field, electroosmotic flow is generated. CE separations based on differences in electrophoretic mobility take advantage of EOF. Because this force influences the migration velocity of analytes to the same extent and it is independent of their properties. An alternative mode of CE like frontal analysis capillary electrophoresis (Fermas, Gonnet et al. 2007) has been reported for coupling with MS as well. Capillary electrophoresis mass spectrometry has been used for separation of heparin-derived disaccharides as well as oligosaccharides (Rhombert, Ernst et al. 1998, Duteil, Gareil et al. 1999, Ruiz-Calero, Moyano et al. 2001, Gunay and Linhardt 2003, Fermas, Gonnet et al. 2007). On-line coupling of CE to MS was first introduced by Duteil et al. using ammonium acetate, which is a MS compatible buffer. In state of the art, only limited amount of CEMS applications has been reported. Because it requires for special cautions to interfere with MS, further development is needed for capillary electrophoresis separation.

1.5.3.2 Fluorophore-assisted carbohydrate electrophoresis

Fluorophore-assisted carbohydrate electrophoresis (FACE) is a simple, fast and versatile technique for quantification and quantitation of glycosaminoglycans (Calabro, Midura et al. 2001, Oonuki, Yoshida et al. 2005, Buzzega, Maccari et al. 2008). Two fluorescent dyes are commonly used in FACE, 8-aminonaphthalene-1,3,6-trisulfonic acid disodium salt (ANTS) and 2-aminoacridone (AMAC). The anionic fluorescent dye ANTS-

labeled derived heparin fractions migrate in the order of chain length, which allows for evaluation of their molecular weights. The nonionic fluorescent dye AMAC-labeled heparin derived disaccharides have shown unique electrophoretic migration pattern on the FACE gel, thus it can be used to profile heparan sulfate disaccharides from unknown samples.

1.5.3.3 Nuclear magnetic resonance spectroscopy

Nuclear magnetic resonance spectroscopy (NMR) has been used as effective tool for characterization of heparin (Pervin, Gallo et al. 1995, Mikhailov, Linhardt et al. 1997). It can provide structural elucidation of heparin such as monosaccharide composition, glycosidic linkage, and sulfonation patterns. In addition, NMR spectroscopy is also useful for directly quantifying the iduronic and glucuronic acid content of heparin. However, the limitation of NMR analysis of heparin is its requirement of a relatively large amount of pure material. Thus it is not suitable for analysis of heparin produced by small biological samples. Sample purity is an important factor for structural determination by NMR spectra. A purity, which is greater than 80% to 90%, is generally required to ensure correct data interpretation. As a consequence, it is more difficult to distinguish positional isomers of heparin within the same sample.

CHAPTER 2

RESEARCH OBJECTIVES AND SPECIFIC AIMS

2.1 Motivation for understanding GAG structures

Both free GAGs and their complexes with proteins are widely known as components of different cells, tissues and organs. They contribute to a wide variety of biological processes and heparin is the most complex GAGs. Almost a century has passed since heparin's discovery in 1916 (Barrowcliffe 2012), but understanding its fine structure still remains to be a challenge for analytical chemists. Heparin is a highly anionic, polydispersed biopolymer with variations in sulfation and hexuronic acid epimerization. The acidity and isomeric properties of heparin makes its structural characterization very difficult to comprehensively unravel. However, investigation of heparin's fine structure is needed to improve our understanding of its biological role.

In 2008, an international healthcare crisis caused by heparin contamination resulted in approximately 100 deaths in the U.S. along with thousands of patients affected. According to capillary electrophoresis and proton NMR analysis (Liu, Zhang et al. 2009), the source of the major contaminant was caused by a highly sulfated "heparin-like" compound. Further investigations found that this heparin was contaminated by oversulfated chondroitin sulfate (OSCS) which was a semisynthetic biopolymer produced via sulfonation of chondroitin

sulfate and provided as a substitute of heparin. Given the structural differences of OSCS, traditional screening tests of pharmaceutical grade heparin could not distinguish the differences.

Current production of commercial-grade heparin is limited to animal sources. The inherent variability of animals, including diet and breed does have an influence on structural details(Liu, Zhang et al. 2009, Zhang, Yang et al. 2011). Hence, additional variations have been added to an already complex structure. Chemical synthesis is generally considered as an alternative approach for preparing heparin from non-animal sources. This led to the introduction of Arixtra[®], a synthetic heparin pentasaccharide drug which mimics the ATIII binding site of heparin. Chemical synthesis of other heparin oligosaccharides is still under investigation.

The biological significance and pharmaceutical use of heparin needs a more exacting and comprehensive understanding of structure. The quality and safety of such drugs are crucial to patients. Therefore, more efficient analytical research strategies should be considered for structural determination of heparin and its analogs at a molecular level.

2.1.1 Limitations of current structural characterization protocols

Due to the structural diversity and chemical instability of its sulfate esters and amides, heparin is difficult to directly characterize intact. Moreover, positional isomers and hexuronic acid epimers add additional challenges. To reduce this complexity, intact heparin is often depolymerized chemically or enzymatically to smaller oligosaccharides proceeding structural analysis. These product oligosaccharides are isolated by size, charge or polarity. As discussed in Section 1.5.1, modern liquid chromatography has been intensively explored for

the separation of heparin and HS derived oligosaccharides. However, at this point, no information has been reported on structural details.

Mass spectrometry and NMR are both useful methods for structural characterization of individual oligosaccharide after separation as they are sensitive to minor structural differences at molecular level. Although NMR is more salt tolerant than MS, it requires a greater sample amounts and purity is essential to avoid false structural conclusions. Also, interpretation of NMR spectra usually requires molecular weight and fragmentation information gathered by MS. On the other hand, MS suffers from loss of sulfo groups during ionization process, formation of a variety of salt adducts, and sophisticated data interpretation generated from the tandem MS spectra. In addition, hyphenated techniques, such as IP-RP-LC-MS/MS and HPLC-NMR, have great potential to improve the efficiency of structural characterization of heparin- and HS- derived oligosaccharides in complex mixtures.

2.1.2 MSⁿ introducing a new sequencing strategy

MS profiles can be used to obtain molecular weight information based on mass-to-charge ratios. Activation of these ions by collision and detailing products repetitively (MSⁿ) introduces a sequencing strategy most successful for glycans of protein and lipids (Ashline, Hanneman et al. 2014, Ashline, Yu et al. 2014). The application of such technology to heparins could proceed along the same lines by preparing suitable derivatives at marker locations. Assuming success with this chemistry, the details of heparin's fine structure would be resolved. Thus, sequential mass spectrometry (MSⁿ) using electrospray ion-trap instrumentation offers steps of activation and dissociation coupled with repeated isolation and detection. Methylation prior to analysis leads to increases in signal and cross-ring

cleavages upon collisional disassembly. MSⁿ creates a tractable pathway to pursue these structural details and has been successfully applied for the determination of structural isomers of N-linked and O-linked glycans in our Glycomics Center. Given these points, complete understanding of heparin oligosaccharide structures could be accomplishable through MSⁿ, if the labile sulfate esters and amides can be bench marked. Consequently, modifications of native heparin oligosaccharide have to be considered to make it suitable for MSⁿ analysis.

A recent study (Huang, Pomin et al. 2011) of structural characterization of chondroitin sulfate oligosaccharides has utilized LC-MSⁿ analysis to resolve isomeric structures. As a follow-up study, the authors applied a sequential chemical derivatization strategy involving permethylation, desulfation, and trideuteroperacetylation to heparin/heparan sulfate-like oligosaccharides (Huang, Liu et al. 2013). To date, MSⁿ has not yet been applied to structural characterization to heparin oligomers.

2.1.3 Research strategies

Permethylation plays an important role in preparing samples for MS analysis. Complete methylation provides a sample for easy clean-up, focuses fragmentation and provides enhanced precursor and product ion sensitivity. Permethylation of most glycans is easily carried out in dimethyl sulfoxide (DMSO) with sodium hydroxide and iodomethane. But heparin, contains O- and N- sulfo groups adding considerable polarity that results in limited solubility in DMSO.

To circumvent this, a dual permethylation strategy was initiated. Specifically, native heparin-derived disaccharides or oligosaccharides were permethylated with methyl iodide,

followed by removal of sulfo groups, then permethylated with deuterated methyl iodide. In consequence, an isotopic label is landed on the position where used to be a sulfo group. At this point, all the sulfo groups have been removed to make it no longer the issue of ionization process in mass spectrometer. The removal of negatively charged sulfo groups also enables MSⁿ analysis in positive ion mode.

In this application, the sulfo groups are removed by solvolytic desulfation after permethylation, which removes both N- and O-sulfates. The free amine group in glucosamine residue is generated during desulfation as shown in Figure 2-1. Acetylation is performed to prevent its conversion to quaternary amine during the second permethylation. The quaternary amine carrying a permanent positive charge behaves quite differently from the salt adducted species during MSⁿ fragmentation, increasing the difficulty of spectra interpretation.

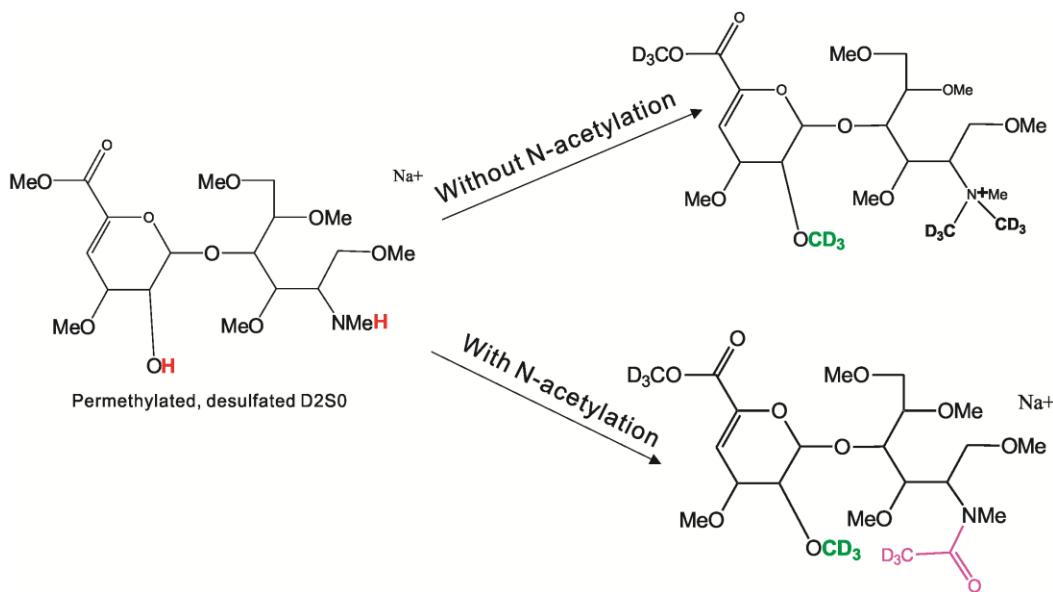


Figure 2-1 Chemical derivatization with/without N-acetylation.

In order to preserve the isotopic labeling, acetylation is carried out with acetic anhydride-*d*₆. However, this step inevitably puts acetyl groups onto hydroxyl groups, but

O-acetylated groups are easily ruptured during CID process, making it always the most abundant in tandem MS spectra. Given that, a second permethylation with deuterated methyl iodide is performed after acetylation to replace O-acetyl groups with deuterio methyl groups, but leaving N-acetyl group untouched. Eventually, O-sulfates are converted to deuterio methyl groups (-OCD₃), while N-sulfates are converted to N-acetyl-*d*₃ groups (-NCOOCD₃). MSⁿ analysis is performed with dual-permethylated products to determine the fine structure.

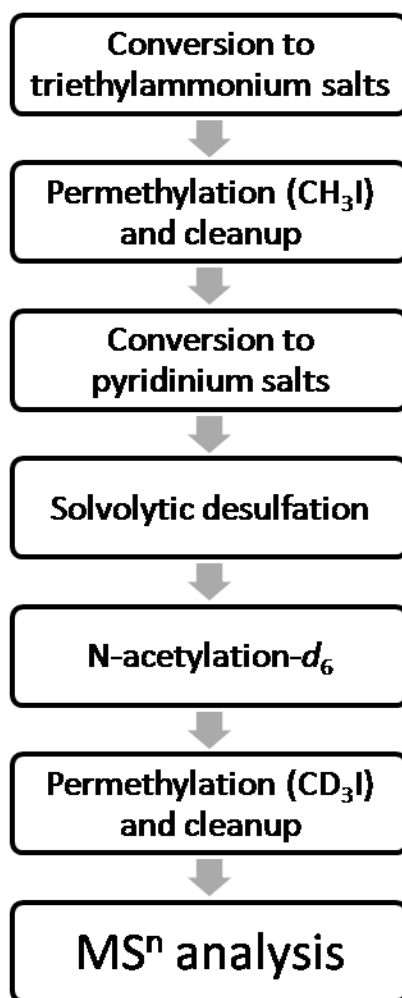


Figure 2-2 Experimental workflow of dual permethylation.

To summarize, as shown in Figure 2-2, native sulfated glycans are converted to triethylammonium salts through a cation exchange column to make them soluble in DMSO.

After permethylation with iodomethane and cleanup, permethylated glycans are passed through another cation exchange column followed by addition of pyridine. Solvolytic desulfation of their pyridinium salts are carried out in solution (10% methanol in DMSO) under heat. Desulfated glycans are N-acetylated to protect amine groups. Finally, deuterio-permethylation is performed. At this point, samples are ready for MSⁿ analysis.

The goal of this unique derivatization approach is to capitalize on the advantages of permethylation and mass spectrometry to provide a novel heparin analog for structural analysis. This workflow has been successfully applied to many heparin disaccharide standards, then, challenged with a heparin pentasaccharide synthetic standard. Once a universal protocol has been established, current effort is to seek comparable materials at increasing molecular weights.

2.2 Specific Aims

Aim 1: Dual permethylation of heparin/heparan sulfate disaccharide standards

As an important step in this chemical derivatization, permethylation was carefully investigated with a series of HS disaccharide standards. These standards possessed four major functional groups - carboxylic, hydroxyl, O-sulfo and N-sulfo group. Permethylation was first performed on the simplest HS disaccharide standard, D0A0 (Δ UA-GlcNAc), a non-sulfated HS disaccharide. After that, permethylation was performed on mono-O-sulfated HS disaccharide standards, D2A0 (Δ UA2S-GlcNAc) and D0A6 (Δ UA-GlcNAc6S), followed by di-O-sulfated HS disaccharide standard, D2A6 (Δ UA2S-GlcNAc6S). Lastly, the chemical derivatization protocol was examined with both N,O-sulfated HS disaccharide standard D2S0 (Δ UA2S-GlcNS). Refer to Figure 3-1 for chemical structures of HS disaccharides.

Similarly, desulfation conditions were studied with mono-O-sulfated HS disaccharide standards (D2A0 and D0A6), then di-O-sulfated HS disaccharide (D2A6) and finally N,O-sulfated HS standard (D2S0). Both methanolic and solvolytic desulfations were performed, and the latter was proven to be a better method with reduced degradation and by-products. Acetylation was only performed on disaccharides with N-sulfo group.

Dual permethylation was successfully applied to D2A0, D0A6, D2A6 and D2S0. Each step of the experimental workflow was checked by MS before processing to the next step. The product was confirmed by its molecular weight and MS² spectra. Reversed-phase liquid chromatography (RPLC) separation coupled to MS was selectively performed to clean up reaction mixture after N-acetylation or the second permethylation. Additionally, UV detection at 232 nm was used at the same time to provide orthogonal validation of the products. At last, MSⁿ analysis was performed with dual-permethylated products to confirm the details of structure.

Aim 2: Dual permethylation of Arixtra[®]

With the standard HS disaccharides conditions established, dual permethylation was applied to Arixtra[®], a synthetic heparin pentasaccharide (GlcNAc/NS6S → GlcA → GlcNS3S,6S → IdoA2S → GlcNS6S). Arixtra[®] will be referred to as Arixtra in the subsequent text.

Unlike the disaccharides, Arixtra reserves uronic acid epimerization. It has eight sulfo groups, three N-sulfo groups and five O-sulfo groups including a very rare 3-O-sulfo group. It was been taken for granted that it should be similar to perform dual permethylation on Arixtra. However, the increasing number of sulfo groups makes it much more anionic and

acidic comparing to disaccharides, thus working with Arixtra requires a different methodology. Consequently, protocols have been adjusted to the synthetic Arixtra.

One of the challenges was to determine how to monitor the intermediate steps of the multistep chemical derivatization (refer to Figure 4-3 and Figure 4-4 in Chapter 4). Negative-ion MS spectra of native Arixtra were very complicated, largely due to the sulfo groups. In contrast to HS disaccharides, Arixtra does not contain unsaturated bond or a reducible hemiacetal terminus for reducing end fluorescence labeling. Under these circumstances, validation of each step was limited to LCMS to determine the yield of full permethylated products. Ion-pair reversed-phase liquid chromatography mass spectrometry using pentylamine in conjunction with acetic acid was performed for the separation of the reaction mixture after first permethylation. The products were observed as their pentylammonium adducts in negative ion mode.

Solvolytic desulfation was carried out after permethylation and initially incomplete desulfation was observed with one additional sulfate. Permethylated maltopentose or beta-cyclodextrin were used as an internal standard during desulfation time study. The products were confirmed by molecular weights and MSⁿ spectra. Percentage of complete desulfation was calculated based on the relative intensity to internal standard in MS profile and products of N-acetylation and deuterio-permethylation were checked by MS as well. The tractable changes of m/z values provided solid evidence of successful derivatization along experimental workflow.

Aim 3: MSⁿ analysis for confirmation of chemical structure of Arixtra[®]

MSⁿ analysis was used to evaluate desulfation, N-acetylation and deuterio-permethylation which confirm the estimated products obtained and identify the by-products. All products were analyzed as sodium adducts in positive ion mode. Detailed assignments of fragmentation ions were included and presented in latter chapters.

Comparisons of mass shifts among derivatized Arixtra with differential isotopic labeling provide information to determine the numbers of N-sulfo and O-sulfo groups, while MSⁿ analysis of selected precursor ions provided structural confirmation of sulfation patterns.

Aim 4: An MSⁿ spectral library of dual permethylated Arixtra[®]

Longer term goals of this project will be to build an MSⁿ spectral library of dual-permethylated heparin disaccharides and oligosaccharides starting with Arixtra. The library will contain dual-permethylated heparin oligosaccharides as well as their MSⁿ fragment pathways and products. For instance, the library will be capable of identifying Arixtra from unknown samples by doing spectral matching. We judge this effort to be an effective approach for detailing heparin structures for both routine and high-throughput applications.

CHAPTER 3

DUAL PERMETHYLATION OF HEPARIN/HEPARAN SULFATE DISSACHARIDES

3.1 EXPERIMENTAL SECTION

3.1.1 Materials

Heparin/heparan sulfate disaccharide standards were purchased from V-laboratories, Inc.(Covington, LA) and were used without further purification. All other reagents were from Sigma-Aldrich (Milwaukee, WI, USA). C₁₈ Sep-Pak cartridges were from Waters (Franklin, MA, USA).

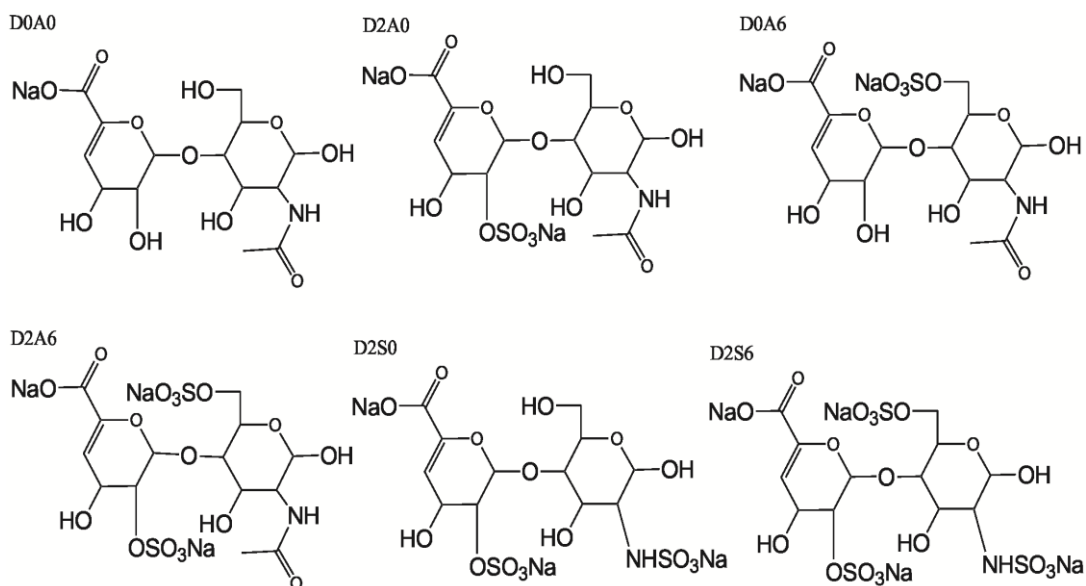


Figure 3-1 Chemical structures of heparin/heparan sulfate disaccharides.

Unsaturated heparin/heparan sulfate disaccharide standards are produced from enzymatic digestion and sold in form of their sodium salts. D0A0 is produced from heparin sulfate by digestion with heparinase III. D2A0 is the minor product of the action of heparinase II on heparin. D0A6 is the product of the action of heparinases II and III on heparin and heparin sulfate. D2A6 is the minor component produced from heparin by heparinase II. D2S0 is produced from heparin by digestion with heparinase I and II. D2S6 is the predominant disaccharide produced from heparin by heparinase I and II. The disaccharide standards are identified by HPLC with a certified purity of 95%, only D0A0 is confirmed by ^{13}C -NMR.

These native disaccharide standards are HPLC clean. However, direct infusion MS analysis of native standards showed presence of larger oligomers (Figure 3-19). The commonly used HPLC method to purify disaccharides from heparinases digested mixtures is strong anion exchange chromatography. This separation method is based on the charge density differences of the compounds. Thus, there is a possibility that disaccharide standard contains contaminants of the same charge density. But the trace amount of contaminants cannot be detected by UV. The presence of larger oligomers does not affect chemical derivatizations dramatically. However, it brings up the relative abundance of background ions especially under acidic conditions.

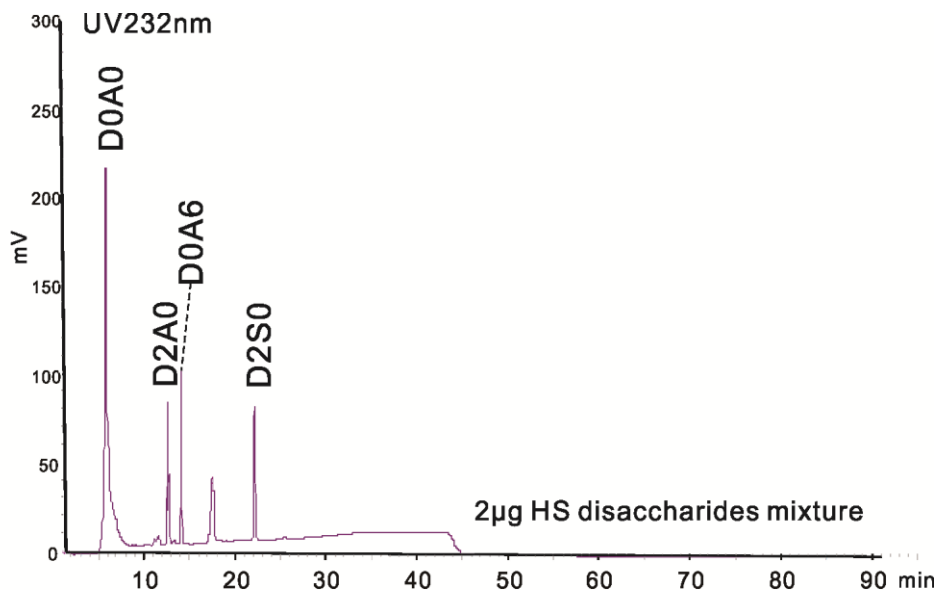


Figure 3-2 SAX chromatogram of underivatized heparin/HS disaccharides mixture.

A mixture of 2 µg heparin/heparan sulfate disaccharide standards was injected on a strong anion exchange column with UV detection at 232 nm.

3.1.2 Chemical derivatizations of heparin/heparan sulfate disaccharide standards

Reduction

The dried heparin/heparan sulfate disaccharide standard (25 µg – 50 µg) was reduced using 10mg/mL borane-ammonia in 28% ammonia/water, followed by cleanup and lyophilization.

To clarify, reduction is not a necessary step of dual permethylation. A saccharide containing reducing end undergoes mutarotation as it reaches equilibrium between its α - and β -forms. Consequently, this appears as wide or split peaks in chromatography. The purpose of reduction is to eliminate its α - and β -anomers.

Conversion to triethylammonium salts

To increase its solubility in dimethyl sulfoxide (DMSO), the reduced HS disaccharide was passed through a self-packed cation-exchange column with Dowex 50Wx8 resin to generate triethylammonium (TEA) salts. The ion exchange resin was pre-cleaned with 3M sodium hydroxide, 3M hydrochloric acid, water, and 5% acetic acid to keep it in hydrogen form. For the cleanup step after permethylation, the resin was additionally washed with 50% methanol/water prior to 5% acetic acid.

1st Permethylation (Iodomethane)

The dried TEA salts were completely dissolved in 200 μL of DMSO and 200 μL of anhydrous suspension of sodium hydroxide in DMSO (150 $\mu\text{g}/\mu\text{L}$), followed by 200 μL of iodomethane. The permethylation was performed at room temperature by vortex for 5 min, then sonication for 10 min. The reaction was quenched by adding 2mL of ion pairing buffer (100 mM triethylamine, pH adjusted to 7 by conc. acetic acid). The reaction mixture was sparged with nitrogen to remove excess iodomethane.

Cleanup after 1st Permethylation

The reaction mixture was applied to a cation-exchange column in triethylammonium form. Then the IE column was washed with 3 mL ion pairing buffer and the flow-through was collected. The flow-through was loaded onto a C₁₈ Sep-Pak cartridge, previously equilibrated with ion pairing buffer. The C₁₈ column was washed with 5 mL of the same ion pairing buffer and 2 mL of 5% acetonitrile/water (to get rid of excess TEA). The permethylated product was finally eluted with 5 mL of 50% methanol/water (v/v), followed by lyophilization.

Conversion to pyridinium salts

The dried permethylated product was completely dissolved in 200 μL of 50% methanol/water, then, loaded onto a cation-exchange column in H^+ form. The IE column was flushed with 5 mL of 50% methanol/water, then added 500 μL pyridine to the solution, followed by lyophilization.

Solvolytic desulfation

The dried pyridinium salts were re-suspended in 100 μL of 10% methanol/DMSO and incubated at 100 $^{\circ}\text{C}$ for 4 hours to remove the sulfate groups, followed by lyophilization. Desulfation of HS disaccharides with only O-sulfo groups was carried out at 80 $^{\circ}\text{C}$ for 3 hours.

N-acetylation

The dried desulfated product was re-suspended in 175 μL of pyridine and 25 μL of acetic anhydride or acetic anhydride- d_6 , then, incubated at 50 $^{\circ}\text{C}$ overnight, followed by lyophilization. This step was to prevent putting a permanent positive charge on free glucosamine (generated from desulfation) during the 2nd permethylation step.

Cleanup after N-acetylation

The dried product was re-suspended in 50 μL of 20% acetonitrile/water (v/v) for cleanup and LC-UV-MS/MS analysis. Fractions of completely desulfated, acetylated species were collected and dried for next step. Partially desulfated species were also collected if observable.

2nd permethylation (Iodomethane-*d*₃)

The 2nd permethylation was performed using spin column procedure, but instead of iodomethane, iodomethane-*d*₃ was used to replace acetyl groups on O-sulfo groups. A spin column (Harvard Apparatus) was packed with sodium hydroxide beads to about 3 cm depth. The packed column was rinsed with acetonitrile once, then DMSO twice. Sample was dissolved in 141.6 μL DMSO, 52.8 μL iodomethane-*d*₃ and 0.9 μL water. Then the mixture was applied to the column to react for 15 minutes. The reaction mixture was collected by spinning the column at 2000 rpm for 2 minutes. 70 μL DMSO and 26 μL iodomethane-*d*₃ was added to the sample tube, then, transferred to the spin column. Spin column at 2000 rpm for 2 minutes to collect all sample. After that, 60 μL iodomethane-*d*₃ was added to the reaction mixture and reapplied to the column to repeat the reaction for another 15 minutes. After reaction, the total reaction mixture was collected by spinning the column at 4000 rpm for 2 minutes. The mixture was transferred to a test tube containing one aliquot of chloroform and one aliquot of 10% acetic acid/water (v/v). At least 5 times water washes of the sample layer (organic layer) were performed during liquid-liquid extraction cleanup. The sample layer was dried for ESI-IT-MSⁿ analysis later.

The protocol is summarized in Figure 3-3.

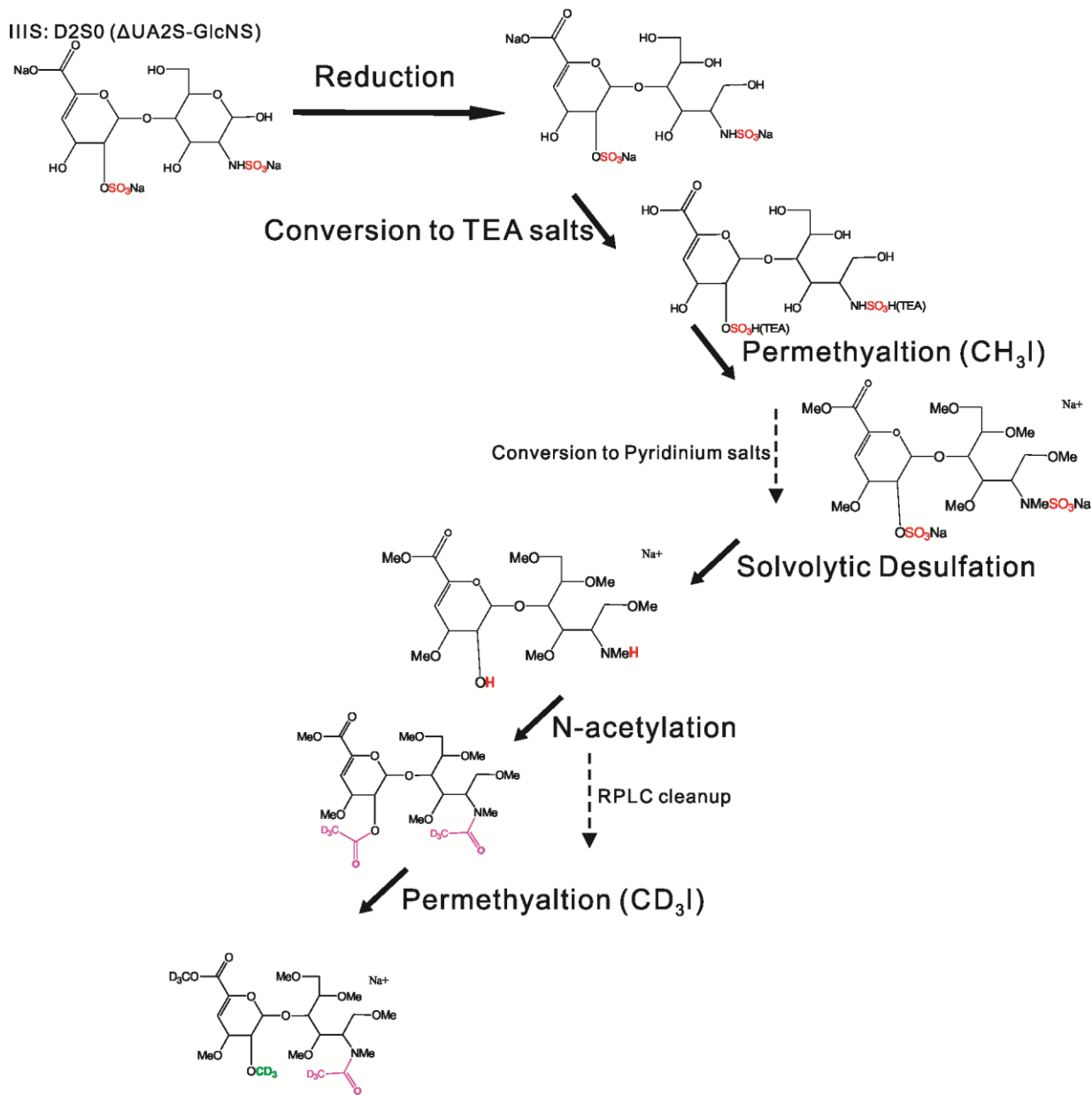


Figure 3-3 Experimental workflow of dual permethylation.

HS disaccharide standard D2S0 was used as a representative example to demonstrate the sequential chemical derivatizations. D2S0 has 2-O-sulfation at unsaturated uronic acid (ΔUA) residue and N-sulfation at glucosamine (GlcN) residue. After dual permethylation, O-sulfo group was replaced by deuterio-methyl group and N-sulfo group was replaced acetyl-D₃ group. The symbol Me represents methyl group. TEA is the abbreviation of triethylammonium.

3.1.3 Glycan analysis

Online LC-UV-MS/MS Analysis

Online reversed phase liquid chromatography (RPLC) separation was performed on a BDS HYPERSIL C₁₈ column (Thermo), 2.1mm x150 mm, 3 μm, with UV detection at 232 nm. Mobile phase A was 25 μM sodium acetate prepared with HPLC grade water. Mobile phase B was acetonitrile. A linear gradient of mobile phase B from 25% to 75% over 30 min was used, with a flow rate of 200 μL/min. Online positive ion MS profiles and MS/MS spectra were obtained from an LTQ (Thermo Fisher Scientific, Waltham, MA) equipped with an electrospray ion source. The capillary temperature was 300 °C. Spray voltage was 4.5 kV and the collision energy was set as 35 eV.

Offline MS and MSⁿ Analysis by Direct Infusion

The Thermo instrument was additionally equipped with a TriVersa Nanomate nanoelectrospray ion source (Advion, Ithaca, NY). Offline MS profiles and MS/MS spectra were obtained from this chip-based nanoESI interface by direct infusion. Samples were dissolved in 50% methanol/water (v/v).

Strong Anion Exchange Chromatography

SAX was performed on a Dionex ProPac PA1 column, 4.0 mm x 250 mm, with UV detection at 232 nm. Mobile phase A was HPLC grade water, pH 3.5 adjusted by concentrated hydrochloride acid (HCl). Mobile phase B was 2 M NaCl, pH 3.5 adjusted by HCl. A linear gradient of mobile phase B from 10% to 100% over 120 min was used, with a flow-rate of 1 mL/min.

3.2 RESULTS AND DISCUSSIONS

3.2.1 Permethylation of non-sulfated heparin/heparan sulfate disaccharide standard

D0A0 is the simplest form of HS disaccharide standard and it does not contain any sulfo groups. But it still has one unsaturated uronic acid residue that makes it an acidic compound. Permethylation of D0A0 was carried out through spin-column procedure and previously described in-solution procedure (NaOH PM). To point out that, because D0A0 does not contain any sulfo group, instead of adding TEA buffer, 10% acetic acid in water has been added after reaction. Saponification by-product is observed under both methods. Saponification is the hydrolysis of a carboxylic acid methyl ester under basic conditions and it happens at uronic acid residue. In Figure 3-4, m/z 516 and m/z 502 represented fully permethylated D0A0 and saponified D0A0, respectively. Comparing to spin-column permethylation, saponification product has reduced from 20% to 10%. This may be because sodium hydroxide beads packed spin column created a stronger basic environment than NaOH-DMSO solution.

In Figure 3-4, tandem MS spectra have confirmed the chemical structures of m/z 516 and m/z 502. Fragment m/z 372 and m/z 268 indicated that there was no underpermethylation on the glucosamine residue. Glycosidic cleavages generated Y-ion m/z 316 and Z-ion m/z 298. Presence of both ions in tandem MS spectra of m/z 516 and m/z 502 also suggested glucosamine residue was permethylated.

Fragment m/z 428 indicated permethylation on the unsaturated uronic acid residue. In the same way, m/z 414 suggested one less methyl group on the unsaturated uronic acid side. In agreement with m/z 372, the underpermethylation happened at carboxylic acid position.

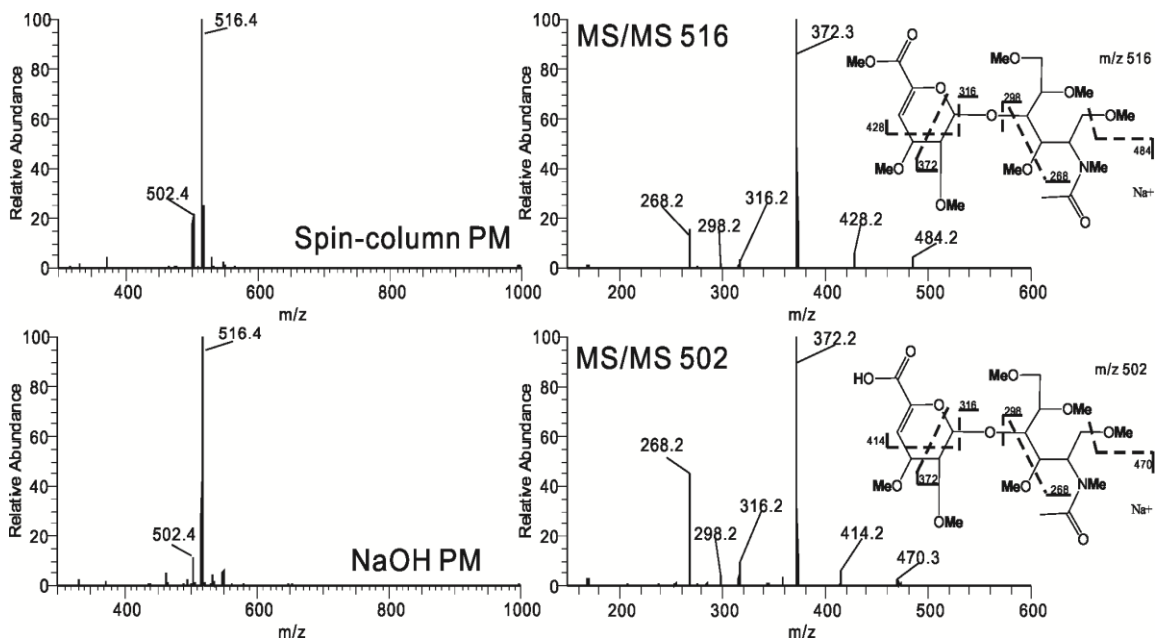


Figure 3-4 Permethylation of non-sulfated disaccharide D0A0.

Positive MS profiles were obtained from reduced D0A0 after spin-column permethylation and NaOH permethylation. Both permethylation product (m/z 516) and saponification by-product (m/z 502) have been observed. Tandem MS were performed on both ions to confirm proposed chemical structures. Fragment m/z 372, m/z 268, m/z 316 and m/z 298 indicate fully methylation of glucosamine residue. Fragment m/z 414 indicates underpermethylation on the uronic acid side. The fragmentation pattern suggests that m/z 502 is a saponification product, not an underpermethylation product.

3.2.2 Permethylation of sulfated heparin/heparan sulfate disaccharide standards

3.2.2.1 Dual permethylation of mono-O-sulfated heparin/heparan sulfate disaccharides

D2A0 and D0A6 were used as examples for investigation of dual permethylation protocols. They are structural isomers and have only one O-sulfo group. There is no N-sulfo group in either molecule. D2A0 has 2-O-sulfation at unsaturated uronic acid (Δ UA) residue while D0A6 has 6-O-sulfation at glucosamine (GlcN) residue. They are relatively simple

candidates for preliminary study of the sequential chemical derivatizations. Because there is no N-sulfation in this case, N-acetylation is excluded from sample preparations.

In Figure 3-5, HS disaccharide standards were observed as molecular ions in negative ion mode MS profile before derivatization and after the first permethylation when the structures still contains sulfo groups. Before removal of sulfo group, positive MS profiles of sulfated glycans are more complicated as a result of various sodium adducts. This leads to signal splitting thus reduces peak intensity. In addition, owing to the poor MS purity of HS disaccharide standards, negative ion MS profile is relatively cleaner than positive MS profile. Moreover, contaminant ions produced along sample preparation, mainly in lower mass range, greatly affected the relative abundance of product ions. As a consequence, contaminant ions became the dominated peaks in positive ion MS profile.

This is not a big issue with mono-O-sulfated HS disaccharide standards. However, as the number of sulfo groups increasing and the sulfonation pattern changing in the same time, positive MS profile is more challenging to elucidate than negative profile. Under these circumstances, MS profile of samples still containing sulfo groups is preferred to be shown in negative mode. MSⁿ analysis is focused on products after removal of sulfo groups.

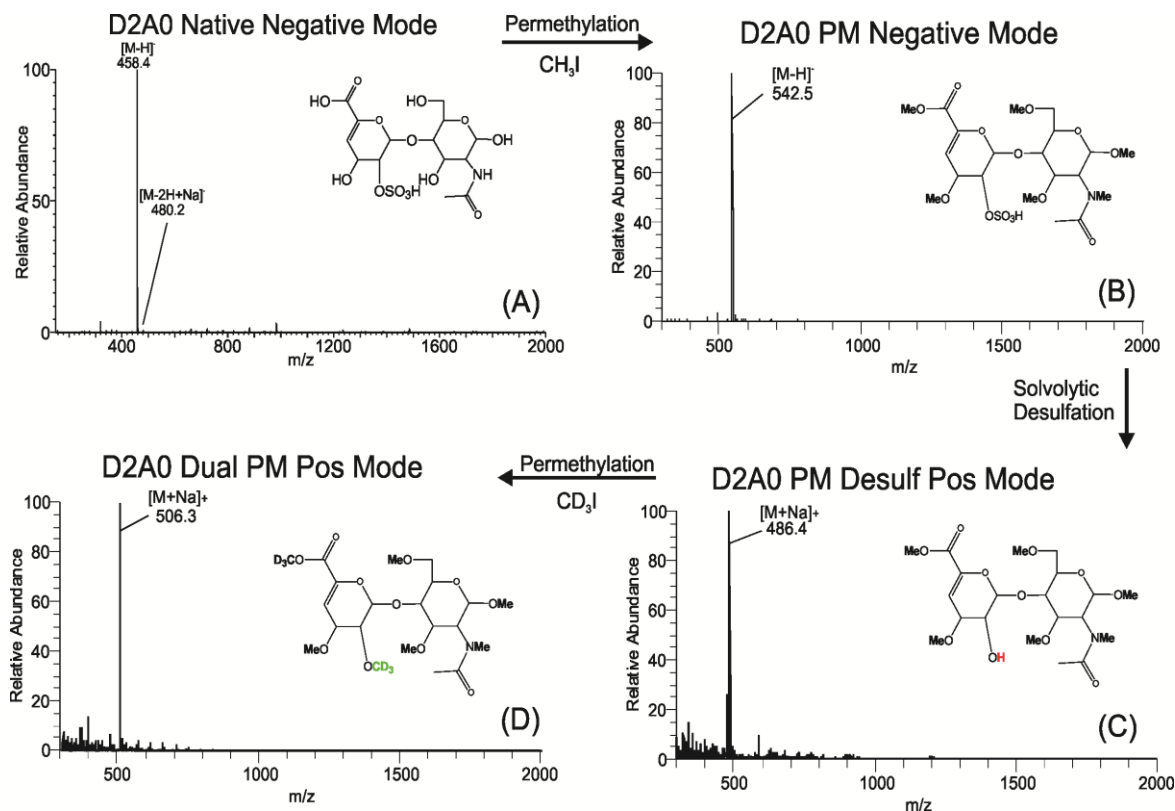


Figure 3-5 Dual permethylation of D2A0 at different stages of chemical derivatization.

Offline MS spectra and chemical structures of D2A0 at different stages of chemical derivatization. Each corresponding molecular ion is labeled. The arrows indicate the workflow of sample preparation. (A) Before chemical derivatization. In negative ion mode, m/z 458 represented native D2A0 without any sodium adducts. A sodiated D2A0 was observed in very low abundance; (B) After CH_3I permethylation, m/z 542 matched the structure shown in Figure 3-5 (B); (C) Solvolytic desulfation, m/z 486 matched the estimated structure; (D) After CD_3I permethylation, O-H group was replaced by O- CD_3 group.

MS analysis was performed at each stage of chemical derivatizations to target m/z values of predicted structures. Since D2A0 and D0A6 are structural isomers, in both positive and negative MS profiles, they were seen as the same molecular ions at the same stage. The targeted molecular ion was further fragmented to confirm the predicted structure. The complete MS characterization of D2A0 and D0A6 was summarized in Figure 3-5 and Figure 3-6, respectively.

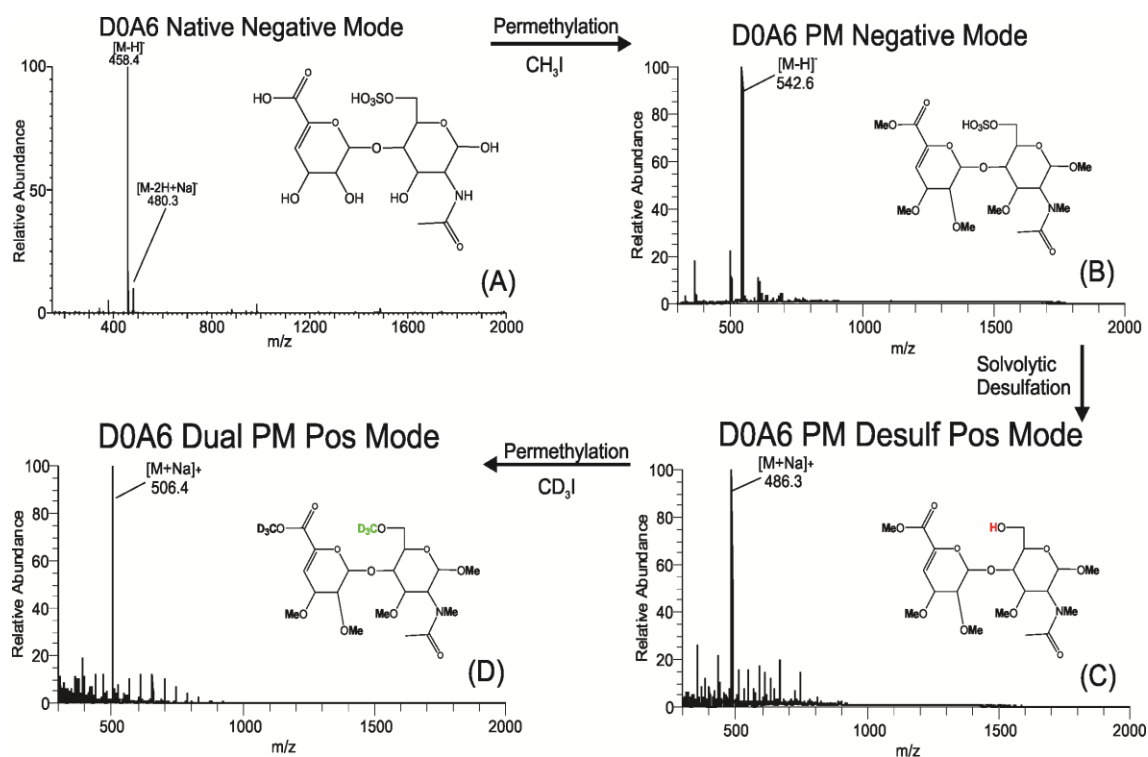


Figure 3- 6 Dual permethylation of D0A6 at different stages of chemical derivatization.

Offline MS spectra and chemical structures of D0A6 at different stages of chemical derivatization. Each corresponding molecular ion is labeled. (A) Before chemical derivatization. The D0A6 standard was purchased in form of its sodium salts. In negative ion mode, m/z 458 represented native D0A6 without any sodium adducts. A sodiated D0A6 was observed in relatively low abundance. (B) After CH_3I permethylation, m/z 542 matched the structure shown in Figure 3-5 (B). (C) Solvolytic desulfation, m/z 486 matched the estimated structure. (D) After CD_3I permethylation, O-H group was replaced by O- CD_3 group.

After MS characterization, MS^n analysis was performed on targeted m/z values to further confirm the predicted structures. Comparisons between D2A0 and D0A6 at stage of CH_3I permethylation, solvolytic desulfation and CD_3I permethylation were summarized in Figure 3-7, 3-8 and 3-9, respectively.

As mentioned previously, positive MS profile is well enough for simple HS disaccharide. In Figure 3-7, m/z 588 represented permethylated D2A0 and D0A6. Sulfo group was found to be sodiated in positive mode. At MS level, it is impossible to distinguish structural isomers.

Tandem MS spectra (Figure 3-7) of m/z 588 showed distinct patterns between D2A0 and D0A6. D2A0 displayed cleavage of the sulfo group (m/z 468), along with several cross-ring cleavages (m/z 412,436,444) in the uronic acid residue and different glycosidic cleavages (m/z 282,300,322). D2A0 has 2-O-sulfo group at unsaturated uronic acid residue resulting in loss of $-\text{OSO}_3\text{Na}$ as the major ion. This ion (m/z 468) was technically present but only at a negligible intensity in MS/MS spectrum of D0A6. This suggested that the 2-O-sulfo group in D2A0 seemed to be much more labile than 6-O-sulfo group in D0A6. In contrast, tandem MS spectrum of D0A6 was dominated by the (retro-Diels-Alder) 0,2-cleavage of the uronic acid (m/z 444), with another uronic acid cross-ring cleavage (m/z 500) and various glycosidic cleavages providing minor peaks (m/z 388). Note that most of the minor peaks were at negligible intensities in MS/MS spectrum of D0A6.

The MS³ and MS⁴ spectra (Figure 3-7) for the two species were quite distinct as well. There were signature ions for both species. However, assignments of these ions were tricky. Note the base peak (m/z 322) in D2A0 MS³ spectrum. The only explanation I can think of for this m/z 322 is if there was a glycosidic cleavage leaving the oxygen with the reducing end residue, and the oxygen picked up a sodium salt from the sodiated sulfo group, instead of a hydrogen. This would result in a species with the right mass (a Y-ion with a sodiated oxide at the 4-carbon instead of a hydroxyl group). This type of ions presented in tandem MS spectra of all other HS disaccharide standards I have worked with.

In the D0A6 MS³ spectrum (Figure 3-7), fragment m/z 340 was the major ion. This ion was observed in MS² spectrum as well but at a negligible level. I believed that this ion is generated by the indicated glycosidic cleavage (m/z 370, negligible in MS²) accompanied by the loss of a methoxyl group as CH₂O. This is another commonly seen fragmentation type in these samples, namely the loss of a methoxyl group or two along with another cleavage. The methoxyl groups can either leave as CH₂O or CH₃OH, giving rise to a peak either 30 m/z (CH₂O) or 32 m/z (CH₃OH) smaller than the peak corresponding to the other cleavage alone. The peak corresponding to the cleavage without the methoxyl loss can be present as well, as is the case here, but these 'extra methoxyl loss' peaks are often more intense than that for the 'normal' cleavage alone. This kind of methoxyl losses become very prominent in later, more derivatized samples. This kind of fragmentations was not commonly seen with larger glycan species, and it may be because collision energy used for these species (i.e. 35) is too high for molecules this small.

Although the assignments of ions in MS³ and MS⁴ spectra are less confidential, the structural elucidation is not counting on MSⁿ analysis of permethylated products. On the other hand, given the issues with disassembling sulfated species, removal of sulfo groups is reasonable to produce more tractable fragmentation pathways.

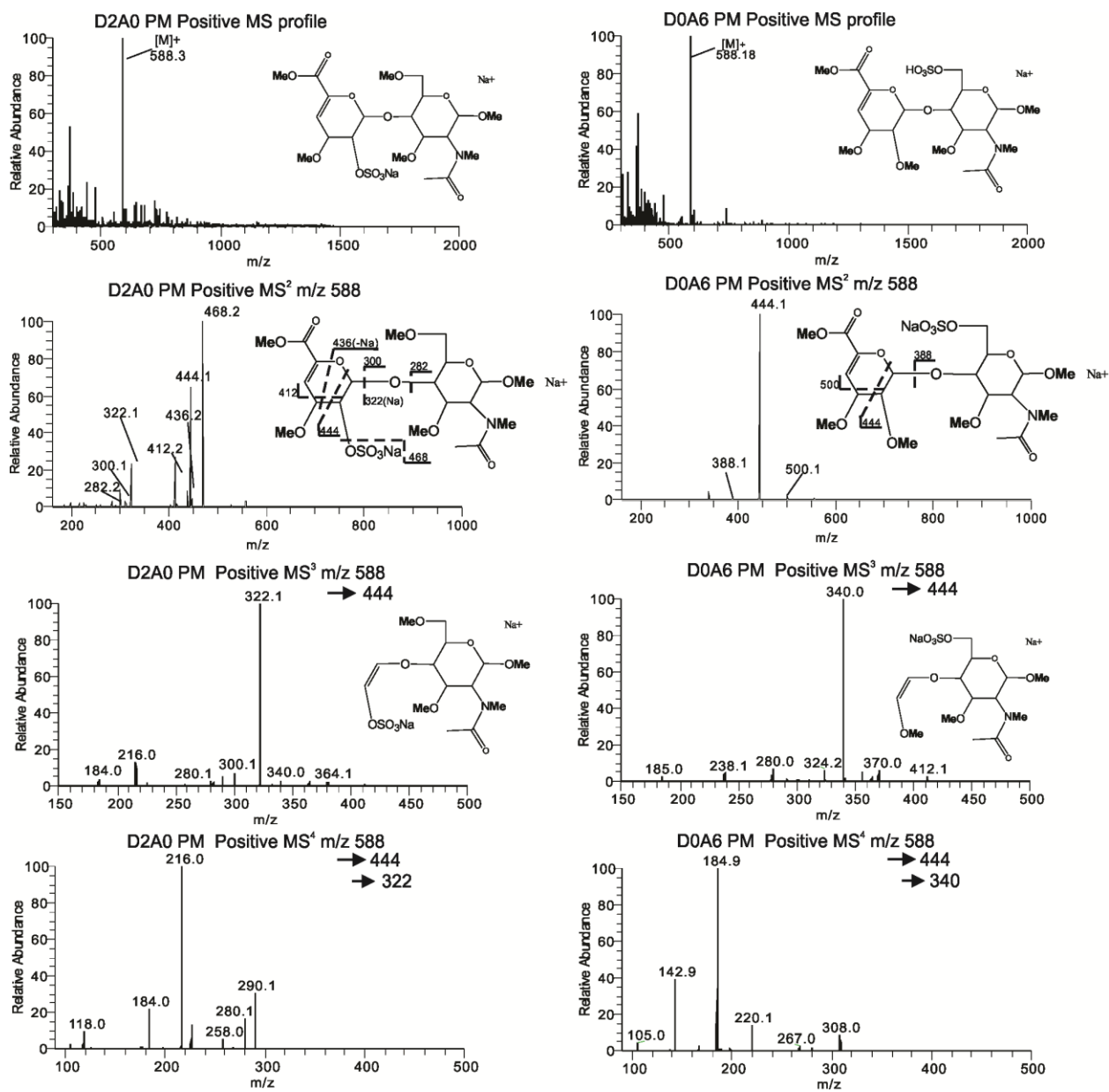


Figure 3-7 Positive ion MSⁿ spectra of permethylated mono-O-sulfated disaccharides.

Positive MS profiles and MSⁿ spectra were compared between for D2A0 and D0A6 after permethylation. D2A0 and D0A6 are structural isomers thus have the same m/z 588 in positive MS profile. D2A0 has 2-O-sulfo group at uronic acid residue while D0A6 has a 6-O-sulfo group at glucosamine residue. MSⁿ spectra of permethylated D2A0 and D0A6 are quite distinct. Notably, fragment m/z 468 generated by loss of sodiated sulfo group was absent in MS² spectrum of D0A6.

After removal of sulfo groups, the following steps are solvolytic desulfation and deuterio methylation. MS structural analysis was performed in positive mode for the last two steps. Comparisons of positive MSⁿ analysis between permethylated D2A0 and D0A6 are summarized in Figure 3-8.

The MS² spectra for both species were dominated by the 0,2-cross-ring cleavage (m/z 342) in the uronic acid residue, with a few other cross-ring and glycosidic cleavages present, as well. The only true signature ions for these species were here in MS², m/z 412 for D2A0 and m/z 398 for D0A6.

The MS³ spectra (Figure 3-8) for both species showed a glycosidic cleavage along with several cross-ring cleavages, and methoxyl loss peaks associated with both. In both species, the associated methoxyl loss peaks were the most intense in the spectra, and we saw several different numbers and combinations of losses. Note that the most intense methoxyl loss peak in both spectra was the one associated with the glycosidic cleavage that yielded a Z-type ion (so m/z 252 in the D2A0 spectrum was associated with m/z 282, and m/z 238 in the D0A6 spectrum was associated with m/z 268). This seems to be a general pattern, as it also appears in the deuterio methylated species.

These two species are hard to distinguish at the MS² level, although some of the smaller peaks like m/z 412 and m/z 398 make it possible. It is a little easier to differentiate the two based on the MS³ spectra, but much of the distinction is based on the differing intensity of peaks that are present for both species.

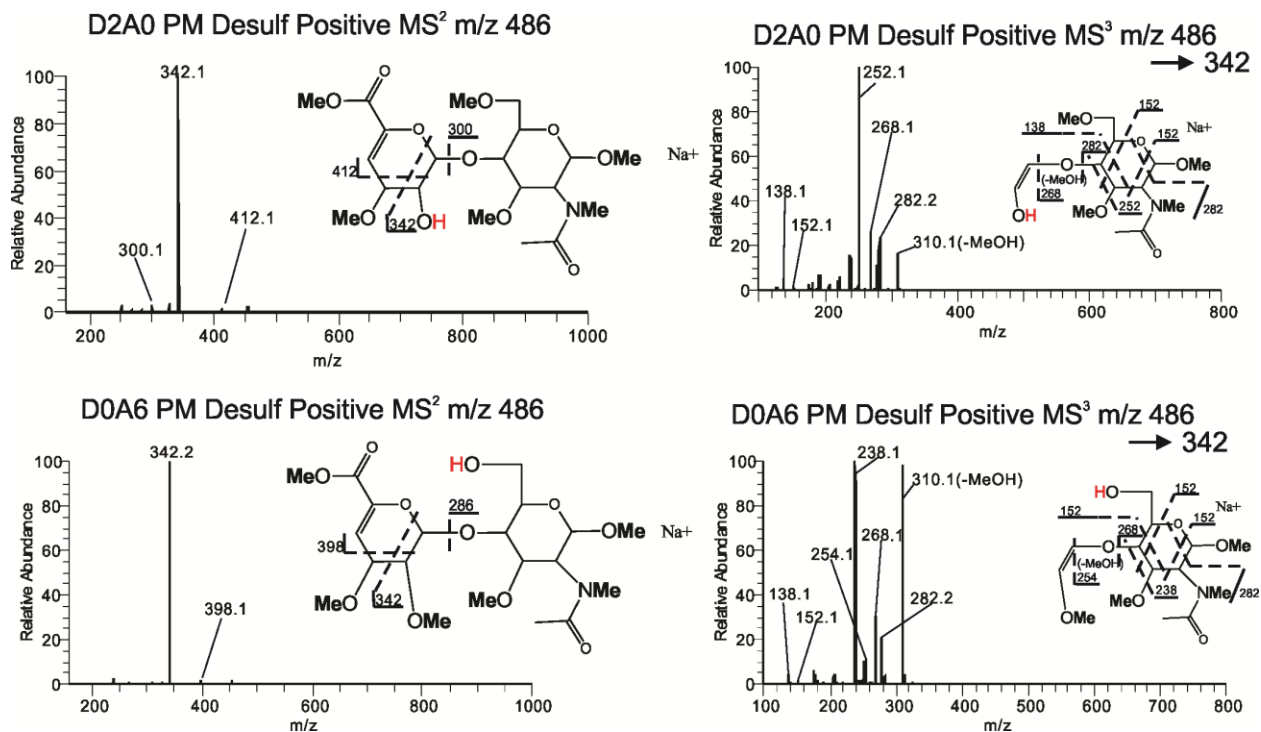


Figure 3-8 MSⁿ spectra of PM desulfated mono-O-sulfated heparin disaccharides.

Positive MSⁿ spectra were compared between for permethylated D2A0 and D0A6 after solvolytic desulfation. D2A0 and D0A6 are structural isomers thus have the same m/z 486 in positive MS profile. D2A0 has a 2-O-sulfo group at uronic acid residue while D0A6 has a 6-O-sulfo group at glucosamine residue. The dominated ion (m/z 342) in MS² spectra was 0,2-cross-ring cleavage in the uronic acid residue of two species. The signature ions are m/z 412, 300 for D2A0 and m/z 398 for D0A6. It was a little difficult to distinguish between D2A0 and D0A6 at the MS² level. The differences became clearer at MS³ level.

Comparisons of positive MSⁿ analysis between dual permethylated D2A0 and D0A6 are summarized in Figure 3-9. As in the earlier permethylated samples, one specific cross-ring cleavage (m/z 359) in the uronic acid residue dominated the MS² spectra for both species, with glycosidic cleavages and other uronic acid cross-ring cleavages present, as well. There were a few low-intensity signature ions present for the two species in the MS² spectra: m/z 300 and 415 are signatures for D2A0, and m/z 303 and 418 were signatures for D0A6.

At MS³ level in Figure 3-9, a number of cross-ring cleavages in the glucosamine residue were seen for both species, along with a number of fragments involving the loss of methoxyl groups. Note that the two species fragmented in the same places at both the MS² and MS³ levels. This is because the two molecules have essentially the same structure. The deuterio methyl group is very similar to a normal methyl group and does not appear to influence fragmentation.

Fragment m/z 327 presented loss of a methoxyl group are seen unambiguously in MS³ spectra (Figure 3-9) of both species. Fragment m/z 268 and m/z 271 in MS³ spectra were loss of a methoxyl group from Y-ions m/z 300 and m/z 303 in MS² spectra, respectively. In the same manner, fragment m/z 252 and m/z 255 were in MS³ spectra are loss of a methoxyl group from Z-ions m/z 282 and m/z 285 in MS² spectra, respectively. These offer clear differences between the D2A0 and D0A6 MS³ spectra.

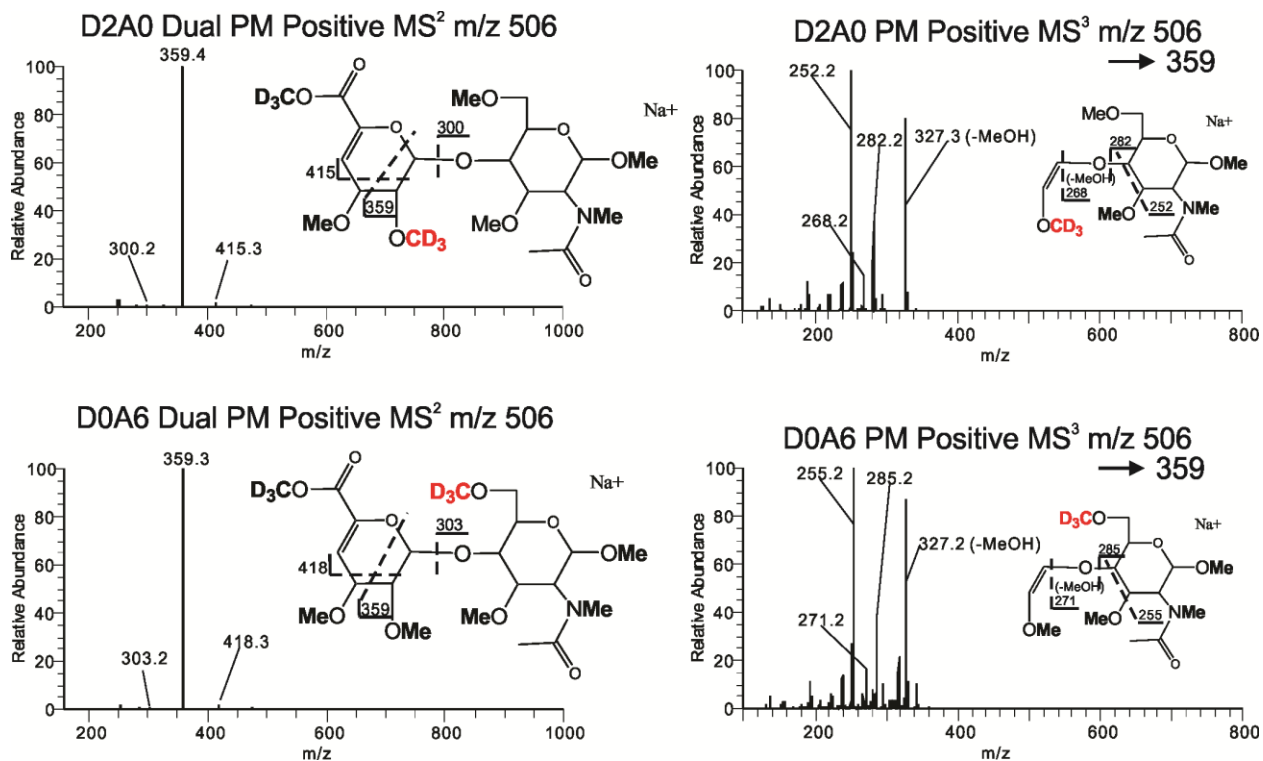


Figure 3-9 MSⁿ spectra of dual permethylated mono-O-sulfated heparin disaccharides.

Positive MSⁿ spectra were compared between for dual permethylated D2A0 and D0A6. D2A0 and D0A6 are structural isomers thus have the same m/z 506 in positive MS profile. D2A0 has a 2-O-sulfo group at uronic acid residue while D0A6 has a 6-O-sulfo group at glucosamine residue. The dominated ion (m/z 359) in MS² spectra was 0,2-cross-ring cleavage in the uronic acid residue of two species. The signature ions are m/z 415, 300 for D2A0 and m/z 418, 303 for D0A6. Similarly, it is a little difficult to distinguish between D2A0 and D0A6 at the MS² level. The differences became clearer at MS³ level.

To summarize, dual permethylation has been successfully applied to mono-O-sulfated heparin disaccharides standards. Since D2A0 and D0A6 are structural isomers, MSⁿ analysis of derivatized species shows ability to distinguish structural details of isobaric heparin disaccharides.

3.2.2.2 Dual permethylation of di-O-sulfated heparin/heparan sulfate disaccharide

After successful application of dual permethylation to mono-O-sulfated heparin disaccharides standards, di-O-sulfated heparin disaccharide standard D2A6 was used to test the established protocol. D2A6 has a 2-O-sulfo group at unsaturated uronic acid residue and a 6-O-sulfo group at glucosamine residue. Derivatized species was analyzed in negative ion mode before removal of sulfo groups while in positive ion mode after desulfation.

As the number of sulfo group increasing, MS profile appears to be more complicated with sulfated glycans. In negative mode MS profile (Figure 3-10), m/z 538 was the native D2A6. In addition, loss of sulfo group (m/z 458) and sodiated species (m/z 560, m/z 582) were observed. In Figure 3-10B, the dominated ion m/z 646 represented permethylated product of reduced D2A6 and one sulfo group picked up a sodium salt. Cleavage of a sodiated sulfo group was observed as ion m/z 544.

Solvolytic desulfation successfully removed two O-sulfo groups. After removal of sulfo groups, derivatized species were analyzed in positive ion mode (Figure 3-10C). The major ion m/z 488 matched the proposed structure. Note that m/z 456 was 32 Da less than m/z 488 which equaled to loss of MeOH. It's likely that this ion was produced from in-source fragmentation.

Deutero permethylation was carried out by spin-column procedure. The free hydroxyl groups generated from solvolytic desulfation were converted to deuteromethoxyl groups. The dominated ion m/z 525 (Figure 3-10) in positive MS profile represented this product. MSⁿ analysis of derivatized species will be discussed later.

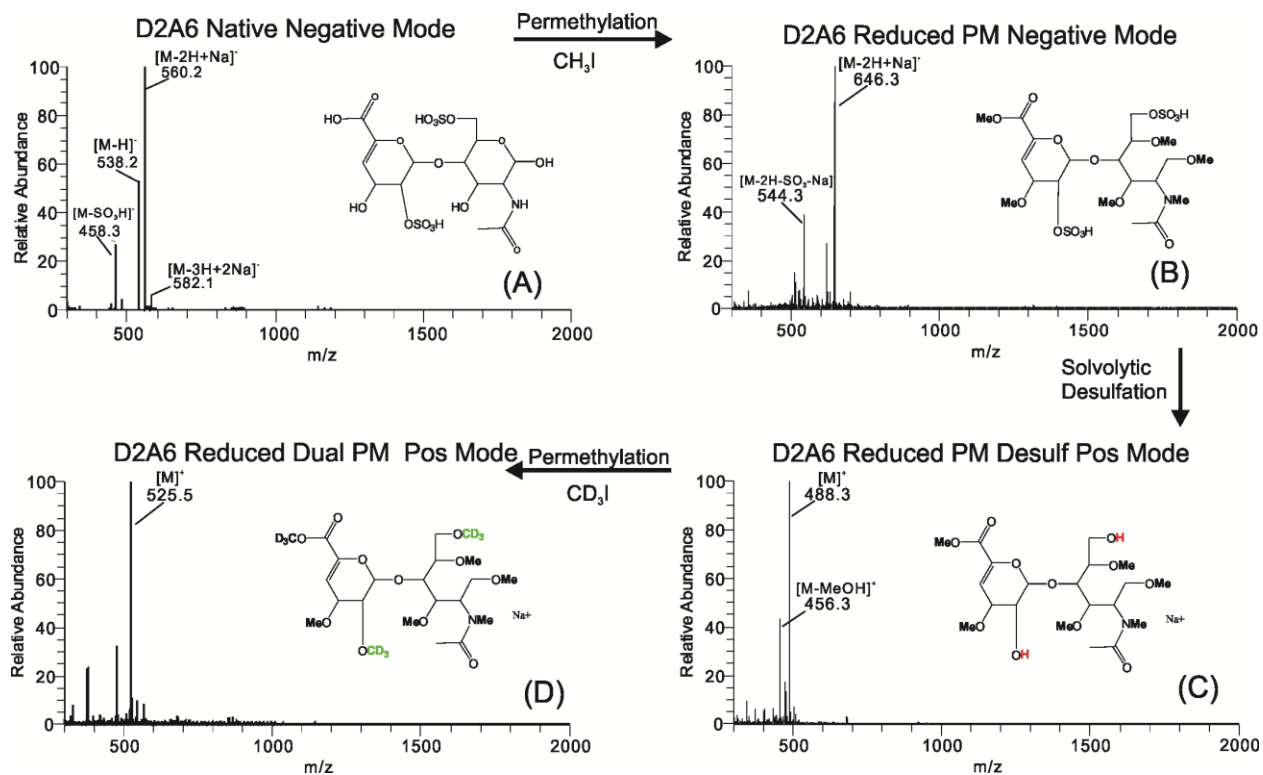


Figure 3-10 Dual PM of reduced D2A6 at different stages of chemical derivatization.

Offline MS spectra and chemical structures of reduced D2A6 at different stages of chemical derivatization. Each corresponding molecular ion is labeled. The arrows indicate the sequence of derivatization. (A) Before chemical derivatization. The D2A6 standard was purchased in form of its sodium salts. In negative ion mode, m/z 538, 560 and 582 represents native D2A6 with 0, 1 and 2 sodium, respectively. Loss of one sulfo group was observed from the ion (m/z 458) without any sodium adducts; (B) After CH₃I permethylation, m/z 646 matched the structure shown in Figure 3-10B with a sodiated sulfo group, m/z 544 indicated loss of a sulfo group; (C) Solvolytic desulfation, m/z 488 matched loss of two sulfo groups. (D) After CD₃I permethylation, O-H groups were replaced by O-CD₃ groups.

Positive tandem MS analysis (Figure 3-11) was performed on permethylated (m/z 692) and desulfated (m/z 488) species. MS² and MS³ analysis was applied to dual permethylated reduced D2A6.

In Figure 3-11, at MS² level, permethylated D2A6 (molecular ion m/z 692) displayed cleavage of the sodiated sulfo group (m/z 572), along with several cross-ring cleavages (m/z 516,548) at the uronic acid residue and different glycosidic cleavages (m/z 404,426,386). Recall from MS² spectra of D2A0 and D0A6 in Figure 3-7. D2A0 has 2-O-sulfo group on unsaturated uronic acid residue resulting in loss of -OSO₃Na as the major ion. D0A6 has 6-O-sulfo group on glucosamine residue resulting in 0,2-cleavage of the uronic acid as the major ion. This cleavage was the second abundant peak in D2A0 MS² spectra. Both cleavages were seen in permethylated D2A6 MS² spectra as the most abundant ions. Additional loss of sodiated sulfo group (m/z 470) was observed as well. The fragmentation pattern is very similar to D2A0 and D0A6.

The MS² spectrum (Figure 3-11) for desulfated D2A6 (molecular ion m/z 488) was dominated by the 0,2-cross-ring cleavage (m/z 344) in the uronic acid residue, with a few other cross-ring (m/z 414) and glycosidic cleavages (m/z 302, 284) were present as well.

After removal of sulfo groups, tandem MS spectra (Figure 3-11) of derivatized species have shown similar fragmentation patterns. The dominated ion was 0,2-cross-ring cleavage in the uronic acid residue (m/z 344). Other signature ions were X-ion from 1,3-cross-ring cleavage in the uronic acid residue (m/z 414), Y-ion (m/z 302), Z-ion (m/z 284) from glycosidic cleavages and ions from cleavages of CH₃OH (m/z 456).

In Figure 3-11 the dominated ion in MS² spectrum of dual permethylated D2A6 (molecular ion m/z 525) was the 0,2-cross-ring cleavage (m/z 378) at the uronic acid residue. Fragment m/z 434 was 1,3-cross-ring cleavage at the uronic acid residue. Fragment m/z 319 was the Y-ion from glycosidic cleavage. Fragment m/z 493 was loss of CH₃OH while fragment m/z 272 was cleavage of CH₃OH from Z-ion.

In the MS³ spectrum (Figure 3-11), fragment m/z 346 represented loss of a methoxyl group of dual permethylated D2A6 (molecular ion m/z 525). Fragment m/z 271 in MS³ spectrum was loss of a methoxyl group from Z-ion m/z 301. Fragment m/z 153 was 0,2-cross ring cleavage of glucosamine residue. Fragment m/z 172 was 0,2-cross ring cleavage of Z-ion m/z 301.

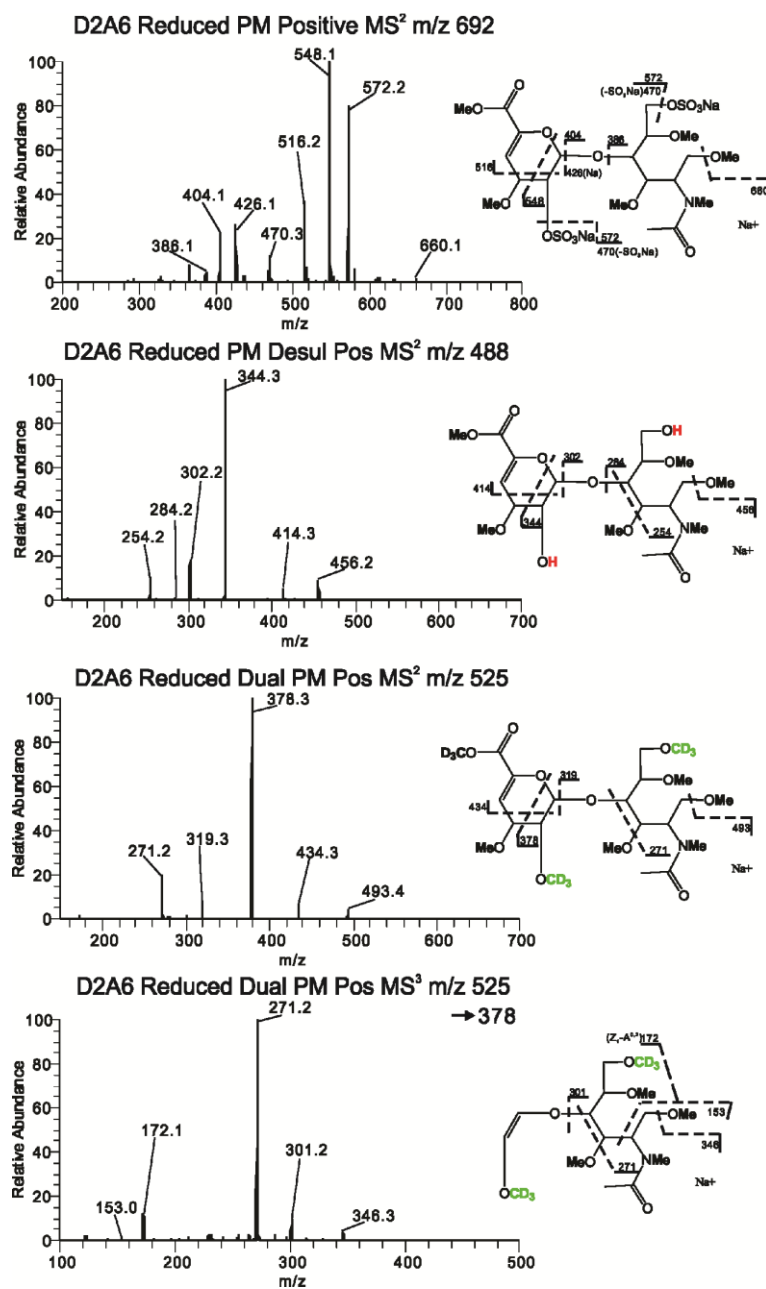


Figure 3-11 MSⁿ spectra of reduced dual permethylated D2A6.

Positive MSⁿ spectra of dual permethylated D2A6 at different stages of chemical derivatization. Each corresponding fragment ion is labeled. D2A6 has a 2-O-sulfo group at uronic acid residue and a 6-O-sulfo group at glucosamine residue. The dominated ion in MS² spectrum was 0,2-cross-ring cleavage in the uronic acid residue of derivatized species. MS³ analysis was performed on dual permethylated D2A6. The dominated ion m/z 271 was loss of a methoxyl group from Z-ion m/z 301.

3.2.2.3 Dual permethylation of O-, N-disulfated heparin/heparan sulfate disaccharide

D2S0 has a 2-O-sulfo group at unsaturated uronic acid residue and one N-sulfo group at glucosamine residue. Unlike O-sulfated heparin disaccharides, a free amino group is generated after solvolytic desulfation. Therefore, acetylation is performed prevent its conversion to quaternary amine after desulfation, prior to deuterio permethylation. Similarly, derivatized D2S0 species were analyzed in negative ion mode before removal of sulfo groups while in positive ion mode after desulfation.

In Figure 3-12, loss of sulfo group (m/z 416) and different sodium adductions were seen of reduced native D2S0 in negative mode MS profile. The dominated ion is m/z 496 which is not sodiated. In the next profile, the dominated ion m/z 618 represents permethylated product of reduced D2S0 and one sulfo group picked up a sodium salt. Cleavage of a sodiated sulfo group was observed as ion m/z 516. This pattern is in consistent with D2A6. Positive MS analysis of permethylated species is summarized in Figure 3-13.

Solvolytic desulfation successfully removed N- and O-sulfo groups with adjustments of reaction temperature and time. After removal of sulfo groups, acetylation with acetic anhydride was performed. The most intense peak of ion m/z 544 in Figure 3-12C matched the predicted structure. MS analysis of derivatized species after desulfation is summarized in Figure 3-14.

Acetylation was carried out using acetic anhydride- d_6 as well. This is to preserve the isotopic labeling to distinguish N-sulfo group. The O-acetyl group generated from acetylation

was converted to deuteromethoxyl group. The dominated ion m/z 522 in positive MS profile (Figure 3-12) represented this product. If acetic anhydride- d_6 was used, the dominated ion would be m/z 525. Comparison of their tandem MS spectra is shown in Figure 3-15.

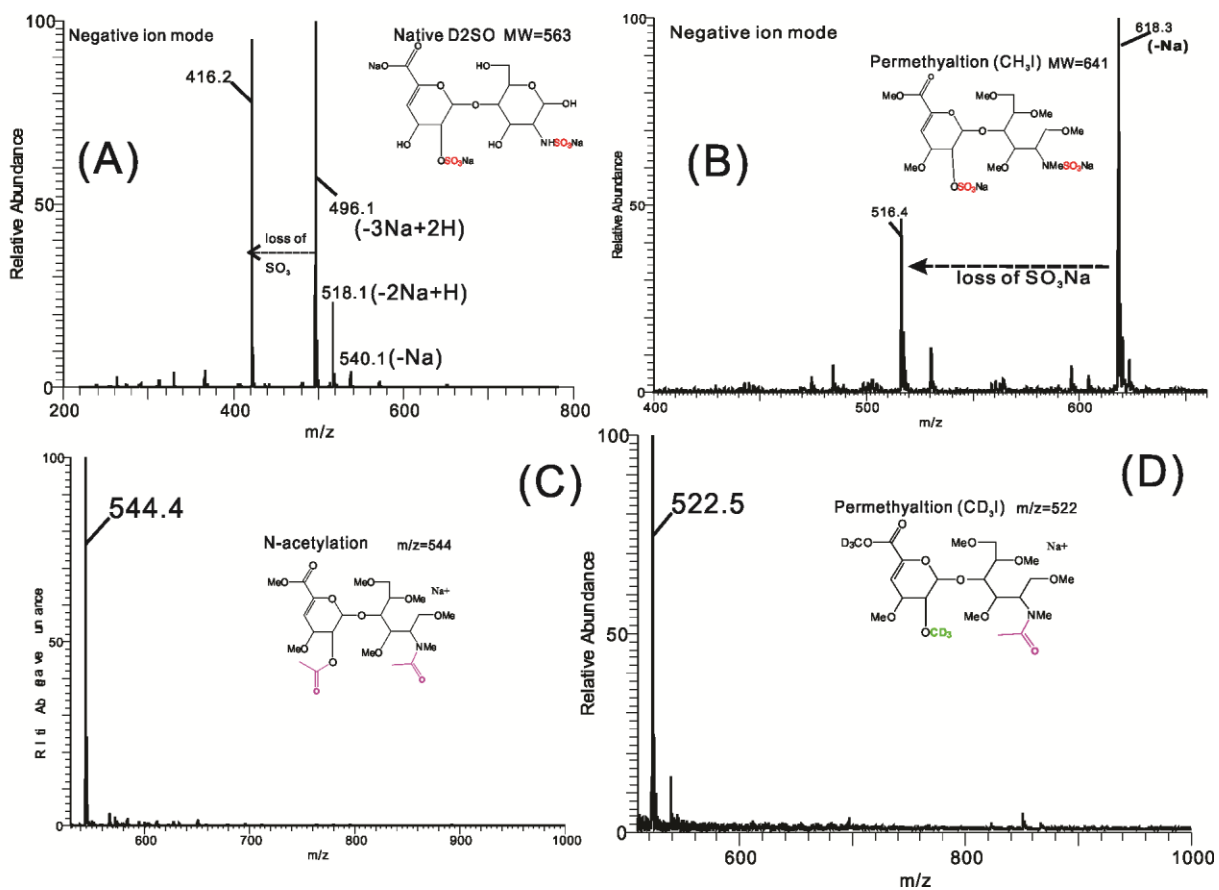


Figure 3-12 Dual permethylation of D2S0 at different stages of chemical derivatization.

Offline MS spectra and chemical structures of D2S0 at different stages of chemical derivatization. Each corresponding molecular ion is labeled. (A) Before chemical derivatization. The D2S0 standard was purchased in form of its sodium salts. In negative ion mode, m/z 540, 518 and 496 indicated loss of 1, 2, 3 sodium, respectively. Loss of one sodiated sulfo group was observed from the ion (m/z 496) without any sodium adducts. (B) After CH_3I permethylation, m/z 618 matched the loss of sodium from the structure shown in Figure 3-12B. Loss of one sulfate group plus an additional sodium was observed in negative ion mode as well. (C) Acetylation, m/z 544 matched the estimated structure. (D) After CD_3I permethylation, O-acetyl group was replaced by O- CD_3 group.

In positive MS profile as shown in Figure 3-13, molecular ion m/z 664 was reduced permethylated D2S0 with sodiated sulfo groups. D2S0 displayed different cleavages of the

sulfo groups, along with several cross-ring cleavages in the uronic acid residue and different glycosidic cleavages. Fragment m/z 544 and 442 represented cleavage of one and two sodiated sulfo groups. Fragment m/z 584 was loss of sulfo group only. The dominated ion in MS^2 spectrum was the 0,2-cross-ring cleavage (m/z 520) in the uronic acid residue. Fragment m/z 488 was 1,3-cross-ring cleavage in the uronic acid residue. Comparing to MS^2 spectra of O-sulfated disaccharides, the abundance of Y-ions m/z 376, 398 were higher. Fragment m/z 632 was loss of CH_3OH .

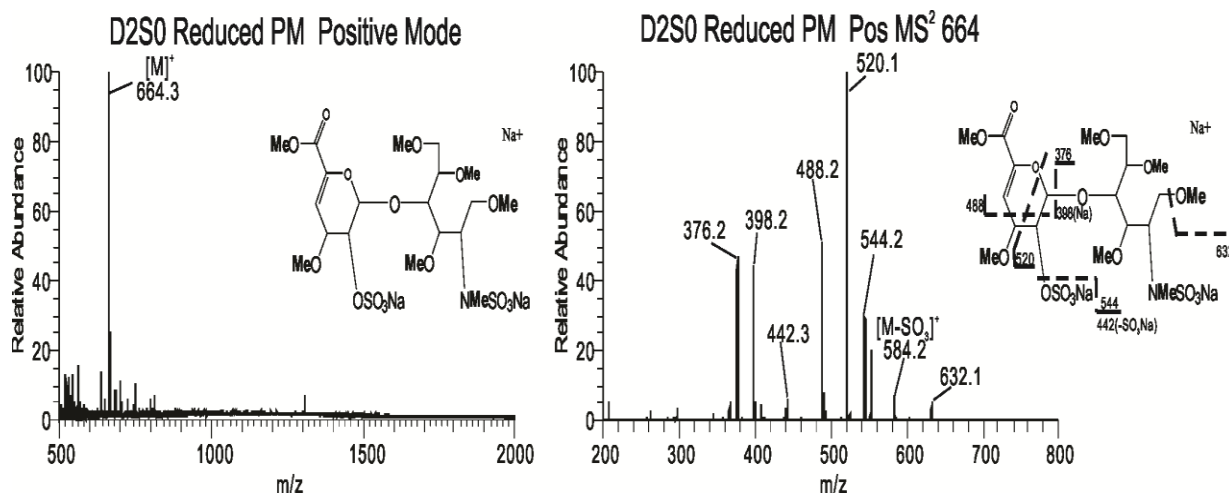


Figure 3-13 Positive ion MS and MS^2 spectra of reduced permethylated D2S0.

After desulfation, positive MS analysis was performed on derivatized species as shown in Figure 3-14. The ion m/z 460 matched the predicted structure. In addition, a pyridine adduct (m/z 540) was present in the profile. MS/MS fragmentation of m/z 540 indicated loss of pyridine. MS² spectrum of m/z 460 was exactly the same as MS³ spectrum of m/z 540-460. The dominated ion was 0,2-cross-ring cleavage (m/z 316) in the uronic acid residue. Fragment m/z 274 was the glycosidic cleavage.

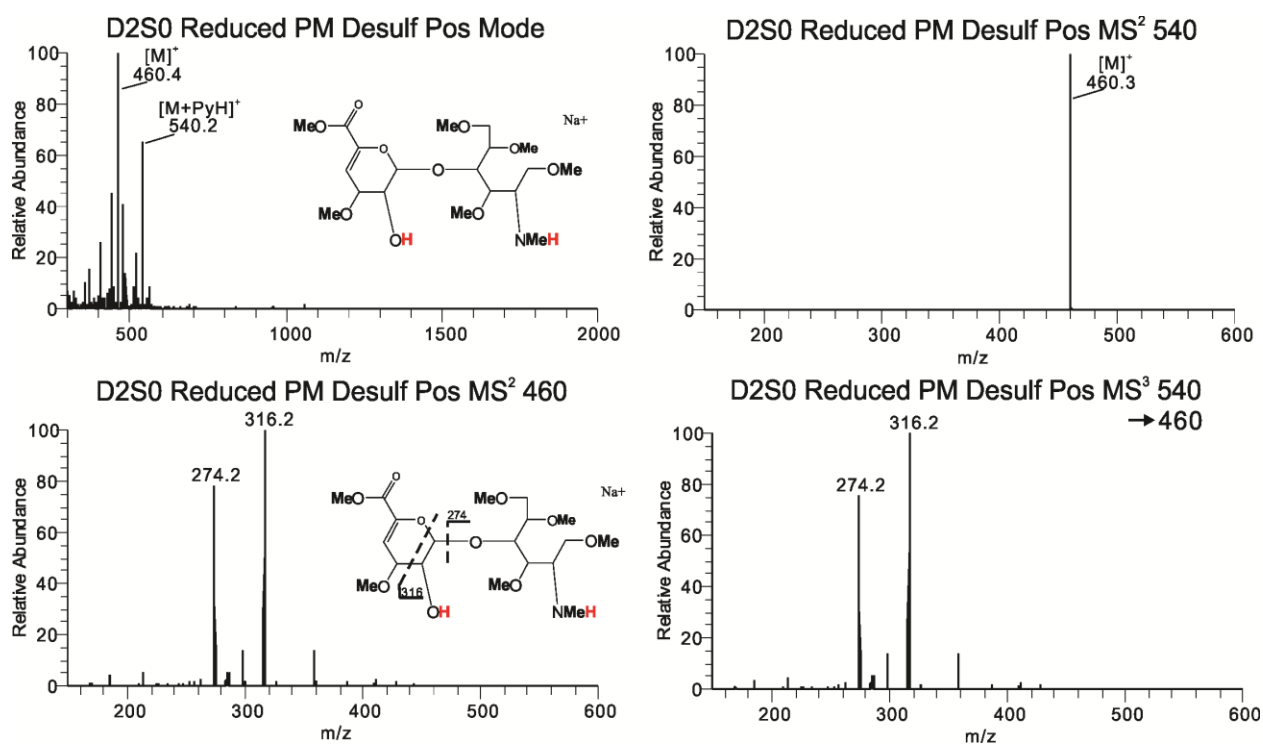


Figure 3-14 Positive ion MSⁿ spectra of reduced PM desulfated D2S0.

In Figure 3-15, acetylation using acetic anhydride gave ion m/z 544 in positive MS profile, while acetylation using acetic anhydride- d_6 gave ion m/z 550. The two ions fragmented in the same places at MS^2 level. This is because the two molecules have essentially the same structure. The deuterio acetyl group is very similar to a normal acetyl group and does not appear to influence fragmentation. The 0,2 cross-ring cleavage in the uronic acid residue dominated the MS^2 spectra for both species. The second abundant peak was cleavage of O-acetyl group. There were a few low-intensity glycosidic cleavage ions present for the two species in the MS^2 spectra.

In Figure 3-15, fragment m/z 400 and m/z 406 were 0,2 cross-ring cleavages in the uronic acid residue. Fragment m/z 484 and m/z 487 were the cleavage of O-acetyl group and O-deutero acetyl group, respectively. Fragment m/z 428 and m/z 431 were 1,3 cross-ring cleavage in the uronic acid residue. A few minor peaks (m/z 298, 316 and m/z 301,319) were from glycosidic cleavages. Fragment m/z 268 and m/z 271 were loss of CH_3OH from Z-ions (m/z 298, 301).

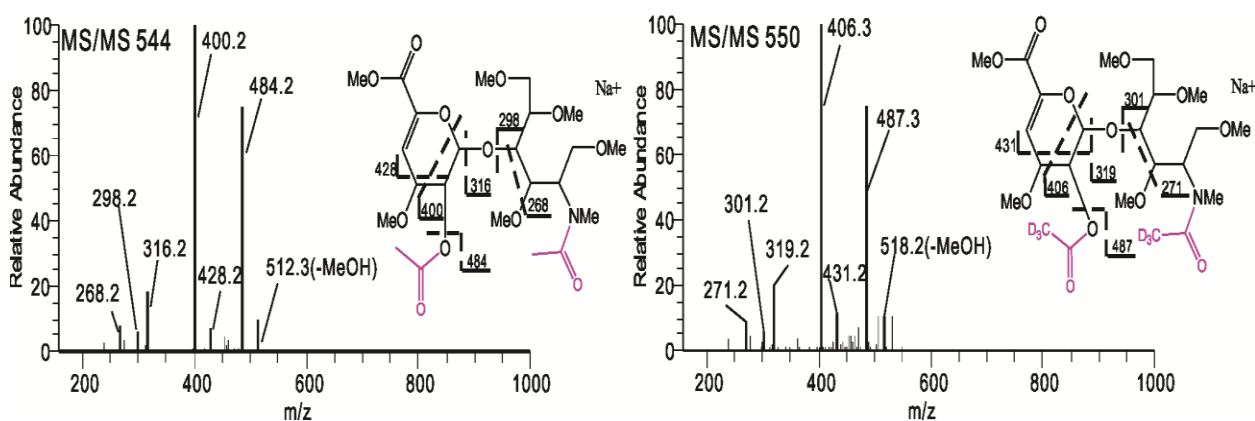


Figure 3-15 MS^2 spectra of reduced PM DESUL acetylated D2S0.

In the same manner, deuterio permethylation of m/z 544 gave ion m/z 522 in positive MS profile, while deuterio permethylation of m/z 550 gave ion m/z 525. The two ions fragment in the same places at MS² level as well. The spectra are shown in Figure 3-16. There were cross-ring cleavages in the uronic acid residue, along with several glycosidic cleavages. The dominated ion was from 0,2 cross-ring cleavage in the uronic acid residue.

In Figure 3-16, fragment m/z 375 and m/z 378 were 0,2 cross-ring cleavage in the uronic acid residue. They were dominated ions in MS² spectra. Fragment m/z 431 and m/z 434 were 1,3 cross-ring cleavage in the uronic acid residue. A few minor peaks (m/z 298, 316 and m/z 301,319) were from glycosidic cleavages. Fragment m/z 268 and m/z 271 were loss of CH₃OH from Z-ions (m/z 298, 301).

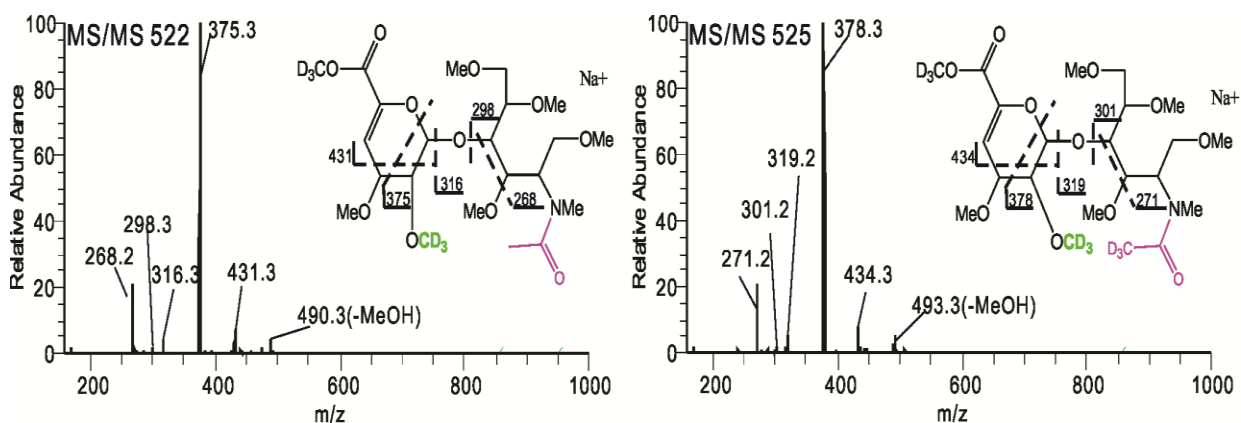


Figure 3-16 Positive ion MS² spectra of reduced dual permethylated D2S0.

If acetylation is not performed after solvolytic desulfation, there is a free amine group generated at the position where used to be a sulfo group. When performing deuterio permethylation on desulfated species, a quaternary amine is produced. Unlike the species associated with sodium, the quaternary amine carries a permanent positive charge. It behaves quite differently from the salt adducted species during MS^n fragmentation, increasing the difficulty of spectra interpretation. In Figure 3-17, the molecular ion m/z 492 in positive MS profile matched predicted structure.

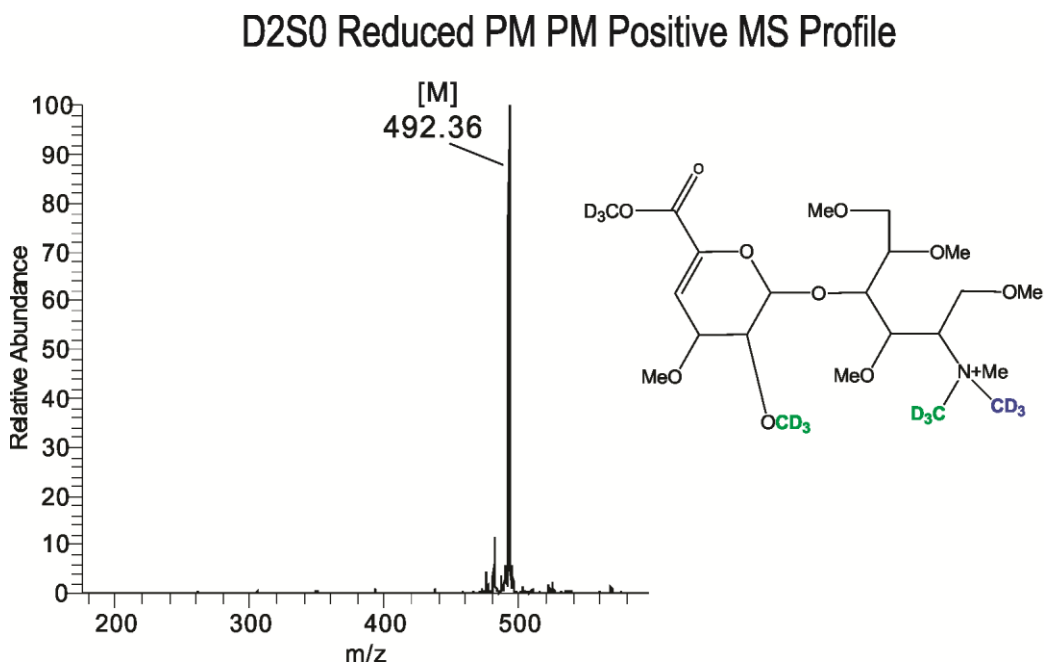


Figure 3-17 Positive ion MS profile of reduced dual PM D2S0 without N-acetylation.

Positive MS profile of D2S0 was obtained after dual permethylation without acetylation. The molecular ion m/z 492 contained a permanent positive charge on the quaternary amine, thus, it was not adducted with sodium.

3.2.3 Sulfation site identification of reduced dual-permethylated heparin/heparan sulfate disaccharides

D2A0 and D0A6 are structural isomer. After dual permethylation, D2A0 and D0A6 have the same m/z values for molecular ions. Note that D2A6 and D2S0 have the same m/z values as well. That is a coincidence as a result of deuterio acetylation of D2S0. In other word, if acetylation is performed on D2S0 (Figure 3-16), the final product will be m/z 522 which has exactly the same structure as D2A0 (Figure 3-18) after dual permethylation.

MS² spectra (Figure 3-18) of all derivatized species shared very similar fragmentation patterns. The dominated ion was 0,2 cross-ring cleavage in uronic acid residue. A few minor peaks were produced from glycosidic cleavages, 1,3 cross-ring cleavage in uronic acid residue and loss of CH₃OH.

The difference of m/z values can be used to distinguish number of sulfo groups at the first place. D2A0 and D0A6 has one sulfo group thus gives m/z 522. While D2A6 and D2S0 has two sulfo group thus gives m/z 525. MSⁿ analysis of targeted m/z values were used for identification of sulfation positions.

There were signature ions in MS² spectra (Figure 3-18) that can tell sulfation position. Fragment m/z 431 in D2A0 MS² and m/z 434 in D0A6 MS² were signature ions from 1,3 cross-ring cleavage in uronic acid residue. Fragment m/z 298, 316 in D2A0 MS² and m/z 301, 319 in D0A6 MS² were signature ions from glycosidic cleavages. Fragment m/z 268 in D2A0 MS² and m/z 271 D0A6 MS² were signature ions from CH₃OH cleavage of Z-ion.

As a result of deuterio acetylation, MS² spectra (Figure 3-18) cannot distinguish the difference in sulfation position. But think of the sample preparation workflow, it is easy to tell whether it contains N-sulfo group by performing acetylation or not.

Although the dominated ions in MS³ spectra (Figure 3-18) were from cleavage of Z-ions, there were signature ions in MS³ spectra to identify sulfation position. Fragment m/z 153 in D2A6 MS³ and m/z 156 is in D2S0 MS³ were 0,2-cross ring cleavage of glucosamine residue. Fragment m/z 172 in D2A6 MS³ spectrum and m/z 169 in D2S0 MS³ spectrum were 0,2-cross ring cleavage of Z-ion m/z 301.

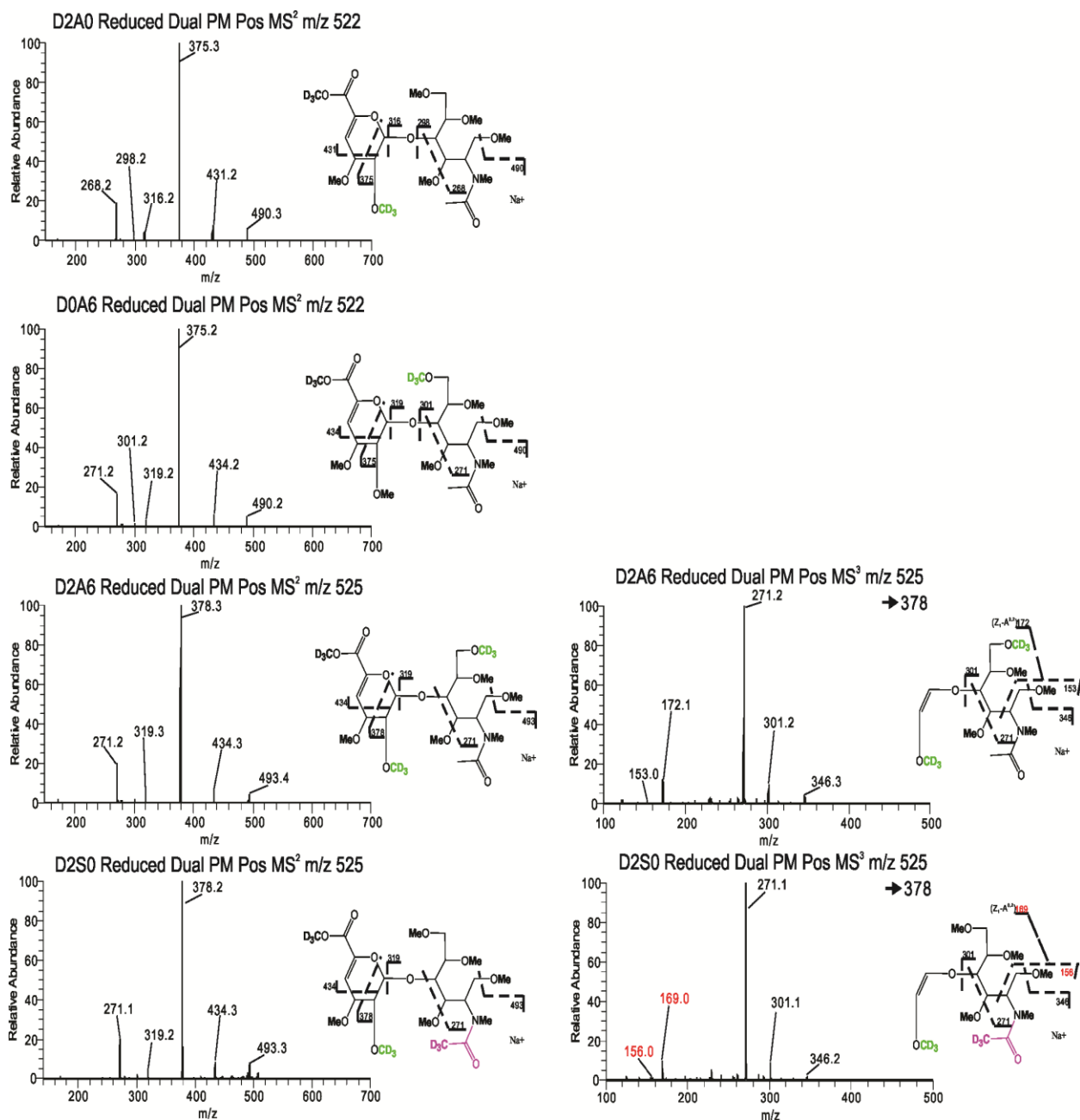


Figure 3-18 Sulfation sites identification of reduced dual-permethylated heparin/heparan sulfate disaccharides.

After chemical derivatization, O-sulfo group was converted to O-methyl group while N-sulfo group was converted to N-acetyl-*d*₃ group. MSⁿ analysis was performed on dual-permethylated HS standards. Numbers of sulfo groups can be determined by mass shift between native species and derivatized species. The position of sulfo groups can be distinguished by MSⁿ spectra.

3.2.4 Investigation of desulfation conditions

D2A0 was used as an example to investigate desulfation conditions. Methanolic desulfation was carried out using 0.5 M hydrochloride acid in methanol at room temperature for 4 hours. Solvolytic desulfation was carried out using 10% methanol/DMSO at 100 °C for 4 hours. D2A0 was purchased in form of its sodium salts. In positive MS profile (Figure 3-19), native D2A0 was ion m/z 504. Ion m/z 526 was the dominated peak which was m/z 504 plus one sodium. Note that there were several peaks in the high mass range of the profile. These larger species may be GAG oligomers with same charge density of D2A0. Comparison between solvolytic desulfation and methanolic desulfation after 4 hours is shown in Figure 3-19. As seen in methanolic desulfation, these larger species were degraded significantly under acidic conditions. In contrast, solvolytic desulfation gave much cleaner MS profile.

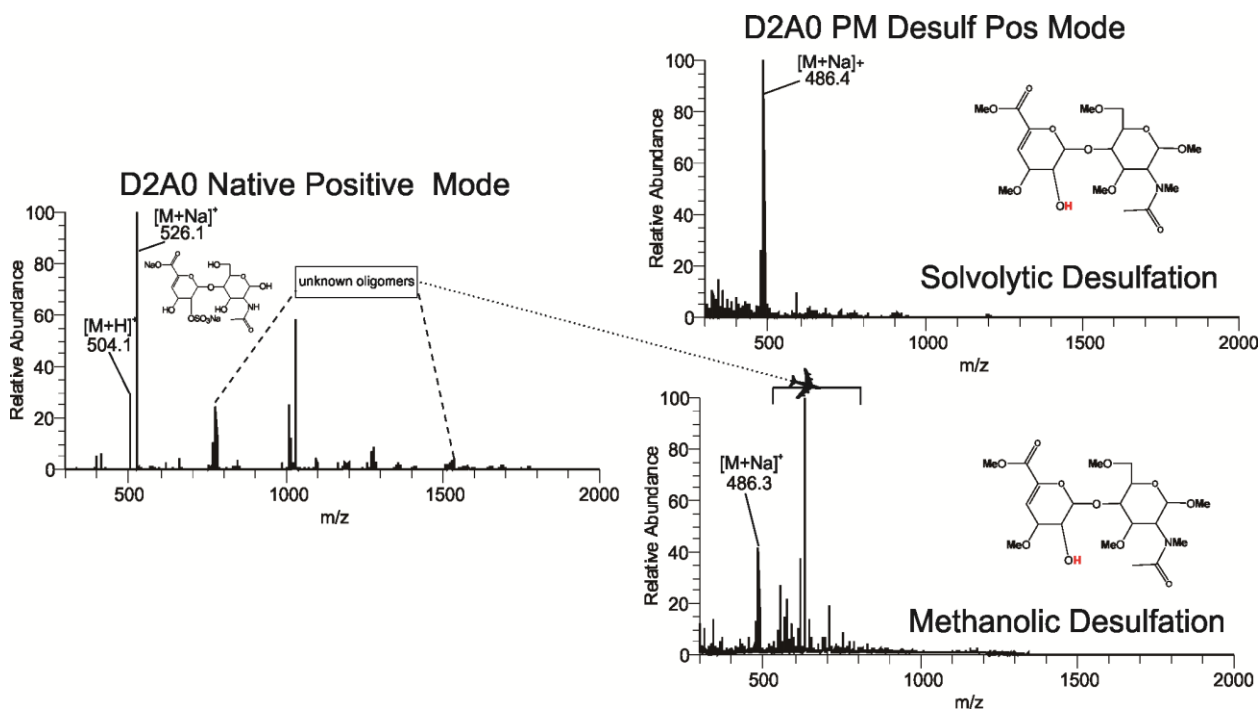


Figure 3-19 Comparison between solvolytic desulfation and methanolic desulfation.

D2S6 was used for time study of solvolytic desulfation. D2S6 has 2-O-sulfation in uronic acid residue, 6-O-sulfation and N-sulfation in glucosamine residue. The non-sulfated disaccharide D0A0 was used as internal standard after reduction and permethylation. D2S6 was first converted to its pyridinium salt before desulfation with no other derivatizations.

Microwave solvolytic desulfation was performed with a CEM Discover LabMate model (CEM Corporation, Matthews, NC). This instrument was equipped with an IR sensor for temperature feedback and control. Temperature was set at 100 °C and the necessary power and pressure was automatically adjusted to maintain that temperature. Note that the reaction was stopped and resumed after each time point.

20 µg dried pyridinium salt of D2S6 and 10 µg internal standard was suspended in 200 µL 10% Methanol/DMSO. In Figure 3-20, the samples were labeled as 403A-heat, 403B-heat, 404A-heat and 404A-microwave, respectively. 10 µL was taken out at each time point then dried. The time points were zero, 1, 2, 4 hours. In Figure 3-20, X axis represented reaction time while Y axis represented relative abundance of desulfated species to internal standard in positive MS profile. As shown in the chart, relative abundance of desulfated species was increasing until 2 hours and dropped at 4 hours. This suggested that degradation of starting material happened after 2 hours' reaction.

Relative peak intensities of desulfated species in positive mode and non-desulfated species in negative mode were plotted as a function of reaction time. At time zero, negative peak intensity of non-desulfated species was set to be 100%. Positive peak intensity of desulfated species at 4 hour was set to be 100%. The relationship is shown in Figure 3-21. Relative peak intensity of desulfated species is increasing while unreacted species is

dropping along with reaction time. After 4 hours' reaction, 90% of starting material was converted to desulfated species.

It seemed like that degradation started after 2 hours but desulfation continues to reach a 90% yield at 4 hour. This trend was further confirmed in Figure 3-22. As reaction time increases, both desulfated species and non-reacted species were decomposed in the same manner. Therefore, the preferred reaction time was 4 hour after balancing degradation and completion.

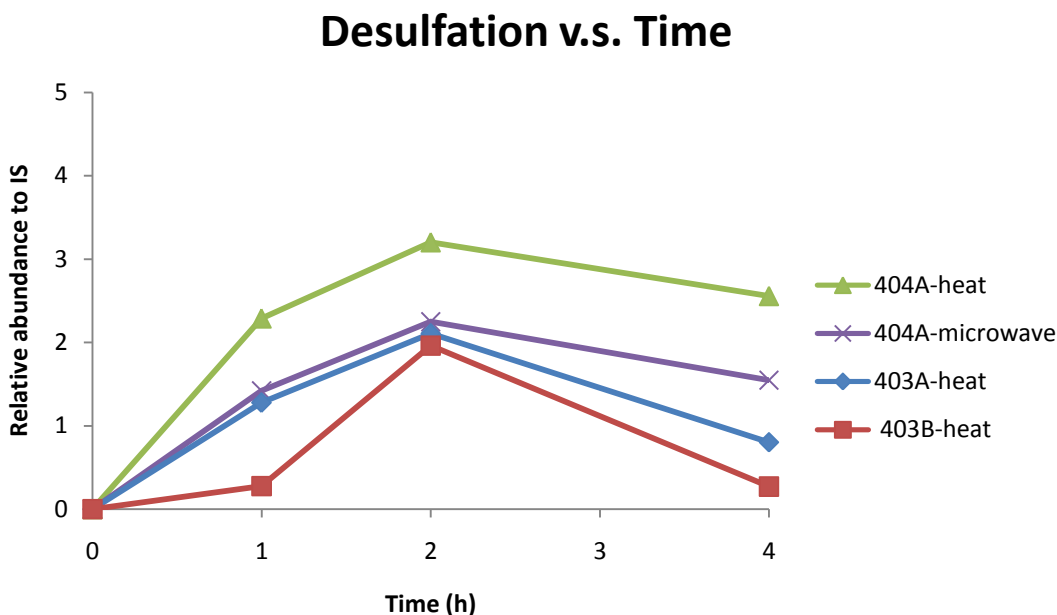


Figure 3-20 Time study of solvolytic desulfation.

The relationship between completion of desulfation and reaction time was plotted in this graph. X-axis represents reaction time, and Y-axis represents relative abundance of desulfated species to internal standard. The internal standard is reduced permethylated D0A0.

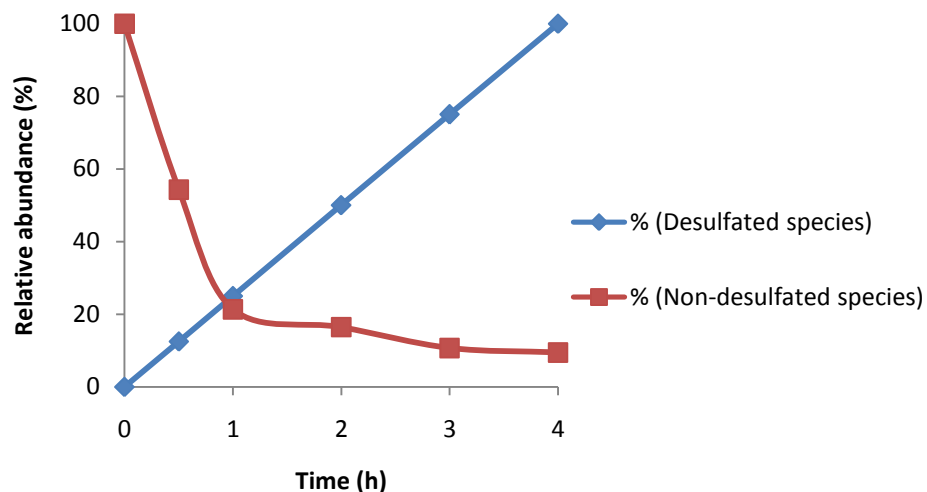


Figure 3-21 Time study of D2S6 in positive and negative ion MS.

Peak intensity of desulfated species was obtained in positive ion mode. For non-desulfated species was obtained in negative ion mode. Negative peak intensity of non-desulfated species was set to be 100%. Positive peak intensity of desulfated species at 4 hour was set to be 100%.

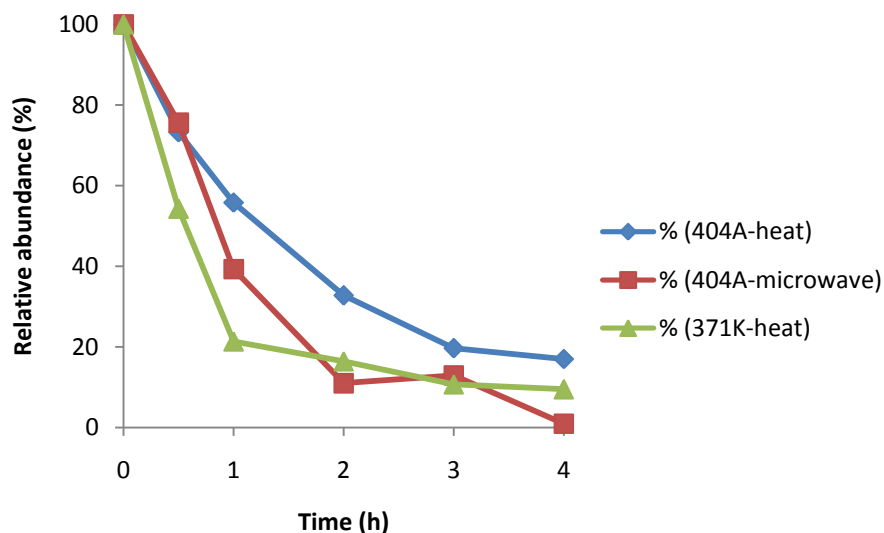


Figure 3-22 Time study of solvolytic desulfation using negative ion MS.

Peak intensity of desulfated species at time zero was set to be 100%. Peak intensities of desulfated species were plotted as a function of reaction time.

3.3 Summary

In conclusion, dual permethylation was successfully applied to heparin disaccharide standards. After derivatization, O-sulfo groups are converted to O-CD₃ groups and N-sulfo groups are converted to N-deutero acetyl groups. The sulfonation pattern can be traced through changes of m/z values and fragmentation spectra. Although acetylation is not a necessary step, as a general approach of identifying sulfation position, acetylation should be included considering presence of N-sulfo groups.

There is an additional attachment of deutero methyl group at uronic acid residue after deutero permethylation. Under strong basic condition, transesterification happens at carboxyl position where it used to be a methyl ester group. Based on working with heparin disaccharide standards, the methyl ester group is always converted to deutero methyl ester group. By not adjusting pH after 1st permethylation and adjusting pH after deutero permethylation, this reaction goes to completion. This additional deutero methyl group may interfere with identification of sulfonation pattern. However, this difference can be distinguished by fragment ions from 1,3 cross-ring cleavage at uronic acid residue, which is always 3 Da more than the theoretical calculation.

Understanding the process of each derivatization step is important for application of dual permethylation to heparin disaccharide and its analogs.

CHAPTER 4

DUAL PERMETHYLATION OF ARIXTRA[®]

4.1 EXPERIMENTAL SECTION

4.1.1 Materials

Arixtra[®], fondaparinux sodium was produced by GlaxoSmithKline (Brentford, Middlesex, UK). PD MidiTrap G-10 desalting columns were purchased from GE healthcare (Piscataway, NJ, USA). All other reagents were from Sigma-Aldrich (Milwaukee, WI, USA). C₁₈ Sep-Pak cartridges were from Waters (Franklin, MA, USA). For convenience, Arixtra[®] is abbreviated as Arixtra in the text.

Arixtra was purchased in form of a pre-filled, single-use syringe. The active substance is 2.5 mg fondaparinux sodium in 0.5 mL solution. The solution contains sodium chloride and hydrochloric acid and/or sodium hydroxide to adjust the pH. Arixtra was diluted to 1mg/mL with water before chemical derivatizations.

The chemical structure of fondaparinux is shown in Figure 4-1. Arixtra is sodiated fondaparinux with 10 sodium and its molecular formula is C₃₁H₄₃N₃Na₁₀O₄₉S₈. Unlike enzymatically digested heparin disaccharides, Arixtra maintains uronic acid epimerizations. It has eight sulfo groups, which are three N-sulfo groups and five O-sulfo groups. The

O-sulfo groups are three 6-O-sulfo groups at glucosamine residue, one 2-O-sulfo group at iduronic acid residue and one 3-O-sulfo group at glucosamine residue.

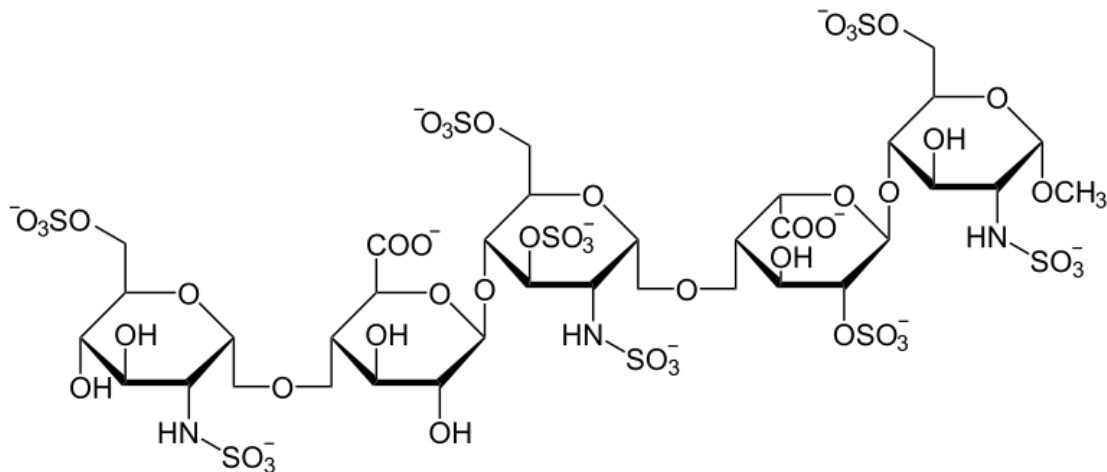


Figure 4-1 Chemical structure of Fondaparinux.

Arixtra is fondaparinux with 10 sodium. Fondaparinux has eight sulfo groups. They are three N-sulfo groups, three 6-O-sulfo groups at glucosamine residue, one 2-O-sulfo group at iduronic acid residue and one 3-O-sulfo group at glucosamine residue.

4.1.2 Chemical derivatizations of Arixtra

Desalting

Arixtra contains around 23 mg sodium salts in 0.5 mL solution of each dose.

Conversion of this salty sample to its triethylammonium (TEA) salts is not efficient owing to the salt contaminants. Incomplete conversion of TEA salts will reduce its solubility in DMSO, thus affects following sample preparation steps. Therefore, a desalting step is added to clean up the sample prior to ion exchange.

PD MidiTrap G-10 columns are pre-packed with Sephadex G-10, which is a gel filtration medium prepared by crosslinking dextran with epichlorohydrin. The packing particle size range is 55-165 μm . This material is stable in all commonly used buffers and has a working pH range from 2-13. This type columns are designed for sample volumes up to 1mL. Sephadex G-10 has an exclusion limit of > 700 molecular weight. Because its separation mechanism is based on size differences, any species have a molecular weight smaller than 700 will be retained in the column.

The PD MidiTrap G-10 column is stored in 20% ethanol. The recovery of sample is dependent on type of biomolecule, typically in the range of 70% to 90%. And an increase in sample concentration can improve recovery. Arixtra is desalted using gravity protocol. The recommended sample volumes of this protocol are 0.4 to 1.0 mL.

The storage solution was discarded. Water was used as equilibration buffer. The column was equilibrated with 20 mL water. The flow-through was discarded. 0.4 mL of 1mg/mL Arixtra was applied to the column. Water was added to reach a total volume of 1.6 mL. The flow-through was collected as the first flow. Then Arixtra was eluted with 1.6 mL water and collected as the second flow or sample flow. Additional 0.6 mL water was applied to the column and collected as the third flow. All the flow-through was lyophilized.

Conversion to triethylammonium salts

To increase its solubility in dimethyl sulfoxide (DMSO), the desalted Arixtra was passed through a self-packed cation-exchange column with Dowex 50Wx8 resin to generate triethylammonium (TEA) salts.

1st Permethylation (Iodomethane)

The dried TEA salts were completely dissolved in 400 μL of DMSO and 400 μL of anhydrous suspension of sodium hydroxide in DMSO (200 $\mu\text{g}/\mu\text{L}$), followed by 400 μL of iodomethane. Anhydrous suspension of sodium hydroxide in DMSO was made from 50% (w/w) NaOH solution. 160 μL of 50% (w/w) NaOH was mixed with 200 μL methanol, followed by addition of 4 mL DMSO. The mixture was sonicated for 15 minutes and centrifuged. DMSO was discarded. The NaOH precipitate was washed by 4 mL DMSO for three times and finally suspended in 400 μL of DMSO.

The permethylation was performed at room temperature by vortex for 5 min, then, sonication for 25 min. The reaction was quenched by adding 2mL of ion pairing buffer (100mM triethylamine, pH adjusted to 7 by conc. acetic acid). The reaction mixture was sparged with nitrogen to remove excess iodomethane.

Cleanup after 1st Permethylation

C₁₈ column cleanup

The reaction mixture was applied to a cation-exchange column in triethylammonium form. Then the IE column was washed with 3 mL ion pairing buffer and the flow-through was

collected. The flow-through was loaded onto a C₁₈ Sep-Pak cartridge, previously equilibrated with ion pairing buffer. The C₁₈ column was washed with 5 mL of the same ion pairing buffer and 2 mL of 5% acetonitrile/water (to get rid of excess TEA). The permethylated product was finally eluted with 5 mL of 50% methanol/water, followed by lyophilization.

G-10 column cleanup

The storage solution was discarded. 30% acetonitrile/water was used as equilibration buffer. The column was equilibrated with 20 mL buffer. The flow-through was discarded. The dried reaction mixture was re-suspended in 600 µL 30% acetonitrile/water. Then the solution was applied to the column. Equilibration buffer was added to reach a total volume of 1.5 mL. The flow-through was collected as the first flow. Then permethylated Arixtra was eluted with 1.7 mL equilibration buffer and collected as the second flow or sample flow. Additional 0.6 mL water was applied to the column and collected as the third flow. All the flow-through was lyophilized.

Conversion to pyridinium salts

The dried permethylated product was completely dissolved in 400 µL of 50% methanol/water, and loaded onto a cation-exchange column in H⁺ form. The IE column was flushed with 5 mL of 50% methanol/water, then added 1 mL pyridine to the solution, followed by lyophilization.

Solvolytic desulfation

The dried pyridinium salts were re-suspended in 100 µL of 10% methanol/DMSO and incubated at 100 °C for 6 hours to remove the sulfo groups, followed by lyophilization.

N-acetylation

The dried desulfated product was re-suspended in 175 μL of pyridine and 25 μL of acetic anhydride or acetic anhydride- d_6 , and incubated at 50 $^{\circ}\text{C}$ overnight, followed by lyophilization. This step was to prevent putting a permanent positive charge on free glucosamine (generated from desulfation) during the 2nd permethylation step.

2nd permethylation (Iodomethane- d_3)

The 2nd permethylation was performed using spin column procedure, but instead of iodomethane, iodomethane- d_3 was used to replace acetyl groups on O-sulfates. A spin column (Harvard Apparatus) was packed with sodium hydroxide beads to about 3cm depth. The packed column was rinsed with acetonitrile once, then DMSO twice. Sample was dissolved in 141.6 μL DMSO, 52.8 μL iodomethane- d_3 and 0.9 μL water. Then the mixture was applied to the column to react for 15 minutes. The reaction mixture was collected by spinning the column at 2000 rpm for 2 minutes. 70 μL DMSO and 26 μL iodomethane- d_3 was added to the sample tube, and transferred to the spin column. Spin column at 2000 rpm for 2 minutes to collect all sample. After that, 60 μL iodomethane- d_3 was added to the reaction mixture and re-applied to the column to repeat the reaction for another 15 minutes. After reaction, the total reaction mixture was collected by spinning the column at 4000 rpm for 2 minutes. The mixture was transferred to a test tube containing one aliquot of chloroform and one aliquot of 10% acetic acid/water. At least 5 times water washes of the sample layer (organic layer) were performed during liquid-liquid extraction cleanup. The sample layer was dried for ESI-IT-MSⁿ analysis later.

The protocol was summarized in Figure 4-2. Arixtra is fondaparinux with 10 sodium. Therefore desalting was applied before ion exchange step. Removal of sodium salt contaminant helped its conversion to TEA salts, thus increased its solubility in DMSO, consequently, it improved the efficiency of permethylation. Another desalting step was applied after permethylation to clean up the sample before its conversion to pyridinium salts. Solvolytic desulfation was performed to remove both N- and O-sulfo groups. N-acetylation with acetic anhydride- d_6 was applied to protect the free amino groups. Then the second permethylation was performed with CD_3I . After the completed procedure, all the N-sulfo groups were converted to N-acetyl- d_3 groups while O-sulfo groups were converted to methyl- d_3 groups.

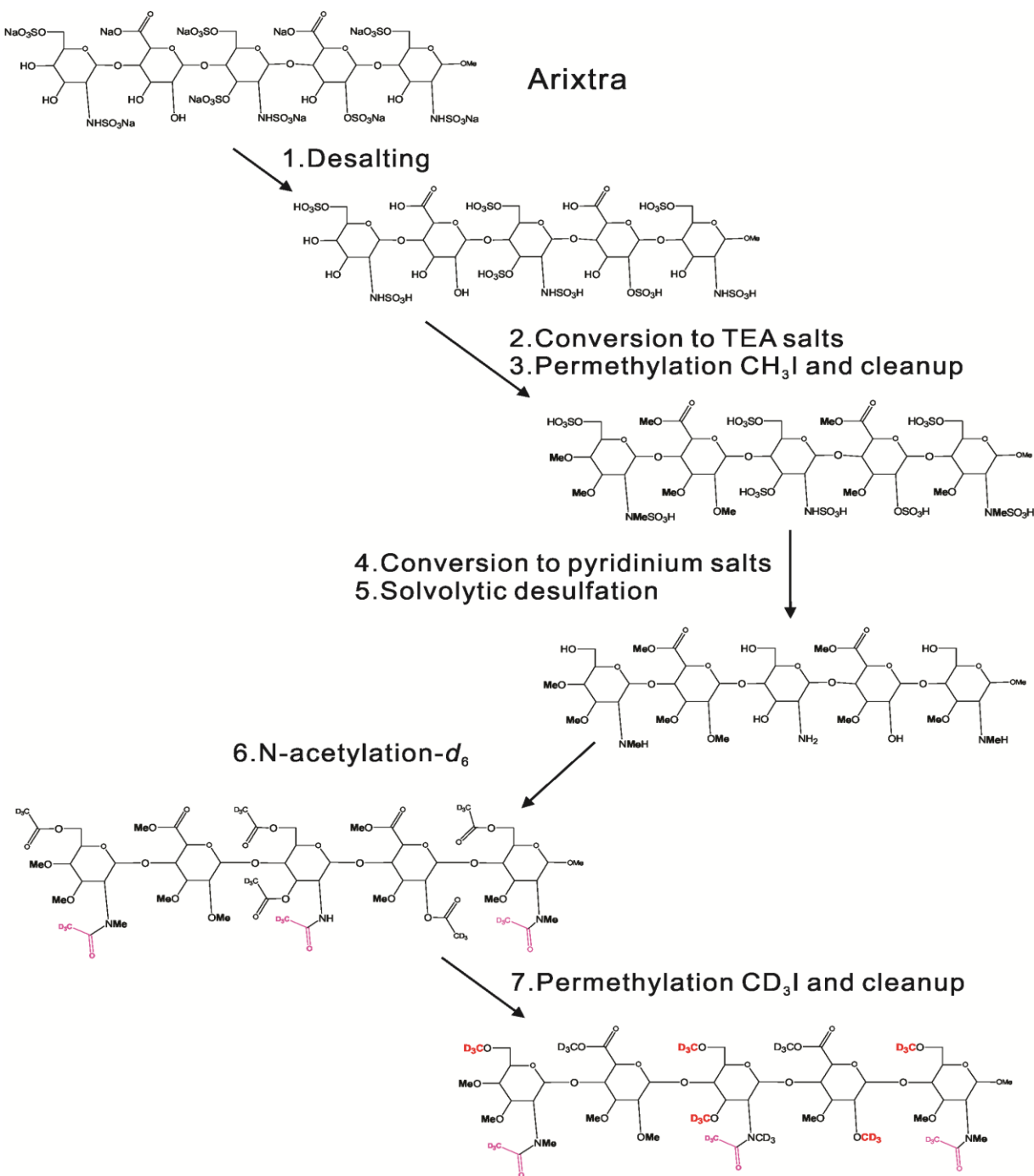


Figure 4-2 Experimental workflow of dual permethylated Arixtra.

The sample contains lots of sodium salts. As the first step, desalting was applied to remove sodium salt contaminant. To make it soluble in DMSO, the sample passed through a cation exchange column to generate its TEA salts. Then, permethylation was performed with CH₃I. After removal of sulfo groups, N-acetylation-*d*₆ and CD₃I permethylation, N-sulfo groups were converted to N-acetyl-*d*₃ groups while O-sulfo groups were converted to methyl-*d*₃ groups.

4.1.3 Glycan analysis

Online IP-RP-LC/MS Analysis

Online reversed phase liquid chromatography (RPLC) separation was performed on a BDS HYPERSIL C₁₈ column (Thermo), 2.1mm x150 mm, 3 μm, with mass spectrometry. Mobile phase A was 10mM pentylamine (PTA), 10 mM acetic acid, 5% Acetonitrile/95% HPLC grade water. Mobile phase B was 10mM pentylamine, 10 mM acetic acid in acetonitrile. The column temperature was maintained at 40 °C. The flow rate was set at 200 μL/min. The gradient was summarized in Table 4-1.

Table 4-1 Gradient profile of RP-IP-LC.

Time (min)	A%	B%
0	95	5
2	95	5
20	87	13
80	31	69
85	31	69
86	95	5
92	95	5

Online positive ion MS profiles and MS² spectra were obtained from an LTQ Velos (Thermo Fisher Scientific, Waltham, MA) equipped with an electrospray ion source. The capillary temperature was 275 °C. The collision energy was set as 35 eV.

LC/MS Analysis

Reversed phase liquid chromatography (RPLC) separation was performed on a BDS HYPERSIL C₁₈ column (Thermo), 2.1mm x150 mm, 3 μm. Mobile phase A was 25 μM sodium acetate prepared with HPLC grade water. Mobile phase B was acetonitrile. A linear gradient of mobile phase B from 25% to 55% over 36 min was used, with a flow rate of 200 μL/min. Online positive ion MS profiles and MS² spectra were obtained from an LTQ Velos (Thermo Fisher Scientific, Waltham, MA) equipped with an electrospray ion source. The capillary temperature was 375 °C. The collision energy was set as 35 eV.

Offline MS Analysis by Direct Infusion

The LTQ was additionally equipped with a TriVersa Nanomate nanoelectrospray ion source (Advion, Ithaca, NY). Offline MS profiles and MSⁿ spectra were obtained from this chip-based nanoESI interface by direct infusion. Samples were dissolved in 50% (v/v) methanol/water.

MSⁿ spectra were also obtained with LTQ Velos equipped with a nanospray ESI source (Thermo Fisher Scientific, Waltham, MA).

4.2 RESULTS AND DISCUSSIONS

4.2.1 MS analysis of native Arixtra

Arixtra is a linear octasulfated pentasaccharide molecule having five O-sulfo groups and three N-sulfo groups. In addition, Arixtra contains five hydroxyl groups in the molecule that are not sulfated and two sodium carboxylates. Native Arixtra contains total 10 sodium in its molecular formula. The solution contains sodium chloride as well. Since Arixtra has eight sodiated sulfo groups, it is highly negatively charged and cannot be detected as molecular ions in positive MS mode. The native Arixtra has been checked by mass spectrometry through direct infusion and coupling with liquid chromatography.

Negative MS profile was obtained with LTQ by direct infusion. The sample was dissolved in 75% methanol/water without any purification. To maintain stable spray in negative ion mode, isopropanol was added to the sample. Most of abundant ions are doubly charged. In Figure 4-3, the dominated ion was m/z 840. This ion represented doubly charged Arixtra of 8 sodium. Singly charged Arixtra were observed as ions m/z 1725 of 10 sodium and m/z 1703 of 9 sodium. Comparing to those doubly charged ions, these singly charged ions were relatively low in abundance. And a series of ions with different salt adductions were present in the profile. They were combinations of various adductions of sodium and sodium chloride (m/z 851, 869, 899, 911, 928). Some peaks were shown in very low intensity thus were not labeled in the MS profile. Besides, ion m/z 800 was the loss of sulfo group.

The sample was analyzed in the same manner after desalting. As shown in Figure 4-4, after removal of salts, there were more types of ions present in negative MS profile. There were three sections in its negative MS profile, doubly charged ions from Arixtra (m/z 738,

749, 789, 800, 840, 851, 869, 899, 911, 928), singly charged ions from Arixtra (m/z 1623, 1703, 1725) and triply charged ions from Arixtra gas-phase dimer (m/z 1129, 1136, 1148). With less protection of sodium, more ions from loss of sulfo groups were observed.

In addition, native Arixtra was looked by ion-pair reversed-phase LC/MS. Arixtra solution was diluted to 100 ng/ μ L. An injection of 5 μ L was used to obtain negative IP-RP-LC/MS profile. Although Arixtra appeared as a single peak in total ion chromatogram, the MS profile (Figure 4-5) was very complicated. There were three types of ions, doubly charged ions from various pentylamine adductions, doubly charged ions or triply charged ions from loss of different numbers of sulfo groups as well as from various pentylamine adductions.

The complexity of native Arixtra MS profile, either from direct infusion or IP-RP-LC/MS, makes it even impossible to assign accurate molecular weight if we have no idea of the structure. Furthermore, fragmentation of ions in native MS profile generates ions with sulfo groups' losses as the most abundant ion. Comparing to this type of ions, other fragmentation ions may contain structural information are present in negligible intensity. For instance, MSⁿ fragmentation pathway of doubly charged molecular ion m/z 840 is 840 to 800, 800 to 760 and so on. 40 Da is the mass for $-\text{SO}_3$ group with a double charge. Therefore, structural determination cannot rely on MSⁿ analysis of native Arixtra.

Arixtra will behave in the same way as long as it has sulfo groups. Thus before removal of sulfo groups, the derivatized sample has been analyzed in negative ion mode.

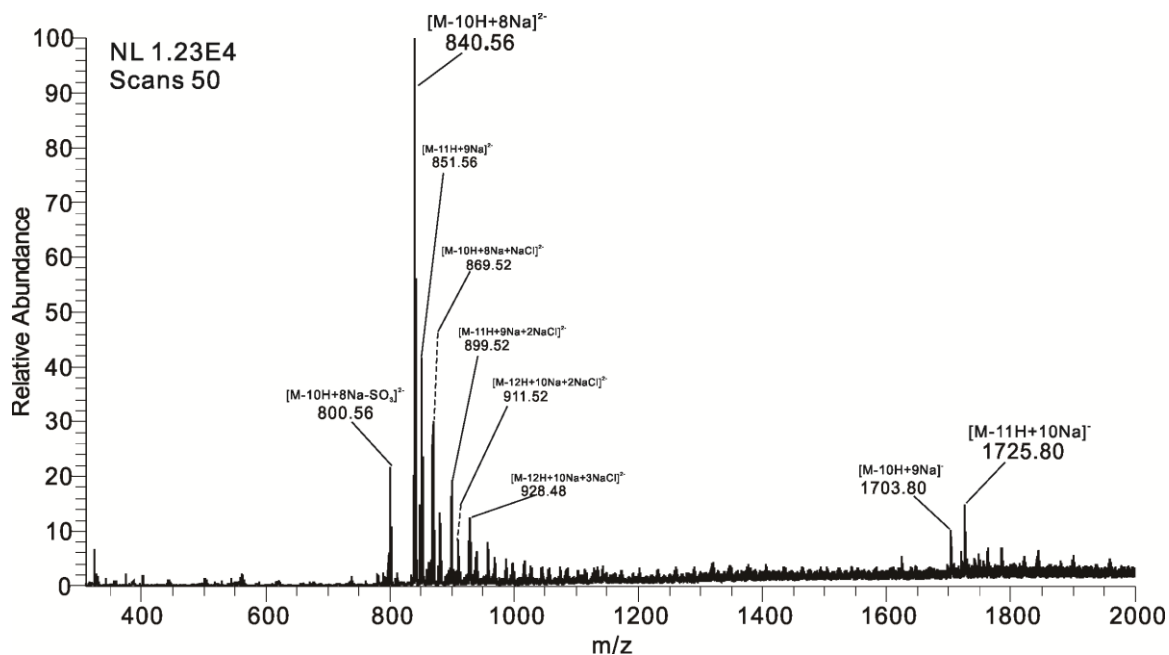


Figure 4-3 Negative ion MS profile of native Arixtra.

Negative ion MS profile was obtained from native Arixtra solution without any purification. Both singly charged and doubly charged molecular ions of Arixtra were present in the profile. The dominated ion m/z 840 was doubly charged Arixtra with 8 sodium. Various salt adductions were observed as ion m/z 851, 869, 899, 911 and 928. In addition, loss of sulfo group was present as ion m/z 800.

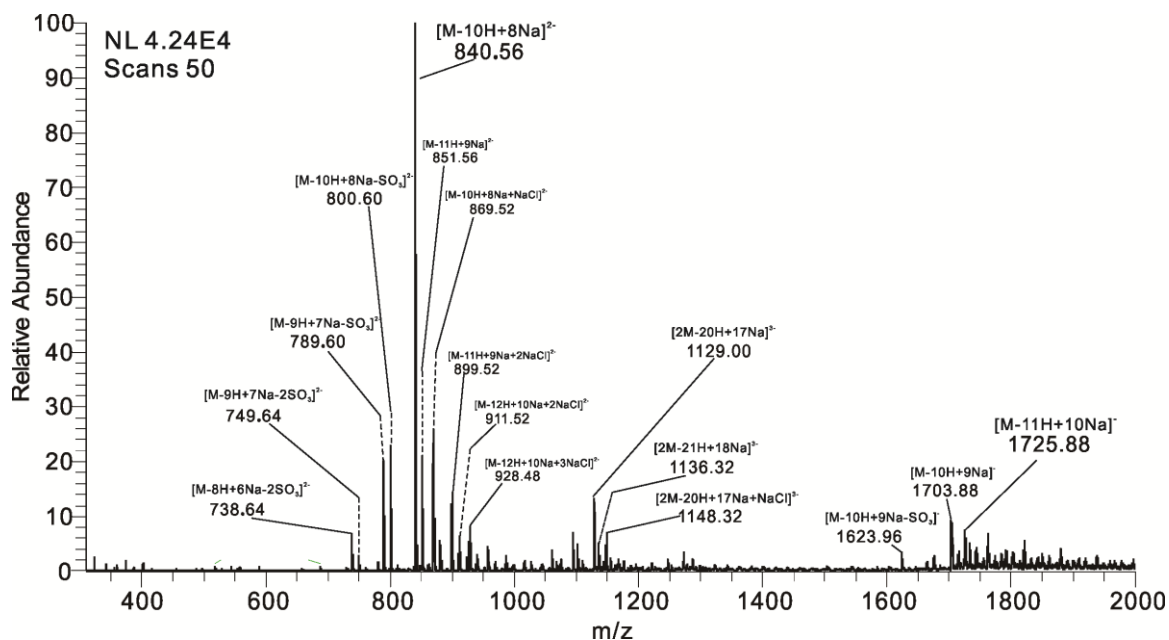


Figure 4-4 Negative ion MS profile of native Arixtra after desalting.

Negative ion MS profile was obtained from native Arixtra solution after desalting. This profile was more complicated than native Arixtra. Both singly charged (m/z 1725) and doubly charged (m/z 840) molecular ions of Arixtra were present in the profile. In addition, there were a section of triply charged ions from Arixtra gas-phase dimer. The dominated ion m/z 840 was doubly charged Arixtra with 8 sodium. Various salt adductions were observed as ion m/z 851, 869, 899, 911 and 928. There were ions from loss of different sulfo groups present as well, m/z 738, 749, 789, 800.

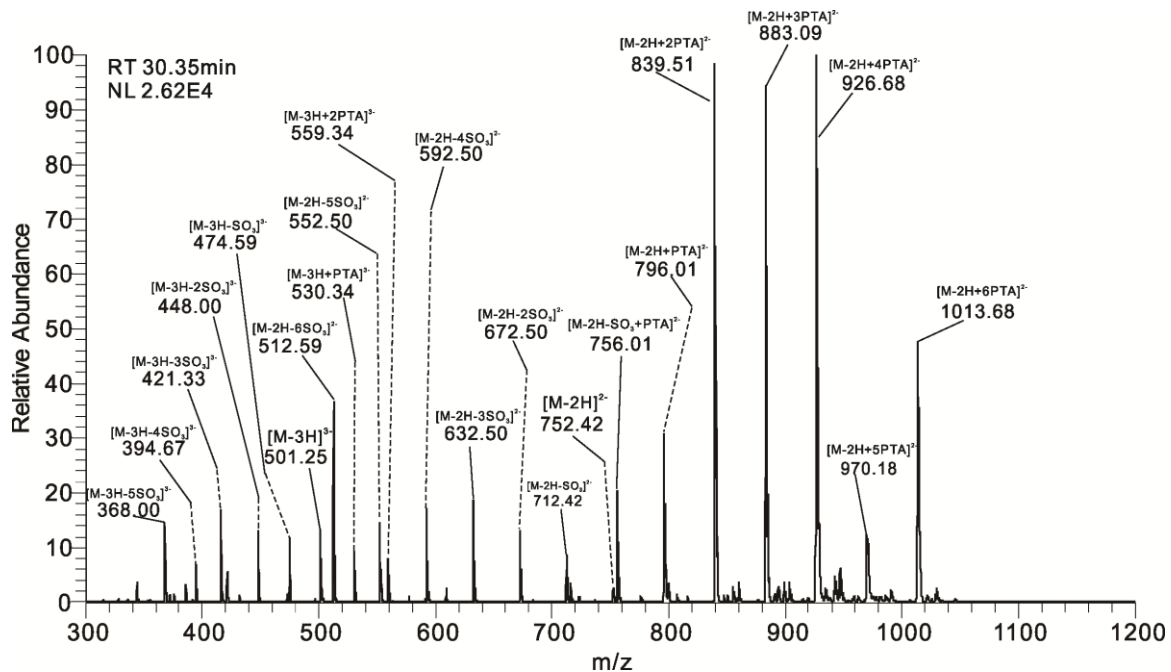


Figure 4-5 Negative ion IP-RP-LC/MS profile of native Arixtra.

Native Arixtra was looked by IP-RP-LC/MS as well. It showed as a single peak in total ion chromatogram. The negative MS profile was obtained at retention time 30.35 minute. The doubly charged ions m/z 752, 796, 839, 883, 926, 970, 1013 represented adduction of 0 to 6 pentylamine, respectively. The triply charged ions m/z 500, 474, 448, 421, 394, 368 represented loss of 0 to 5 sulfo groups, respectively. Ions with various combinations of sulfo groups loss and pentylamine adduction were present as well.

4.2.2 Recovery of desalting and ion exchange

Arixtra is a chemically synthesized methoxy derivative of the unique pentasaccharide sequence of heparin. As shown in Figure 4-1, the rightmost monosaccharide unit of Arixtra does not contain a hemiacetal structure thus cannot be reduced or labeled. Unlike heparin disaccharide standards, Arixtra does not have any chromophores. Given the specialty of Arixtra, general liquid chromatography approaches with UV detection or fluorescence labeling are not achievable for its analysis. Therefore, ion-pair reversed-phase liquid chromatography coupling with mass spectrometric detection is adapted as a tool to investigate the recovery of the desalting column and ion exchange column.

To point out that, this method is not considered as a precise way to measure sample recovery owing to ionization process in mass spectrometer. In this case, Arixtra is not detected as a single molecular ion. The MS profile comprises various adductions of ion pairing agent as well as sulfo group losses. Therefore, using peak area of Total Ion Chromatogram (TIC) is a semi-quantitative way to calculate the recovery. However, it still helps us to get a sense of how much material is recovered after desalting column and ion exchange column. Since the goal is structural analysis of Arixtra, as long as there is enough material to perform MSⁿ analysis, inevitable sample loss during each step is acceptable.

The recovery was calculated on basis of Arixtra's peak area in total ion chromatogram. The external standard was 100 ng/μL native Arixtra. The injection volume was 5 μL for standard and samples. Peak area of external standard was averaged each day before and after sample injections. The second flow from desalting was used as samples to measure recovery.

The recovery of desalting column is summarized in Table 4-2. The starting amount for recovery study was 200 µg and 400 µg of native Arixtra solution. With a starting amount of 200 µg, the average recovery is 72%. While the average recovery from 400 µg native Arixtra is slightly higher as 76%. The recovery is in the suggested range (70% to 90%) of this type desalting column. To keep in mind, the recovery did not suggest the efficiency of salt removal.

For ion exchange step (Table 4-3), the recovery refers to the sample recovered from desalting step not from the starting amount. The sample was collected from the second fraction of desalting then applied to the cation exchange column. The recovery was calculated in the same manner as for desalting. The results suggest that nearly no sample loss when passing through the ion exchange column. Again, the recovery did not suggest the efficiency of conversion to TEA salts. It is worth noting that the recovery of ion exchange column was more than 100%. Because of the peak area of TIC is related to the ionization process. Presence of salt can cause ion suppression in mass spectrometer. After desalting, the salt contaminant was greatly reduced thus resulted in enhanced ion signal.

In summary, the recovery of desalting column and ion exchange column gave a rough amount of how much Arixtra left for permethylation step. Since the ion exchange column itself did not cause sample loss, the efficiency of its conversion to TEA salts was related to the efficiency of salt removal by desalting column.

This kind of information helps investigation of permethylation conditions. Later studies of permethylation suggest that although the starting amount of material does not affect the recovery, the conversion of TEA salts is more efficient with less starting material.

Table 4-2 Recovery of desalting columns.

Sample Name	Starting amount (µg)	Recovery	Average
A025	200	75%	72%
A027	200	71%	
A028	200	70%	
A031	400	75%	76%
A033	400	79%	
A034	400	73%	

The samples were analyzed with RP-IP-LC/MS. Native Arixtra was diluted to 100 ng/ µL. This solution was used as external standard with an amount of 500ng. The injection volume was 5 µL for both standard and samples. 200 µg and 400 µg were selected as the starting amount and resulted in an average recovery of 72% and 76%, respectively.

Table 4-3 Recovery of IE columns.

Sample Name	Starting amount (µg)	Recovery (IE)
A0272-IE	200	104%
A0281-IE	200	110%
A0282-IE	200	98%
A0301-IE	400	122%
A0302-IE	400	121%
A0303-IE	400	124%

The samples were analyzed with IP-RP-LC/MS. Native Arixtra was diluted to 100 ng/ µL. This solution was used as external standard with an amount of 500 ng. The injection volume was 5 µL for both standard and samples. The starting amount was the amount of material loaded onto the desalting column. The fraction was collected and applied to cation exchange column. The results suggested no sample loss during ion exchange step not from the starting point.

4.2.3 Investigation of permethylation conditions

Permethylation is an important step of chemical derivatizations. The completion of permethylation is related to a lot factors, such as solubility in DMSO, NaOH concentration in DMSO, quenching solution, reaction time. Its solubility in DMSO is based on the efficiency of conversion to its TEA salts which is affected by sample amount of desalting. Variation in sample amount applied to desalting, ion exchange and permethylation leads to different reaction chromatographic profiles under the same condition of permethylation.

The permethylated samples were analyzed by IP-RP-LC/MS. By monitoring the changes in base peak chromatograms, reaction conditions were carefully studied of different factors. The commonly seen base peaks and predicted compositions were listed in Table 4-4. To simplify the profile, each peak was assigned with a number. M represented fondaparinux hydrogen. No sodium adduction was observed in LC/MS profile. The dominated base peak of most completed reaction was m/z 953 (peak #1) which was permethylated Arixtra with adduction of three pentylamine. Elimination of a -OSO₃H group (peak #4) was always seen when m/z 953 was present. In addition, three minor base peaks (#5,6,7,) were observed, and most times peak #5 was overlapped with peak #7. Peak #5 was structurally identical to peak #4 with one less adduction of pentylamine. Peak #7 was generated by elimination of a -OSO₃H group from peak #2. Peak #2 was permethylated Arixtra with one less methyl group. The rest base peaks were mostly seen in MS profiles of incomplete reaction.

Please see APPENDIX A for LC/MS profiles of permethylated Arixtra.

Table 4-4 Compositions and their corresponding m/z values in IP-RP-LCMS profile.

Label	Base peak (m/z)	Composition
0	839 or 926	Unreacted Arixtra
1	953	[M-2H+3PTA] ²⁻
2	946	[M-H-Me+3PTA] ²⁻
3	939	[M-2Me+3PTA] ²⁻
4	904	[M-2H-OSO ₃ H+3PTA] ²⁻
5	860	[M-2H-OSO ₃ H+2PTA] ²⁻
6	853	[M-H-Me-OSO ₃ H+2PTA] ²⁻
7	804	[M-H-Me-2OSO ₃ H+2PTA] ²⁻
8	890	[M-2Me-OSO ₃ H+3PTA] ²⁻
9	790	[M-3Me+H-2OSO ₃ H+2PTA] ²⁻
10	846	[M-2Me-OSO ₃ H+2PTA] ²⁻

The permethylated samples were analyzed by PR-IP-LC/MS. Base peaks were obtained from negative MS profiles. M represents fondaparinux hydrogen. No sodium adduction has been observed in LC/MS profile. Peak #1 was permethylated Arixtra with adduction of three pentylamine. Peak #2 was permethylated Arixtra with one less methyl group, three pentylamine adduction as well. Elimination of a -OSO₃H group (peak #4) was always seen when peak #1 was present. In addition, three minor base peaks (#5,6,7,) were observed, and most times peak #5 was overlapped with peak #7. Peak #5 was structurally identical to peak #4 with one less adduction of pentylamine. Peak #7 was generated by elimination of a -OSO₃H group from peak #2. The rest base peaks were mostly seen in MS profiles of incomplete reaction.

4.2.3.1 Variations of sample amounts

The completion of permethylation is closely related to the amounts of sample applied to the column at each step before permethylation. The variations of starting amounts of each step are listed in Table 4-5. And the corresponding base peak chromatograms are shown in Figure 4-6. The desalting step was using gravity protocol, thus, 400 μL sample of specific concentration was applied to the column. The sample solution was diluted to correct concentration to make micro grams. The dried fraction after desalting was dissolved in 400 μL water before applied to ion exchange column. All the listed samples were permethylated for the first time under the same conditions. The reaction solution comprised 400 μL DMSO, 400 μL 200 $\mu\text{g}/\mu\text{L}$ NaOH in DMSO and 400 μL iodomethane. The quenching solution was 2 mL ion pairing buffer. The reaction time was set to 30 minutes. By comparing the six representative samples, the best combination was found to be S4.

In Table 4-5, the desalting amount means the amount of native Arixtra applied to the desalting column. After desalting, the second fraction was dried and dissolved in water. The water solution was split to fractions with equal amount before passing through ion exchange column. The amount of sample used for ion exchange column and permethylation was estimated amount.

Table 4-5 Variations of sample amounts in Figure 4-6.

Sample	Desalting (μg)	IE-TEA (μg)	PM-CH ₃ I (μg)
S1	100	100	100
S2	200	200	200
S3	200	200	100
S4	200	100	100
S5	400	100	100
S6	400	50	50

Permethylation of sulfated glycans is a fickle process affected by a lot factors. Ion-pair reversed-phase chromatography is capable for separation of structurally closed compositions. Recall the IP-RP-LC/MS data of native Arixtra (Figure 4-5), the MS profile was much more complicated than the base peak chromatogram. The base peak at certain retention time is a signature for a specific composition. Under the same reaction conditions, influence of sample amount on permethylation was compared using base peak chromatograms.

The completion of permethylation is largely relied on the solubility in DMSO. Insufficient conversion to TEA salts leads to underpermethylation. The efficiency of ion exchange is related to salt concentration and the column capacity. For example, both sample 4 and sample 5 used 100 μg for ion exchange, but sample 5 ended up with unreacted Arixtra as a consequence of different sample amount of desalting. Sample 2 and sample 4 used 200 μg for desalting, but sample 2 has unreacted Arixtra after permethylation as a result of sample overloading on ion exchange column.

It is interesting to find out that sample 1 contained base peaks mainly from underpermethylation. Because based on observations of sample 2,4,5, it seems like less starting amount of desalting has better yield of fully permethylated Arixtra. A possible explanation is the permethylation is affected by outcome pH after reaction. The pH is a consequence of sample and quenching solution. Arixtra is an acidic compound, thus more starting material leads to a lower pH under the same circumstances. The sample mixture should be acidic after reaction to avoid underpermethylation from saponification. This was proven in sample 6 which underpermethylation is present as well.

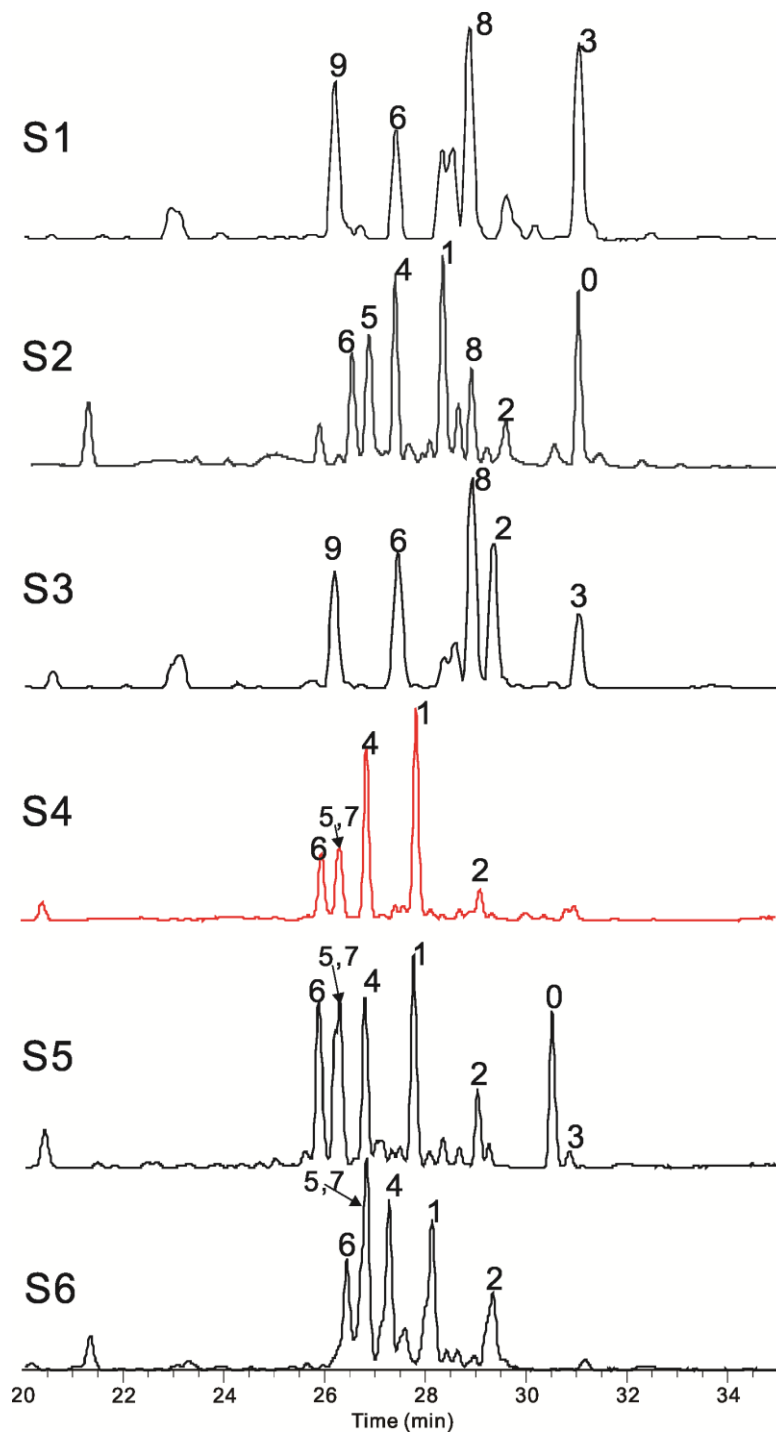


Figure 4-6 Comparison of different sample amounts for permethylation.

The optimized condition was found with S4 using 100 μg Arixtra as starting material. Permethylation conditions: reaction solution was 400 μL of DMSO, 400 μL of 200 $\mu\text{g}/\mu\text{L}$ NaOH in DMSO and 400 μL iodomethane; quenching solution used 2 mL ion pairing buffer (100 mM triethylamine in 5% acetonitrile/ 95% water, pH 7), reaction time was 30 minutes.

4.2.3.2 Multiple times of permethylation

To reduce the species from underpermethylation, the reaction was performed for multiple times. Permethylation was carried out under the same conditions and repeated three times. The reaction solution comprised 400 μL of DMSO, 400 μL of 200 $\mu\text{g}/\mu\text{L}$ NaOH in DMSO and 400 μL iodomethane. The quenching solution was 2 mL ion pairing buffer (100 mM triethylamine in 5% acetonitrile/ 95% water, pH 7). The reaction time was set to 30 minutes. The selected example has fully permethylated, incomplete permethylated species as well as non-reacted species at the first permethylation. After the second permethylation, there was no unreacted Arixtra present in the base peak chromatogram. The unreacted Arixtra was converted to underpermethylated species and fully permethylated species. In the meantime, peaks from elimination of $-\text{SO}_3\text{H}$ were more intense than the first permethylation. In addition, more junk peaks showed up in earlier time range. Those peaks may come from decomposition of the later peaks under strong base condition. After the third permethylation, the dominated peaks are products of elimination of $-\text{OSO}_3\text{H}$ from permethylated Arixtra. Intact fully permethylated Arixtra was not seen in base peak chromatogram.

In conclusion, repeat permethylation helped to convert underpermethylated species to fully permethylated species. However, species generated from elimination of $-\text{OSO}_3\text{H}$ and decomposition were always accompanied with repeating permethylation under strong base condition. The more times of repeating reaction, the more side products have been seen in IP-RP-LC/MS profiles.

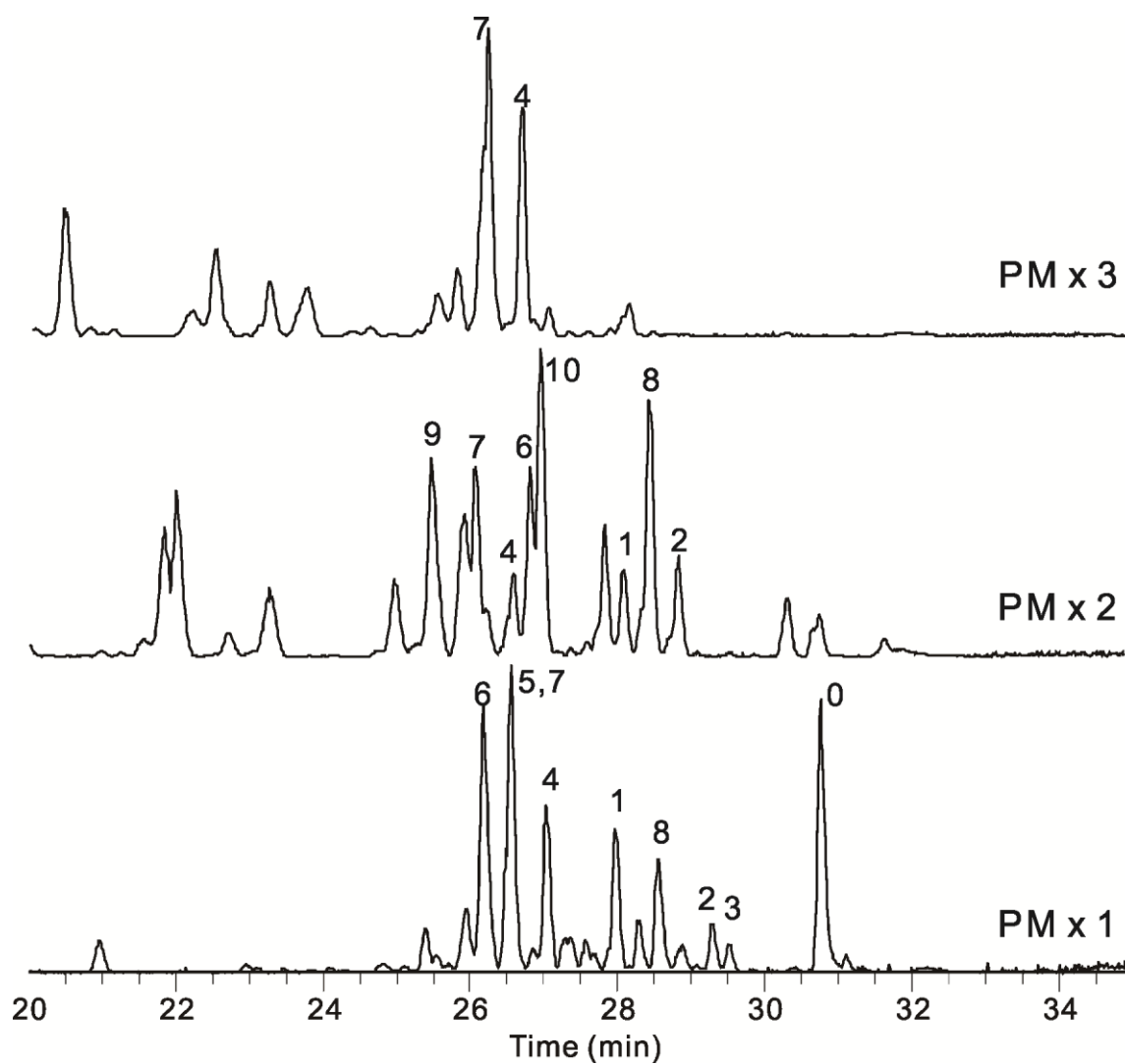


Figure 4-7 Comparisons of multiple permethylation.

Ion-pair reversed-phase liquid chromatography was used to separate the reaction mixture after each permethylation. Base peak chromatograms of native Arixtra after different times of permethylation were shown in Figure 4-7. Repeat permethylation helped to convert underpermethylated species to fully permethylated species. However, more side products were generated after multiple permethylation.

4.2.3.3 Quenching solutions

Permethylation was carried out in solution. Based on the previous investigations, the reaction solution comprised 400 μL of DMSO, 400 μL of 200 $\mu\text{g}/\mu\text{L}$ NaOH in DMSO and 400 μL iodomethane. The reaction time was set to 30 minutes. The quenching solution had a total volume of 2 mL. The ion pairing buffer was 100 mM triethylamine in 5% acetonitrile/95% water, pH is adjusted to 7 with acetic acid. The quenching solutions were water, water/ion pairing buffer, water/10% acetic acid and ion pairing buffer. The reaction mixture was analyzed by ion-pair reversed-phase liquid chromatography coupling with mass spectrometry. Fully permethylated species and side products were shown in base peak chromatograms.

Owing to the presence of NaOH, the permethylation was performed under strong basic conditions. Arixtra has two uronic acid residues, thus, saponification of carboxyl esters happened when the outcome pH is basic. Therefore, addition of 2 mL water to reaction mixture ended up with underpermethylated species as the dominated peaks. As the acidity of quenching solution increasing, saponification side products were gradually reduced. Under the same conditions, as shown in Figure 4-8, the best base peak chromatogram was obtained using 2 mL IP buffer as quenching solution. However, side products from elimination of $-\text{OSO}_3\text{H}$ groups were still present with these conditions.

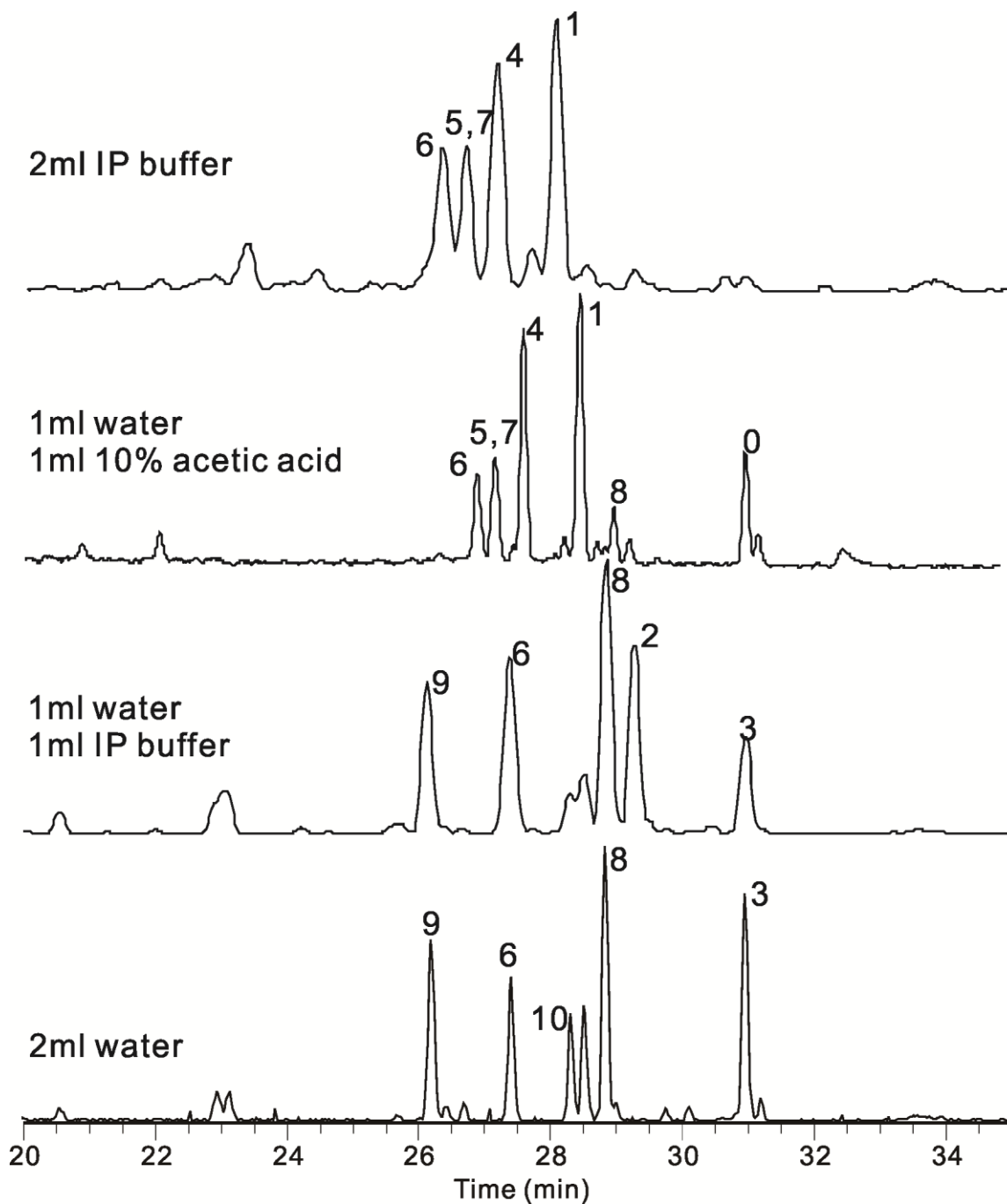


Figure 4-8 Comparisons of different quenching solutions.

The optimized condition was found with using 2 mL ion pairing buffer (100 mM triethylamine in 5% acetonitrile/ 95% water, pH 7) as quenching solution. Permethylation conditions: 100 µg Arixtra was used as starting material; reaction solution was 400 µL of DMSO, 400 µL of 200 µg/ µL NaOH in DMSO and 400 µL iodomethane; reaction time was 30 minutes.

4.2.3.4 Concentration of sodium hydroxide in DMSO

Permethylation in solution involves formation of $\text{CH}_3\text{SO}_3\text{CH}_2^-$ anion, which is considered to be the effective basic agent. This anion is generated from dimethyl sulfoxide and sodium hydride. Therefore, the concentration of NaOH will affect the permethylation process. In principle, an increase in NaOH concentration will improve yield of permethylation. However, the permethylation process of this highly sulfated acidic pentasaccharide is affected by many factors. An increase in NaOH concentration also means higher outcome pH after reaction. Therefore, more NaOH does not help to get fully permethylated species in this case. As the concentration of NaOH increasing, the dominated base peaks have been drifted to underpermethylated species.

In Figure 4-9, the concentration of sodium hydroxide in DMSO varied from 200 $\mu\text{g}/\mu\text{L}$ to 400 $\mu\text{g}/\mu\text{L}$. We may increase the volume of quenching solution to shift the outcome pH. But the total sample volume was limited to 1 mL due to desalting column capacity. At this point, the best reaction condition was achieved by using 400 μL anhydrous solution of 200 $\mu\text{g}/\mu\text{L}$ sodium hydroxide in dimethyl sulfoxide. And with this reaction condition, 2 mL IP buffer (100 mM triethylamine in 5% acetonitrile/ 95% water, pH 7) was proved to be the best quenching solution. Multiple times of permethylation led to decomposition of permethylated species; and it is time-consuming. Hence, the permethylation was preferred to be completed at one time.

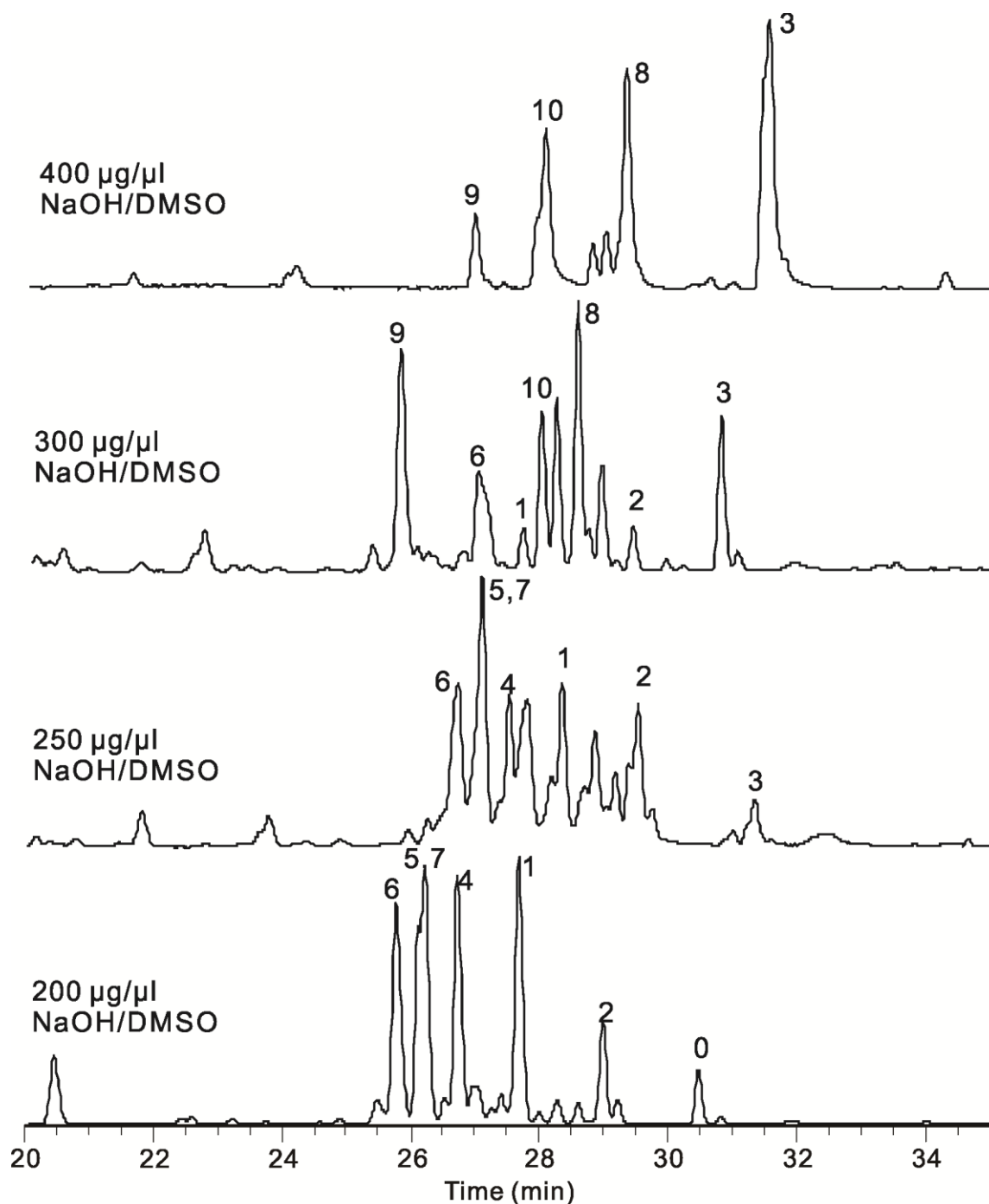


Figure 4-9 Comparisons of different NaOH/DMSO concentrations.

The optimized condition was found with using 200 µg/ µL NaOH/DMSO in reaction solution. Permethylation conditions: 100 µg Arixtra was used as starting material; reaction solution was 400 µL of DMSO, 400 µL of 200 µg/ µL NaOH in DMSO and 400 µL iodomethane; quenching solution used 2 mL ion pairing buffer (100 mM triethylamine in 5% acetonitrile/ 95% water, pH 7); reaction time was 30 minutes.

4.2.3.5 Reaction time

The last thing to test is reaction time. Under the same conditions, different reaction times were tested for permethylation. As seen in Figure 4-10, the established reaction conditions gives the same major peaks in base peak chromatograms. However, when the reaction time was 60 minutes, species generated from elimination of $-\text{OSO}_3\text{H}$ groups and underpermethylation resulted in more intense peaks than those from 30 minutes. Unreacted Arixtra was observed with reaction time of 10 minutes and 20 minutes (data not shown).

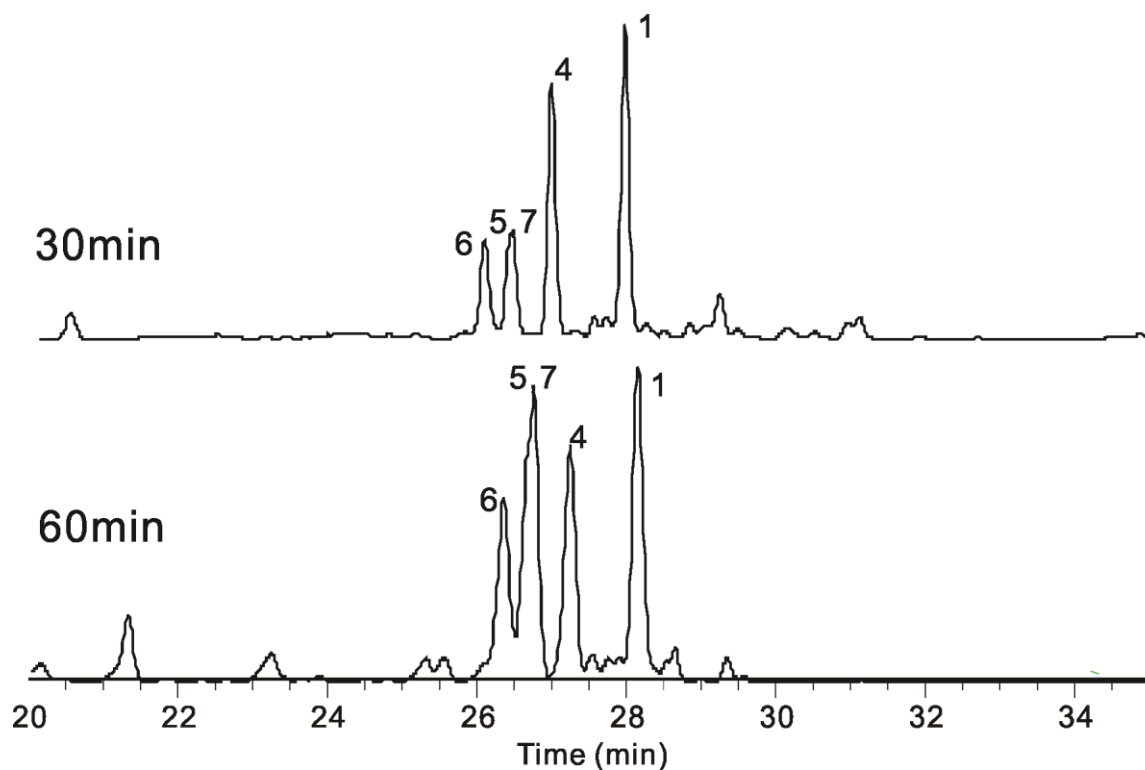


Figure 4-10 Comparison of different reaction times.

4.2.3.6 Microwave assisted permethylation

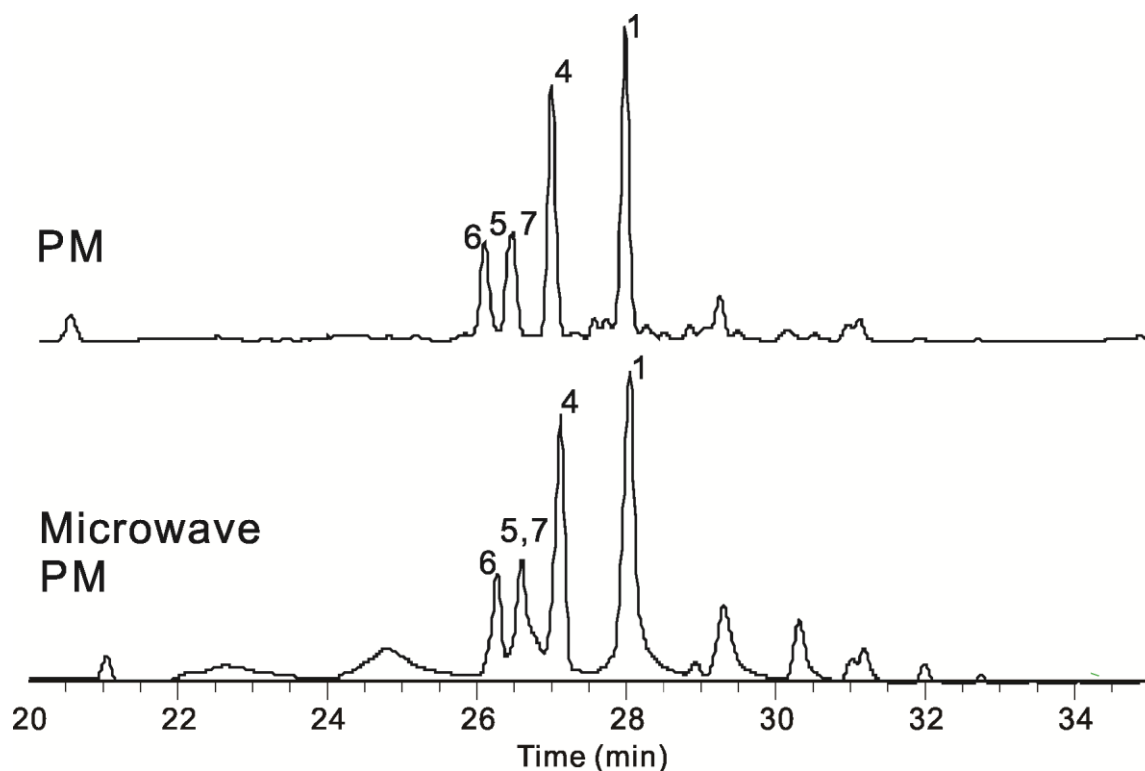


Figure 4-11 Comparison between permethylation and microwave-assisted permethylation.

Known that microwave radiation can accelerate chemical reactions, microwave permethylation is performed with Arixtra. The reaction solution comprised 400 μL DMSO, 400 μL 200 $\mu\text{g}/\mu\text{L}$ NaOH in DMSO and 400 μL iodomethane. The quenching solution was 2 mL ion pairing buffer. The reaction time was set to 30 minutes. Under the same conditions, as shown in Figure 4-11, no significant improvement has been observed with microwave permethylation.

In summary, the most completed reaction has been reached using 200 μg Arixtra as starting material, 100 μg for ion exchange and permethylation. The best condition of

permethylation was using 400 μL DMSO, 400 μL 200 $\mu\text{g}/\mu\text{L}$ NaOH in DMSO and 400 μL iodomethane as reaction solution, 2 mL ion pairing buffer as quenching solution, 30 minutes as reaction time.

4.2.3.7 Underpermethylation at 3-O-sulfated N-sulfoglucosamine (GlcNS) moiety

An underpermethylation site was found at sulfated glucosamine residue containing 3-O-sulfation. The detected m/z value of permethylated Arixtra in negative MS profile was 14 Da less than the theoretical calculation. A similar underpermethylation site was previously reported (Huang, Liu et al. 2013) when performing permethylation with synthesized Arixtra-like heptamer. This finding is consistent with another earlier report regarding NMR studies (Langeslay, Jones et al. 2012) about a deactivated hydrogen bond within the Arixtra structure.

The position of underpermethylation site was followed up after desulfation, acetylation as well as deuterio permethylation. The traceable mass shift after each derivatization step confirmed the presence of one under-methylated position. MSⁿ analysis was performed to locate the underpermethylation site. Please refer to Figure 4-19, 4-28 and 4-29 for detail information.

4.2.4 Solvolytic desulfation of Arixtra

4.2.4.1 Time study of solvolytic desulfation with permethylated Arixtra

Arixtra has five O-sulfo groups and three N-sulfo groups. There are three types of sulfate esters. They are three 6-O-sulfations present at glucosamine residue, one 2-O-sulfation at iduronic acid residue and one 3-O-sulfation group at glucosamine residue. 3-O-sulfation is a relatively rare modification of heparin/heparan sulfate.

Solvolytic desulfation was carried out on permethylated Arixtra after its conversion to pyridinium salts. The dried sample was dissolved in 200 μL 10% methanol/DMSO and heated at 100 $^{\circ}\text{C}$ for 6 hours. Permethylated β -cyclodextrin was used as an internal standard for the reaction. The reaction was investigated using conventional heating block as well as microwave radiation.

Microwave solvolytic desulfation was performed with a CEM Discover LabMate model (CEM Corporation, Matthews, NC). This instrument was equipped with an IR sensor for temperature feedback and control. Temperature was set at 100 $^{\circ}\text{C}$ and the necessary power and pressure was automatically adjusted to maintain that temperature. Note that the reaction was stopped and resumed after each time point.

In contrast to heparin disaccharides, incomplete desulfation was found with Arixtra. To investigate the influence of reaction time on extent of desulfation, a fraction of 10 μL reaction mixture was taken at different time point and dried. The dried fractions were re-suspended in 40 μL 50% methanol and infused to mass spectrometer. Positive MS profile

was obtained for each fraction. With the addition of an internal standard, the relative abundances of desulfated species and internal standard were recorded for each time point.

The ratio of relative abundance of desulfated species to internal standard is plotted as a function of reaction time in Figure 4-12. The blue line represented completely desulfated product (M) while the red line represented incomplete desulfated species with one sulfo group. The results indicated that the completely desulfated product and incomplete desulfated specie reaches at a constant ratio after six hours' reaction. In addition, a plateau between complete desulfation and incomplete desulfation has been reached for conventional heating as well as microwave desulfation.

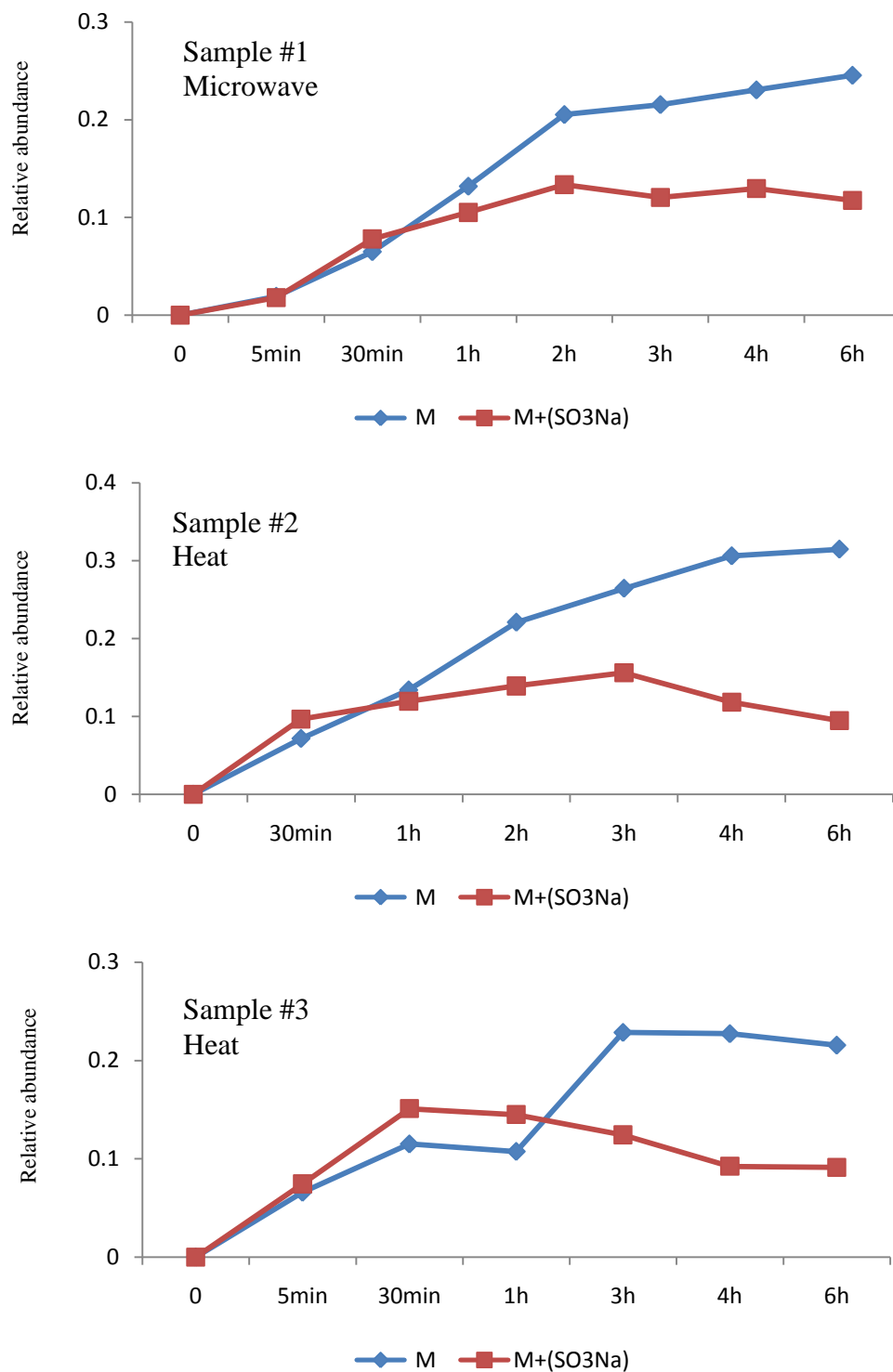


Figure 4-12 Desulfation time study of permethylated Arixtra.

4.2.4.2 Influence of methanol concentration on incomplete desulfation of permethylated

Arixtra

The time study shows incomplete desulfation of permethylated Arixtra with current procedure. Therefore further investigation of desulfation conditions was carried out to make the desulfation to completion.

Permethylated Arixtra was converted to its pyridinium salt before solvolysis. Although the process of solvolysis has not yet been fully understood, the generally accepted mechanism involves liberation of sulfo groups from its pyridinium salt in DMSO. In the process of reaction, pyridinium salts are decomposed in dimethyl sulfoxide when heated. The liberated sulfates will form sulfur trioxide-dimethyl sulfoxide complex and release pyridine in the meantime. Methanol may act as acceptors of sulfur trioxide to drive the reaction to the right side, thus accelerate solvolysis process.

Given this reason, the influence of methanol concentration in DMSO on incomplete desulfation was studied. Relative abundances of full desulfated specie and incomplete desulfated specie in positive MS profile were recorded. Ratio of the two species versus reaction time was shown in Figure 4-13. Permethylated β -cyclodextrin was used as an internal standard for the reaction. Solvolytic desulfation using solution of 5%, 10% and 15% methanol in DMSO was plotted as a function of time, respectively. It was clear to see that 10% methanol remained to be the best choice. Either increasing or decreasing the methanol concentration did not improve complete desulfation.

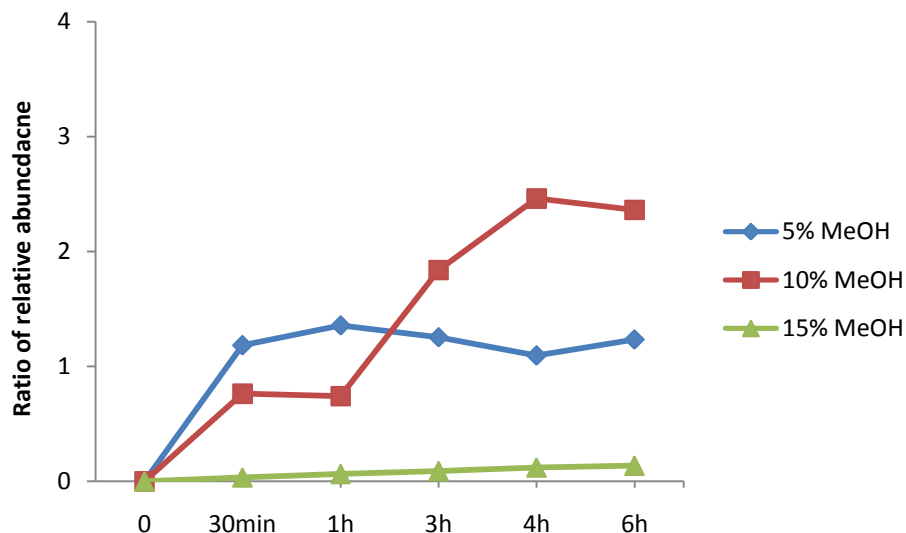


Figure 4-13 Investigation of methanol concentration on incomplete desulfation.

Y-axis represented ratio of relative abundance of full desulfated specie to permethylated β -cyclodextrin (internal standard) in positive MS profile. X-axis represented reaction time.

4.2.4.3 Influence of temperature on incomplete desulfation of native Arixtra

As another important factor of solvolytic desulfation, temperature affects the rates of decomposition of pyridinium salts in DMSO. As shown in previous study, microwave radiation did not accelerate desulfation significantly. The highest temperature that can be reached by heating block is limited to 100 °C, thus, microwave instrument was used to reach higher temperature for desulfation. There is no particular reason to use native Arixtra for this study besides the conveniences and to save time.

In Figure 4-14, microwave solvolytic desulfation at different temperatures was plotted as a function of time. Permethylated β -cyclodextrin was used as an internal standard for the reaction. The investigated temperatures were 100 °C, 120 °C and 150 °C. The Y-axis was relative abundance. The reaction did not go any longer than 30 minutes because of

significant degradation side products have been seen at higher temperature. However, the graph did suggesting improvement of desulfation at higher temperature.

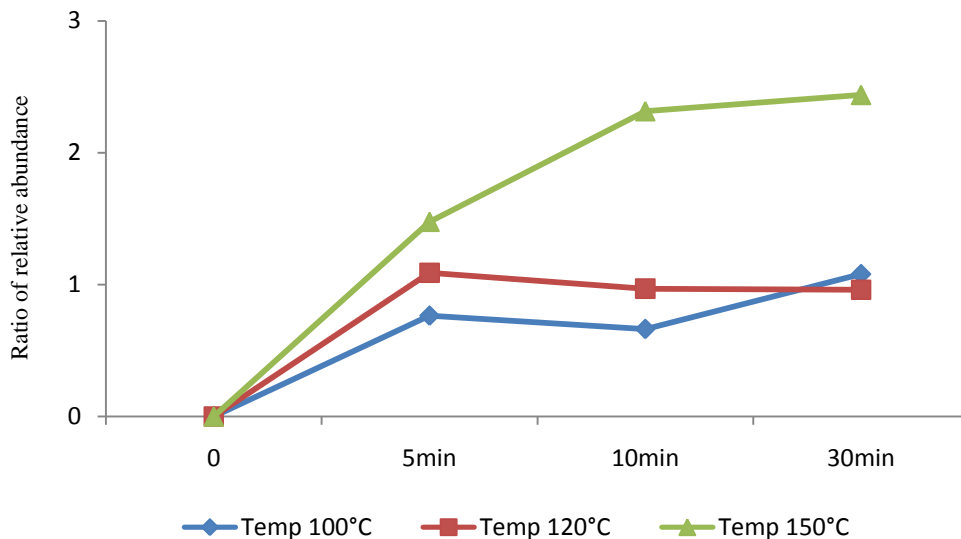


Figure 4-14 Investigation of temperature on incomplete desulfation.

Y-axis represented ratio of relative abundance of complete desulfated species to incomplete desulfated species in positive MS profile. X-axis represented reaction time.

In conclusion, the most effective way to improve desulfation was found to be increasing reaction temperature. But higher temperature can cause serious degradation leading to a large amount of sample loss. Generally speaking, the ratio of desulfated product and O-sulfated specie was in the range from 2 to 1 after solvolytic desulfation. That meant a yield of 50 to 67% completely desulfated Arixtra. With mass spectrometric detection, it was easy to differentiate the two species. Incomplete desulfation led to sample loss during derivatization process. However, as long as there is enough material to finish derivatization steps and detectable in mass spectrometer, the goal of this approach is achievable with appreciation of the great sensitivity provided by MS analysis.

4.2.5 MSⁿ analysis of desulfated Arixtra

After removal of sulfo group, the derivatized species can be analyzed in positive mode. There is only one sulfo group present in the incomplete species. Its molecular ion can be seen in positive MS profile but the sulfo group is sodiated. That makes a mass difference of 102 between complete and incomplete desulfated product.

In Figure 4-15, the positive MS profile of desulfated Arixtra was obtained after desulfation for six hours. Permethylated β -cyclodextrin was used as an internal standard for the reaction which is molecular ion m/z 1451. Complete desulfated permethylated Arixtra resulted in m/z 1030 while incomplete desulfated product was m/z 1132. Both ions were singly charged.

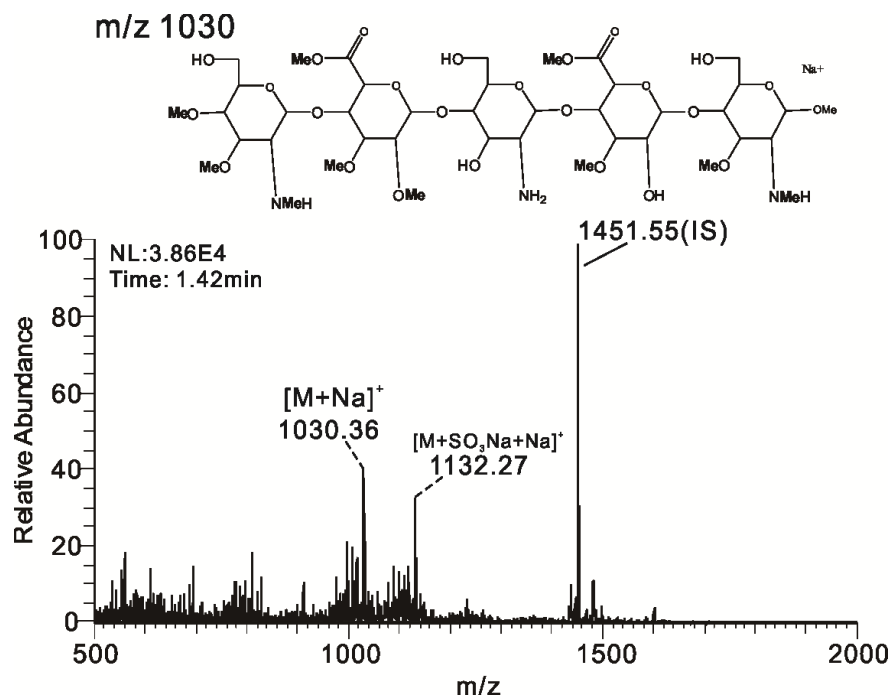


Figure 4-15 Positive ion MS profile of desulfated PM-Arixtra.

In Figure 4-16, at MS² level, the major fragmentations included glycosidic cleavages, cross-ring cleavages and loss of MeOH. It is interesting to note that the glycosidic cleavages were found only at the α-linkage positions. This was also observed in MS² spectrum of molecular ion m/z 1132 (Figure 4-17) produced by incomplete desulfation.

There are two cross-ring cleavages in the MS² spectrum (Figure 4-16). ^{0,2}X ion came from glucuronic acid unit while ^{0,2}A ion came from glucosamine unit. The dominated ion in MS² spectrum was Z₁ ion m/z 809. Later, it was selected as the precursor ion to perform sequential MSⁿ disassembly.

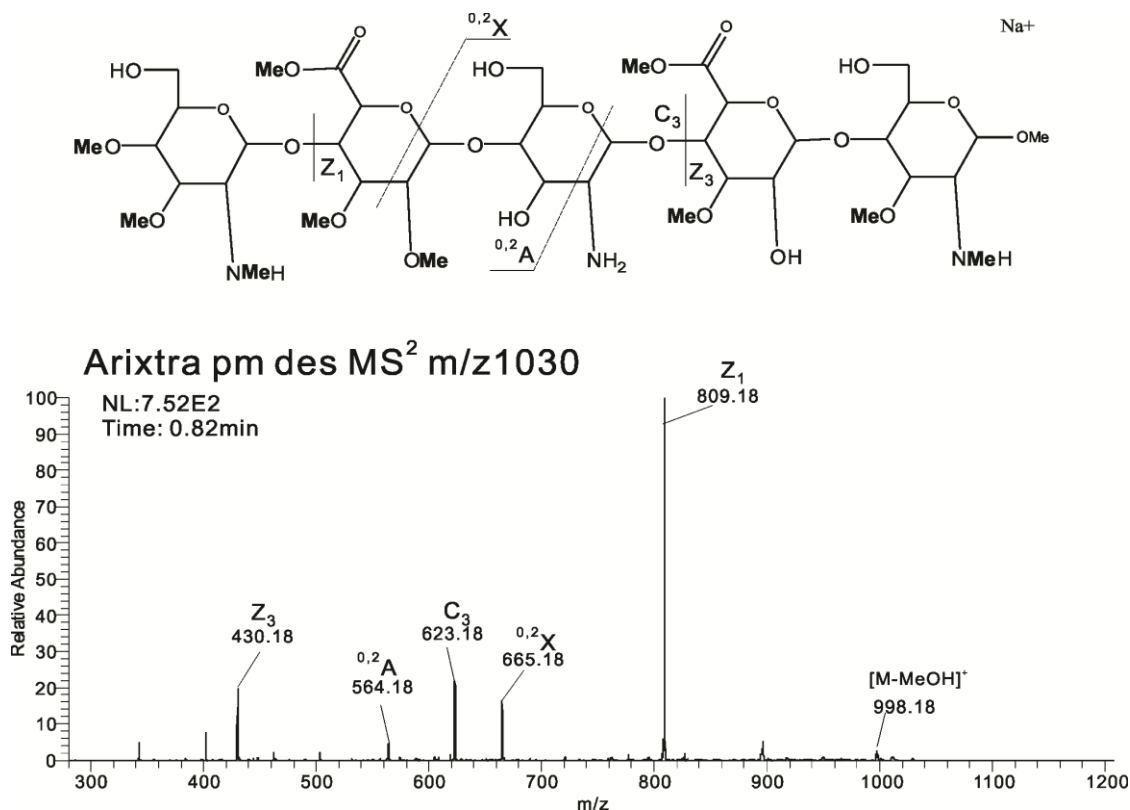


Figure 4-16 Positive ion MS² spectrum of m/z 1030.

In Figure 4-17, incomplete desulfation of permethylated Arixtra resulted in m/z 1132. In addition to the three types of cleavages present in MS² of m/z 1030, loss of -OSO₃Na (m/z

1012) was seen with MS² of m/z 1132. As previously reported, incomplete desulfation was found at 6-O-position of the glucosamine moiety when in adjacency to the 2-O-sulfoiduronic acid group. Fragment m/z 532 indicated the unsuccessful removal of this 6-O-sulfo group. However, there was one more possible position related to incomplete desulfation based on the MS² spectrum. ^{2,4}A and ^{0,2}A ion suggested that the 3-O-sulfo group was not removed successfully.

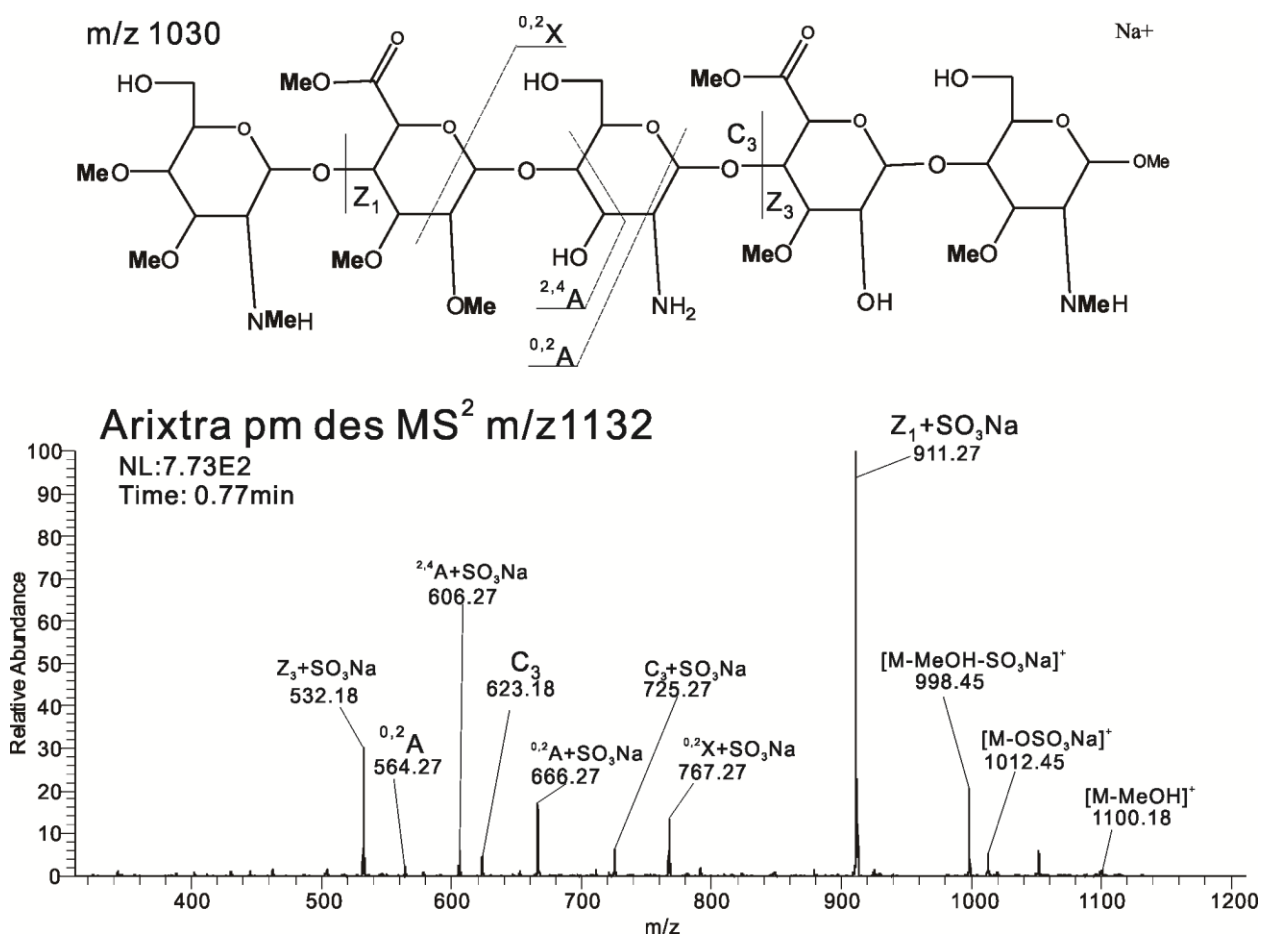


Figure 4-17 Positive ion MS² spectrum of m/z 1132.

MS³ analysis (Figure 4-19) was performed with fragmentation ions originated from glycosidic cleavages to confirm the assignments. The monosaccharide units of Arixtra were labeled in numerical order from 1 to 5 in Figure 4-18. The selected ions were Z₁ ion m/z 809, Z₃ ion m/z 430 and C₃ ion m/z 623. Z₁ ion m/z 809 was originated from cleavage between 6-O-sulfated glucosamine residue #5 and glucuronic acid residue #4. The glycosidic cleavage between iduronic acid residue #4 and 3-O-sulfated glucosamine residue #3 resulted in Z₃ ion m/z 430 and C₃ ion m/z 623.

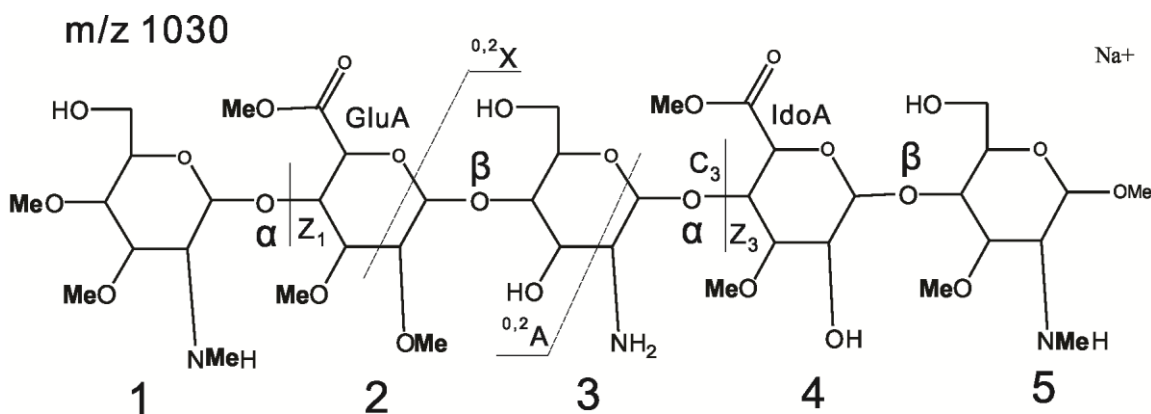


Figure 4-18 Annotation of chemical structure for precursor ion m/z 1030.

At MS³ level (Figure 4-19) of Z₁ ion m/z 809, glycosidic cleavage between iduronic acid residue #4 and 3-O-sulfated glucosamine residue #3 resulted in Z₃ ion m/z 430 and fragment m/z 402. Another dominated ion m/z 665 was seen as the 0,2-cross-ring cleavage at the glucuronic acid residue #2. Disassembly of Z₃ ion m/z 430 and C₃ ion m/z 623 confirmed the sequence of the monosaccharide units. In MS³ spectrum (Figure 4-19) of C₃ ion m/z 623, fragment m/z 402 is the glycosidic cleavage between glucuronic acid residue #2 and glucosamine residue #1. Fragment m/z 444 and m/z 462 were the glycosidic cleavages between glucuronic acid residue #2 and 3-O-sulfated glucosamine residue #3. In MS³

spectrum (Figure 4-19) of Z₃ ion m/z 430, fragment m/z 244 was the glycosidic cleavage between iduronic acid #4 and glucosamine residue #5.

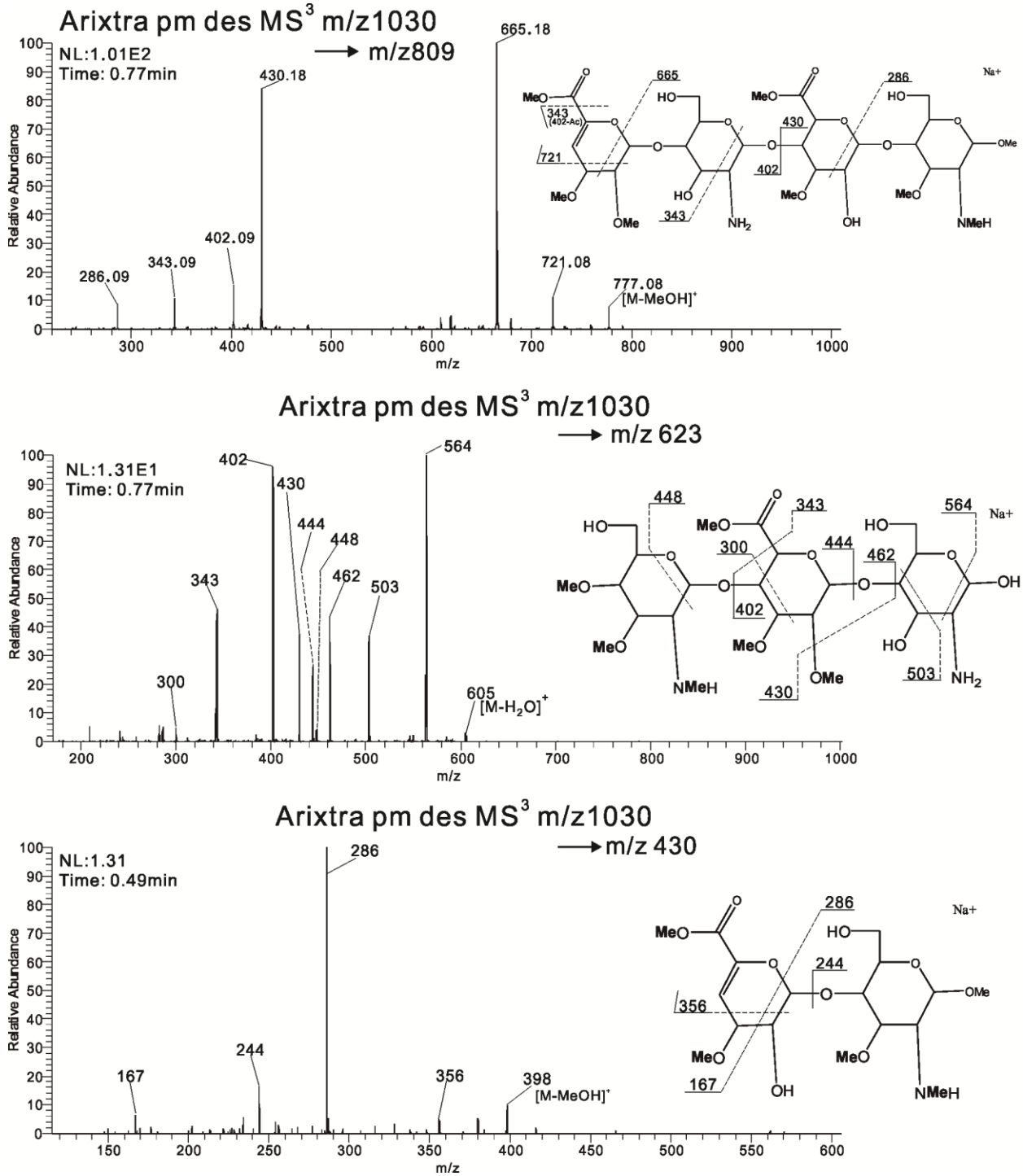


Figure 4-19 MS³ analysis of complete desulfated Arixtra.

In addition, sequential MSⁿ disassembly of Z₁ ion was performed through two tractable pathways to confirm the monosaccharide units and the positions where used to be sulfo groups. Pathway I (Figure 4-20) was m/z 1030-809-430. Pathway II (Figure 4-21) was m/z 1030-809-665-430-286. At MS⁴ level (Figure 4-20) of pathway I, fragment m/z 244 was the glycosidic cleavage between iduronic acid residue #4 and glucosamine residue #5. The 0,2-cross-ring cleavage at the iduronic acid residue resulted in fragment m/z 286 and m/z 167. However, the linkage information of monosaccharide #2 and #3 was missing owing to absence of glycosidic cleavage between glucuronic acid residue #2 and 3-O-sulfated glucosamine residue #3. Thus, pathway II was performed to provide supplementary information for this linkage, which is summarized in Figure 4-21.

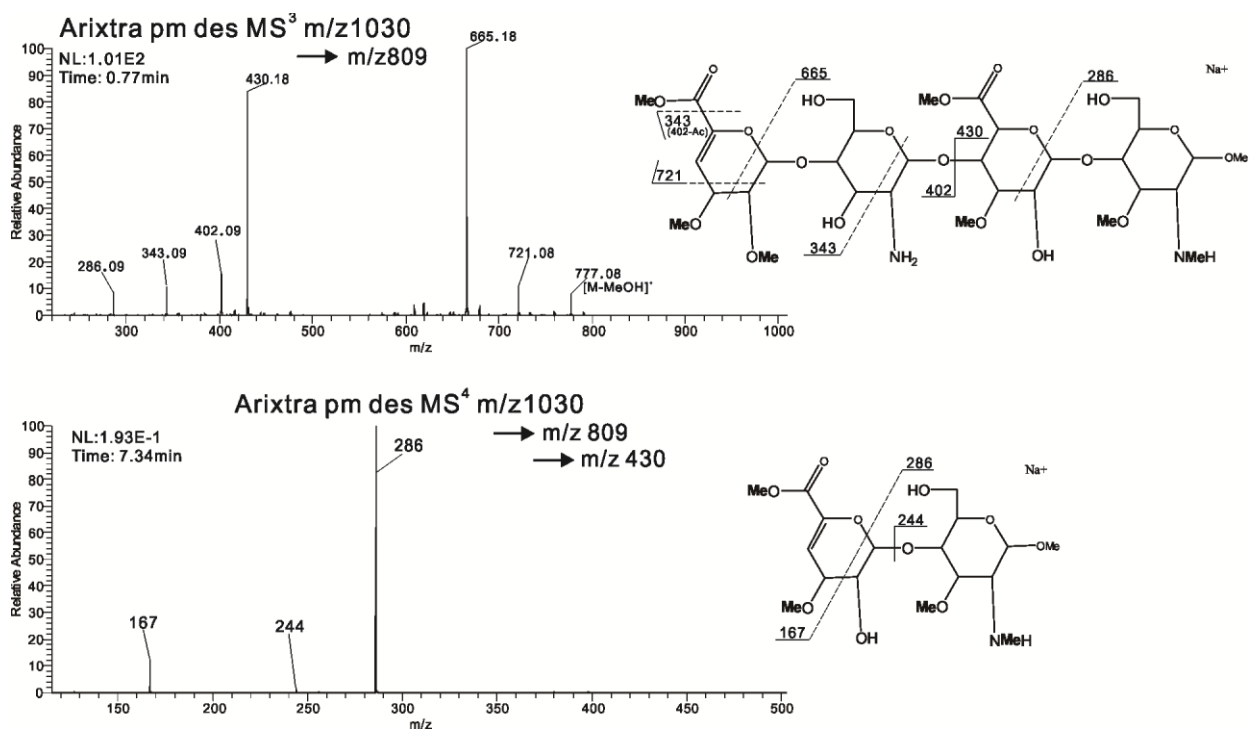


Figure 4-20 Sequential MSⁿ disassembly of Z₁-ion, pathway I.

At MS³ level (Figure 4-21), fragment m/z 665 from 0,2-cross-ring cleavage glucuronic acid residue #2 was selected as precursor ion for sequential disassembly. In MS⁴ spectrum (Figure 4-21), fragment m/z 591 was the glycosidic cleavage between glucuronic acid residue #2 and 3-O-sulfated glucosamine residue #3. At MS⁵ level (Figure 4-21), the precursor ion m/z 430 was confirmed for the predicted structure. The 0,2-cross-ring cleavage at the iduronic acid residue resulted in fragment m/z 286 and m/z 167. Fragment m/z 356 was the 2,4-cross-ring cleavage at the iduronic acid residue. When further fractionating m/z 286 into smaller subsets at MS⁶ level (Figure 4-21), the spectrum consisted of fragment ions from neutral loss of MeOH and water. Either the glycosidic cleavage or cross-ring cleavage was absent at this stage. This suggested that disassembly of such small monosaccharide unit will not provide useful structural information.

The determination of sulfonation pattern was more complicated at this step. For example, in MS⁵ spectrum of Figure 4-21, fragment m/z 356 and m/z 244 indicated that there was a hydroxyl group on the GlcNS residue #5. Fragment m/z 286 suggested the hydroxyl group was at 6-O-position. Furthermore, fragment m/z 167 suggested another hydroxyl group was present at the 2-O-position of the iduronic acid residue #4. In the meantime, fragment m/z 416 in MS⁴ spectrum (Figure 4-21) suggested hydroxyl group is present at the same position as well. In MS³ spectrum (Figure 4-19) of ion m/z 623, hydroxyl group at 6-O-position of GlcNS residue #1 was confirmed by fragment m/z 300, m/z 444 and m/z 462. Fragment m/z 503 and m/z 564 indicated 3-O-sulfation and 6-O-sulfation of the GlcNS residue #3, respectively.

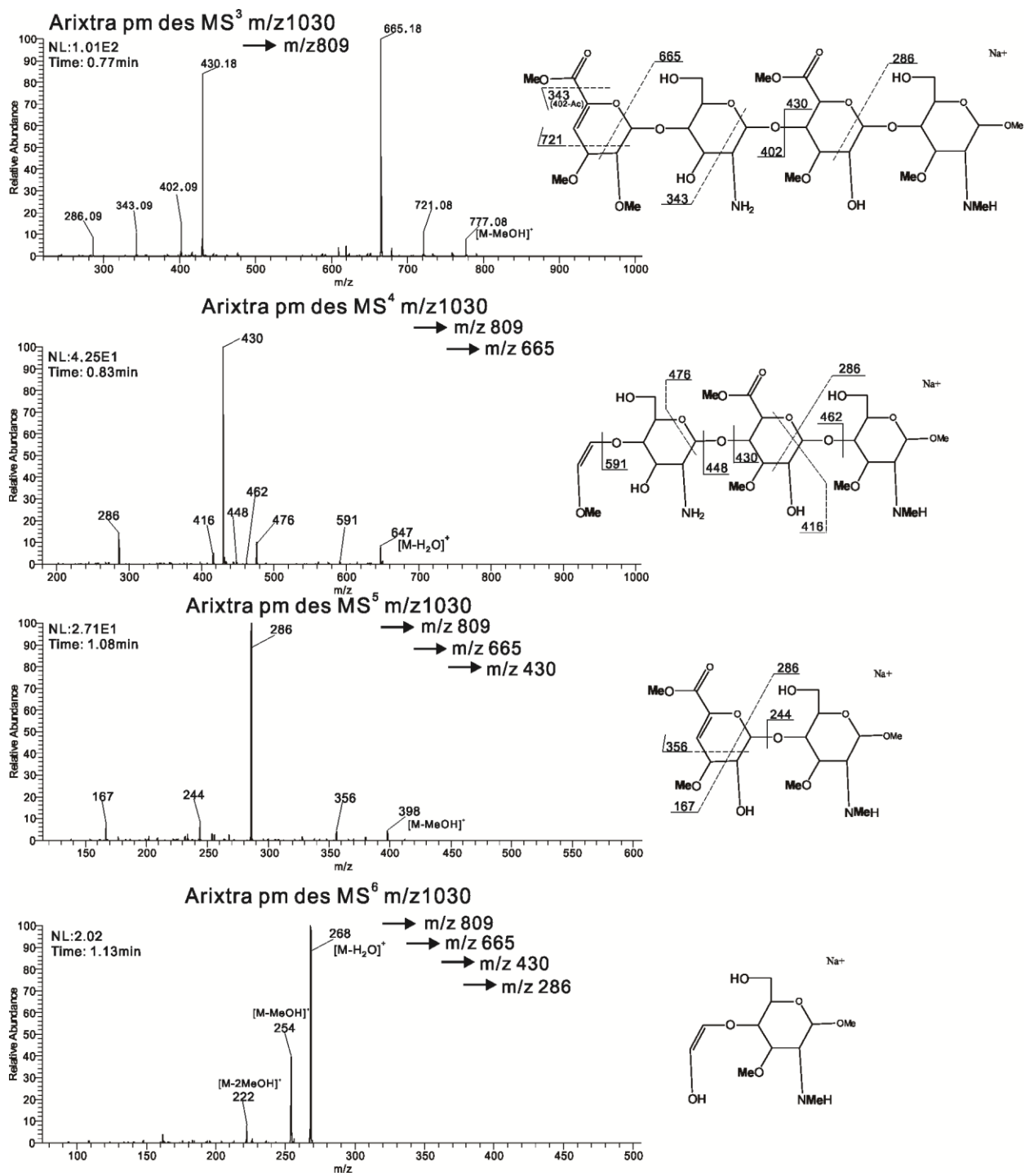


Figure 4-21 Sequential MSⁿ disassembly of Z₁-ion, pathway II.

In conclusion, complete desulfation of Arixtra was confirmed using tractable pathways to disassemble the precursor ion m/z 1030. The determination of sulfonation patterns at this step is a comprehensive task. It needs carefully selection of precursor ions. However, the following steps will further assistant the assignments for sulfo groups' positions.

4.2.6 MSⁿ analysis of permethylated-desulfated Arixtra following N-acetylation

The purpose of the acetylation is to acetylate the amine groups to prevent carrying a permanent positive charge in the following permethylation step. However, it is inevitably putting acetyl groups on the hydroxyls. Moreover, N-acetylation is much faster and easier than per-O-acetylation. Given that, the positive MS profile is extremely complicated owing to inefficient per-O-acetylation. But it will not affect the final product of the derivatization.

In Figure 4-22, the positive MS profile was obtained for desulfated Arixtra after N-acetylation with acetic anhydride- d_6 . After per-O-acetylation, complete desulfated permethylated Arixtra m/z 1030 resulted in m/z 1390, while incomplete desulfated product m/z 1132 resulted in m/z 1447. Both ions are singly charged. The main purpose of using acetic anhydride- d_6 was to prevent putting on a positive permanent charge on the GlcNS moiety after release of N-sulfo groups. Another purpose was to put an isotopic label on the GlcNS moiety. Please see APPENDIX B for the detailed assignments of ions in the profile.

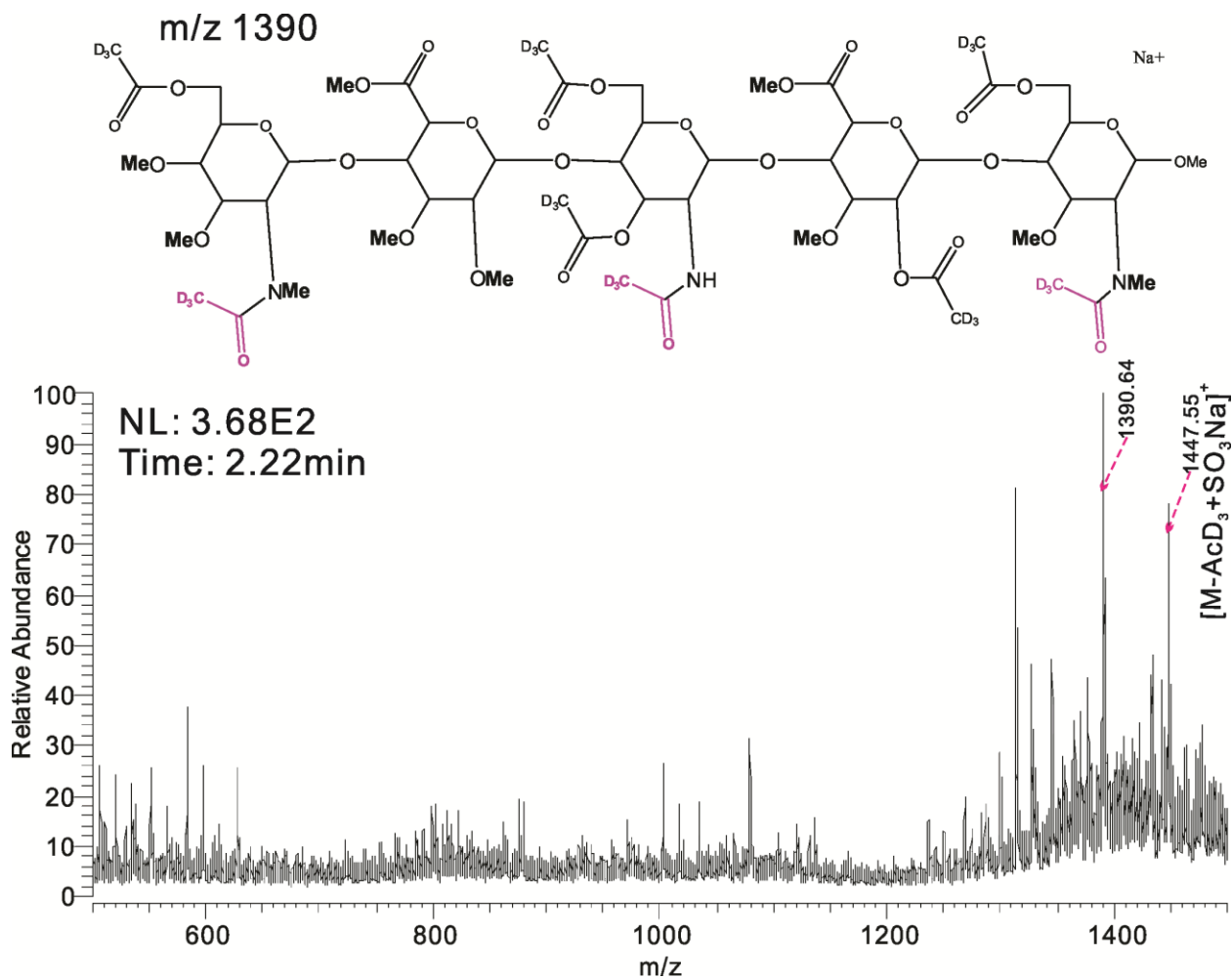
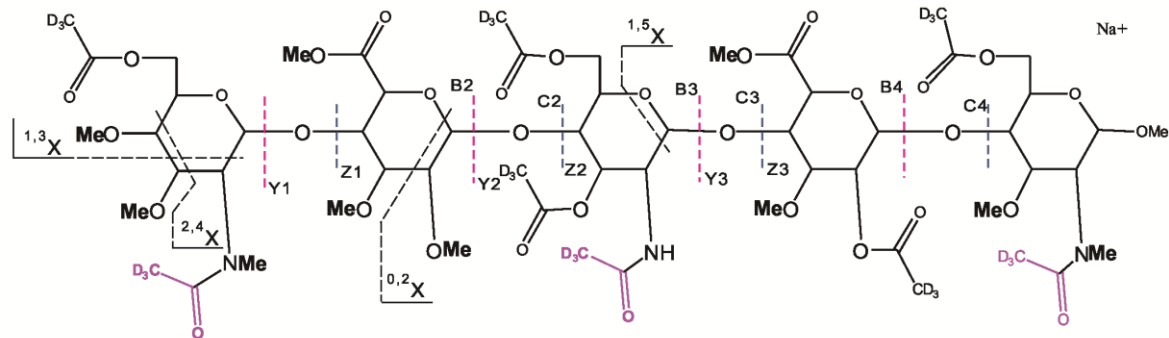
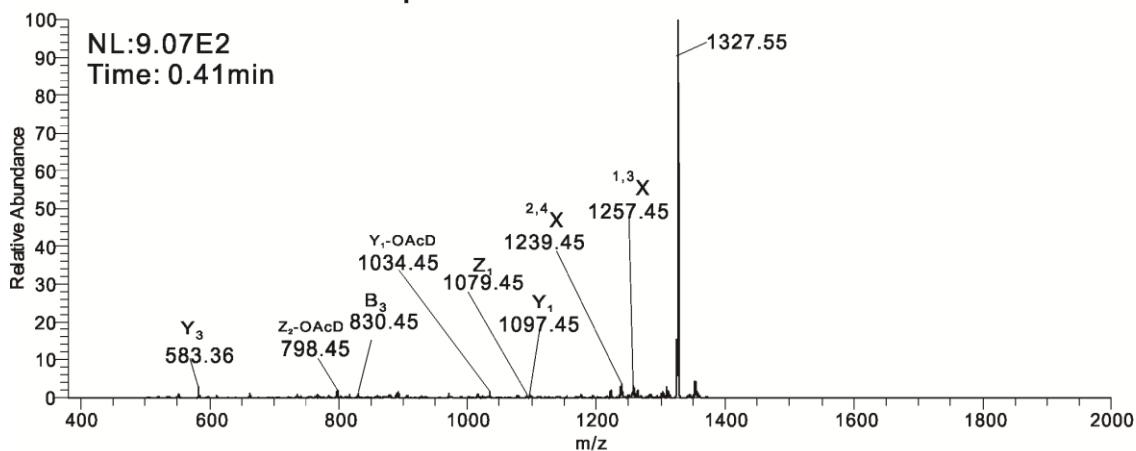


Figure 4-22 Positive MS profile of desulfated PM-Arixtra after acetylation.

An issue with CID MSⁿ analysis of per-O-acetylated Arixtra in ion trap mass analyzer is the indiscriminate loss of an O-acetyl group at MS² level (Figure 4-23). This loss dominated the tandem MS spectrum, which caused that the fragment ions containing structural information were seen only at negligible intensity. Given that, it was extremely difficult to assign fragment ions.



Arixtra pm des AcD MS² m/z 1390



Arixtra pm des AcD MS³ m/z 1390

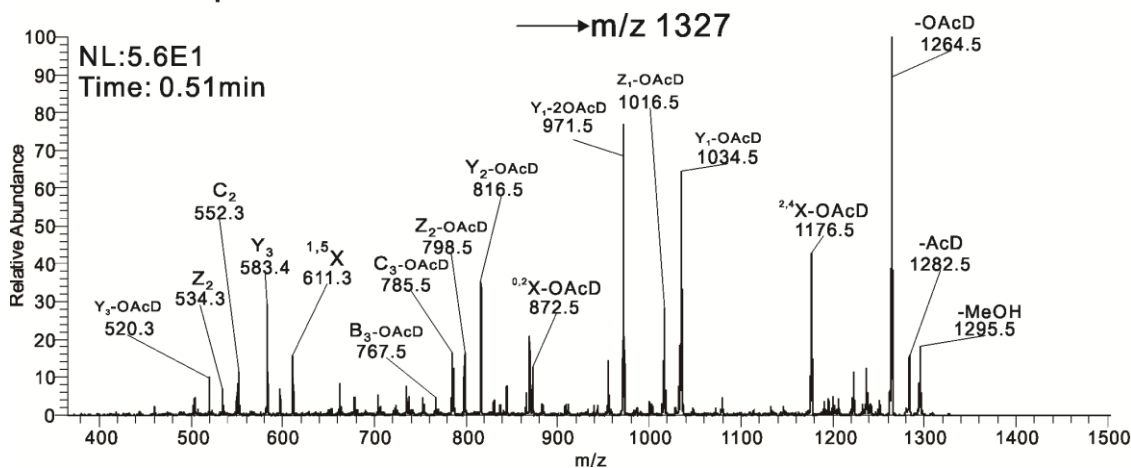


Figure 4-23 MSⁿ analysis of derivatized Arixtra after acetylation.

MS² and MS³ spectra of ion m/z 1390 from the LTQ ion trap analyzer. At MS² level, the dominated ion m/z 1327 came from loss of an O-acetyl group. Sequential glycosidic bond cleavage and cross-ring cleavage fragments were observed at MS³ level.

4.2.7 MSⁿ analysis of fully derivatized Arixtra

Owing to the lability of O-acetyl groups under CID energy, the second permethylation was performed to replace the acetyl groups with deuterio methyl groups. After the sequential derivatizations (Figure 4-24), N-sulfo groups were converted to N-deutero acetyl group while O-sulfo groups were converted to O-deutero methyl groups. Number of N-sulfo groups can be calculated by the times of 3 Da mass differences between acetic anhydride derivatized species and acetic anhydride-*d*₆ derivatized species.

Similarly, number of O-sulfo groups can be calculated by the times of 3 Da mass differences between methylated species and deuterio methylated species. As a reminder, there is an additional attachment of deuterio methyl group at uronic acid residue after deuterio permethylation. Under strong basic condition, transesterification happens at carboxyl position where used to be a methyl ester group. Based on experience of working with heparin disaccharide standards, this methyl ester group is always converted to deuterio methyl ester group. Since Arixtra has two uronic acid groups, the additional mass differences should be excluded from the calculation.

The determination of O-sulfo group positions is based on MSⁿ analysis of selected precursor ions in addition to mass shifts. The selection of precursor ions for step-wise disassembly relies on their fragmentation patterns in MS² spectra. Since Arixtra is a linear pentasaccharide with a protected non-reducing end, the last derivatization with methyl iodide leads to undistinguishable glycosidic cleavages from both sides of the structure.

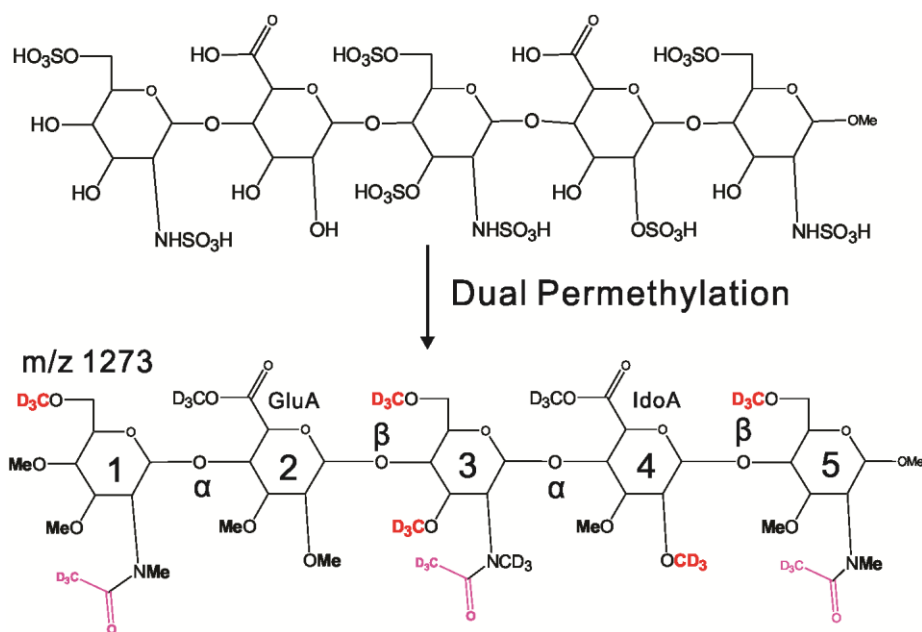


Figure 4-24 Chemical structures of Arixtra before and after dual permethylation.

Different isotopic labels have been applied to permethylated, desulfated Arixtra to confirm the predicted structure. The use of acetic anhydride and acetic anhydride- d_6 in combination with methyl iodide and deuterio methyl iodide results in four different molecular ions at MS level. The estimated structures and corresponding m/z values are summarized in Figure 4-25. Both singly charged and doubly charged species were observed in positive MS profiles in Figure 4-26. For example, m/z 1240 was the singly charged ion while m/z 631 was its doubly charged ion.

Number of N-sulfo groups can be calculated by the times of 3 Da mass differences between acetic anhydride derivatized species (m/z 1240 and m/z 1264) and acetic anhydride- d_6 derivatized species (m/z 1249 and m/z 1273), respectively. The mass difference of 9 Da indicated that there were three N-sulfo groups in Arixtra.

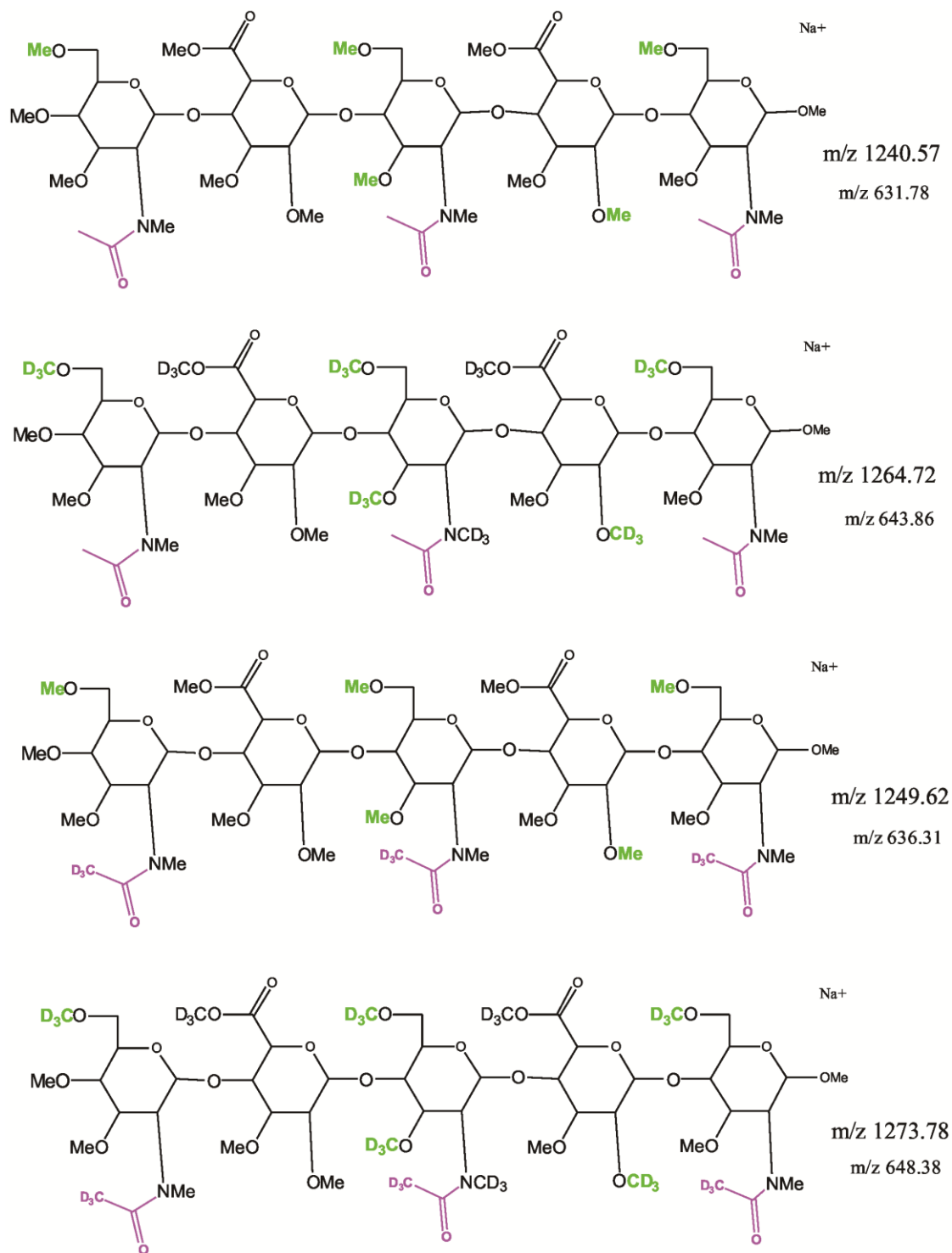


Figure 4-25 Chemical structures of fully derivatized Arixtra with different isotopic labels.

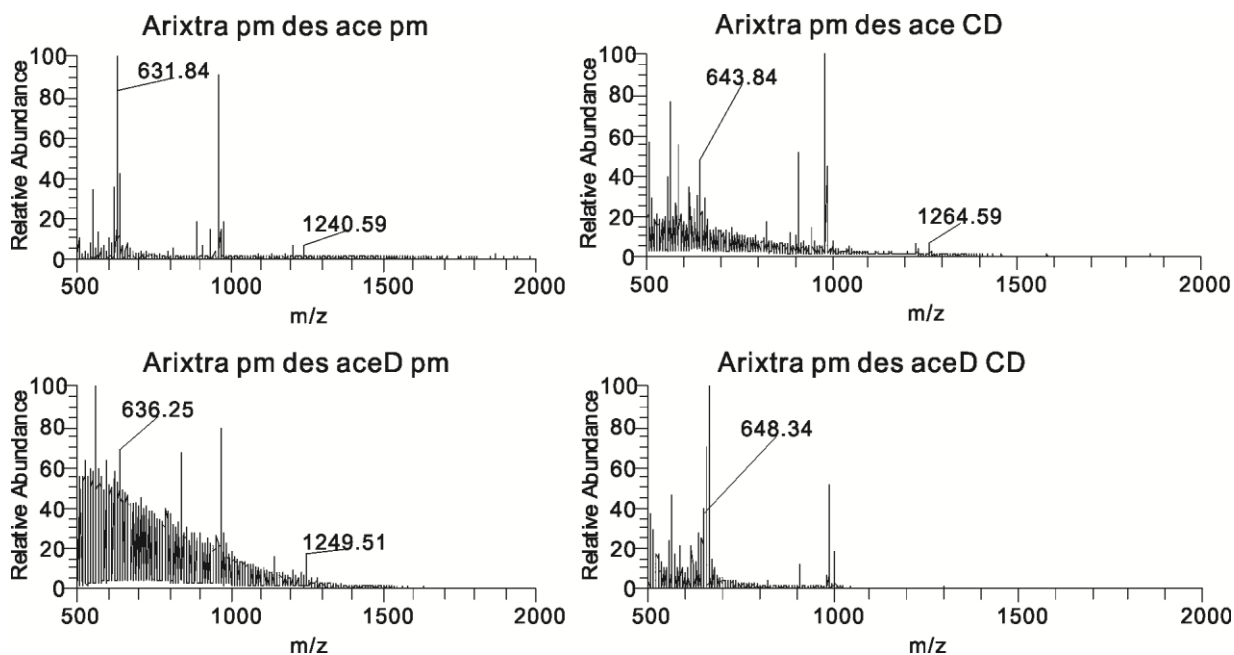


Figure 4-26 Positive ion MS profiles of fully derivatized Arixtra. After dual permethylation, the derivatized Arixtra was cleaned up with RP-LC/MS. The fractions were collected from a C₁₈ column and analyzed by direct infusion. Positive MS profiles were obtained from fully derivatized Arixtra with different isotopic labels.

There are three types of O-sulfo groups in heparin structures, 6-O-sulfo group at glucosamine residue, 2-O-sulfo group at uronic acid residue and a very rare 3-O-sulfo group at glucosamine residue. Number of O-sulfo groups can be calculated by the times of 3 Da mass difference between methylated species (m/z 1240 and m/z 1249) and deuterio methylated species (m/z 1264 and m/z 1273), but excludes the mass shifts caused by transesterification. For example, after acetylation with acetic anhydride, derivatized Arixtra was permethylated with methyl iodide (m/z 1240) and deuterio methyl iodide (m/z 1264). The total mass shift is 24 Da. This means that eight deuterio methyl ester groups have been added after the second permethylation. Since there are two uronic acids in Arixtra, it should have six O-sulfo groups.

MS² analysis of each singly charged molecular ion is summarized in Figure 4-27. The fragmentation pattern is very similar. When derivatized Arixtra was permethylated with methyl iodide, the glycosidic bond rupture resulted in the same m/z values from both sides of the structure at MS² level. As seen in MS² spectra (Figure 4-27) of m/z 1240 and m/z 1249, Y₁ and C₄, Z₁ and B₄, C₂ and Y₃, Z₂ and B₃-ions shared the same m/z values. In this case, the two molecular ions were not good candidates for MSⁿ disassembly.

In contrast, when derivatized Arixtra was permethylated with deuterio methyl iodide, C₂ and Y₃, Z₂ and B₃-ions were observed with different m/z values at MS² level (Figure 4-27). However, Y₁ and C₄, Z₁ and B₄-ions were not distinguishable due to the structural specialty of Arixtra. Therefore, C₂ and Y₃, Z₂ and B₃-ions were selected for further fragmentation. The molecule broke into two parts as a result of glycosidic bond cleavage between saccharide #2 and #3 (Refer to Figure 4-24 for order of saccharide). C₂ and Z₂, B₃ and Y₃-ions represented fragments from glycosidic bond cleavages. However, disassembly of Z₂-ions led to Y₃-ions as the dominated peak at MS³ level (Figure 4-30). Fragmentation ions from glycosidic bond cleavage between saccharide #4 and #5 were present at negligible intensity. Hence, this information was lost if Z₂-ion was selected as precursor ion.

In MS² spectrum (Figure 4-27) of ion m/z 1264, B₃-ion m/z 760 and Y₃-ion m/z 527 were selected for MS³ (Figure 4-29) analysis. Similarly, B₃-ion m/z 766 and Y₃-ion m/z 530 were selected for MS³ (Figure 4-28) from MS² spectrum (Figure 4-27) of ion m/z 1273.

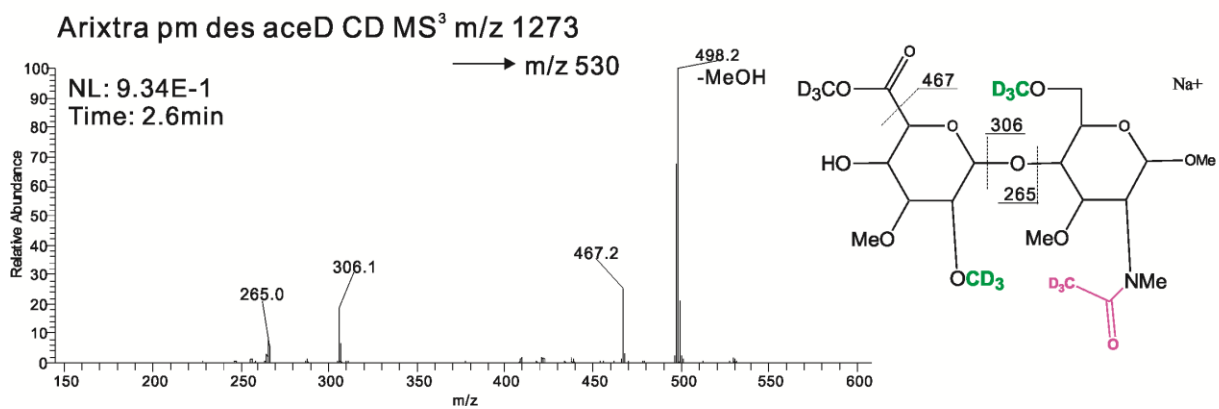
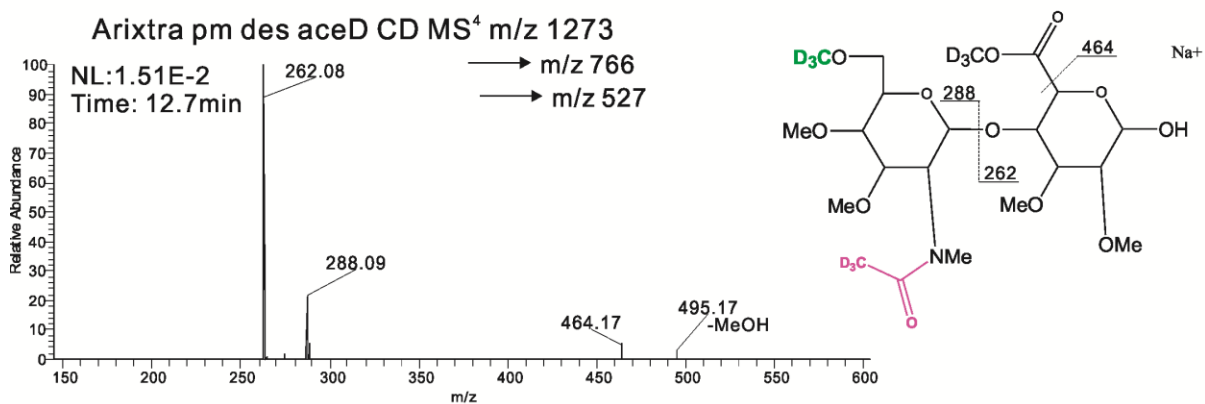
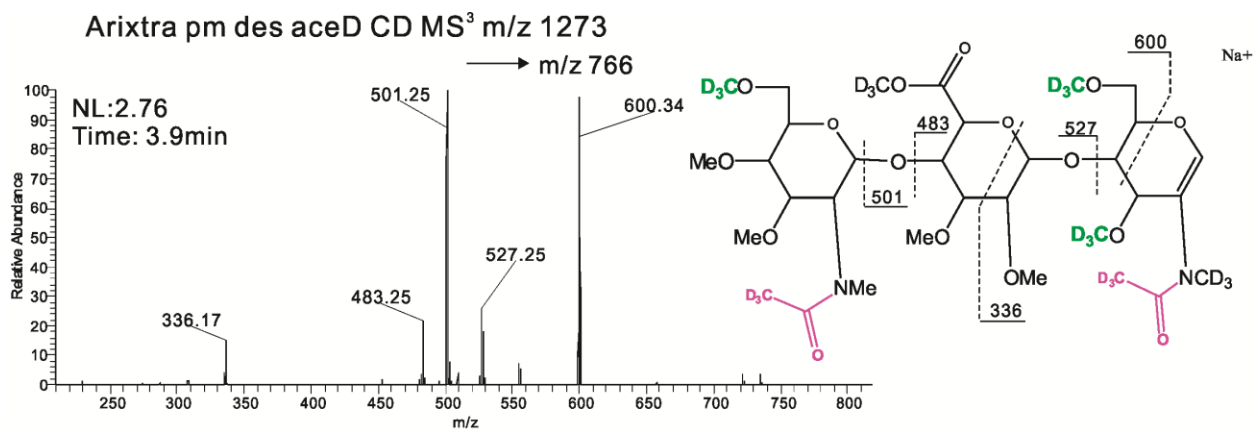


Figure 4-28 MSⁿ analysis of fully derivatized Arixtra, m/z 1273.

At MS³ level (Figure 4-28) of B₃-ion m/z 766, glycosidic cleavage between glucuronic acid residue #2 and GlcNS residue #1 resulted in fragment m/z 501 and m/z 483. C₃-ion m/z 527 was the glycosidic cleavage between glucuronic acid residue #2 and 3-O-sulfated GlcNS residue #3. Another dominated fragment m/z 600 was the 3,5-cross-ring cleavage at the 3-O-sulfated GlcNS residue #3. The other cross-ring cleavage resulted in fragment m/z 336, which was the 3,5-cross-ring cleavage at glucuronic acid residue #2.

In MS⁴ (Figure 4-28) of C₃-ion m/z 527, fragment m/z 262 and m/z 288 were the glycosidic cleavages between glucuronic acid residue #2 and GlcNS residue #1. Loss of deuterated carboxylic acid group glucuronic acid residue #2 and one MeOH resulted in fragment m/z 464 and m/z 495, respectively.

At MS³ level (Figure 4-28) of Y₃-ion m/z 530, fragment m/z 306 and m/z 265 were the glycosidic cleavages between iduronic acid residue#4 and GlcNS residue #5. Loss of deuterated carboxylic acid group at iduronic acid residue#4 and one MeOH resulted in fragment m/z 467 and m/z 498, respectively.

In MS⁴ spectrum (Figure 4-28) of C₃-ion m/z 527, ion m/z 288 suggested that there was one sulfo group at 6-O-position of GlcNS residue #1. Fragment m/z 336 and m/z 600 at MS³ level of B₃-ion m/z 766 indicated 3-O-sulfation and 6-O-sulfation of the GlcNS residue #3, respectively. Fragment m/z 265 at MS³ level of Y₃-ion m/z 530 suggested that one sulfo group was present at the 2-O-position of the iduronic acid residue #4. In the meantime, fragment m/z 306 suggested that 6-O-sulfation was present at GlcNS residue #1.

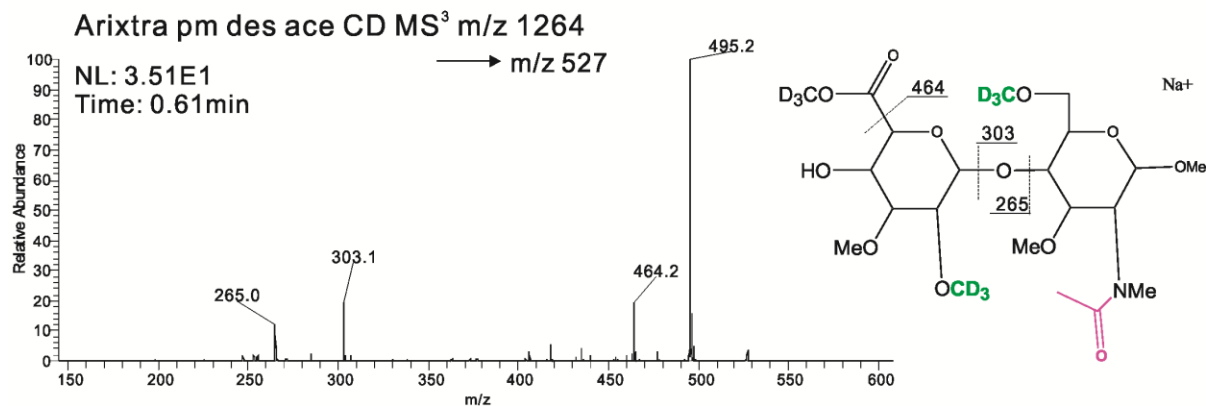
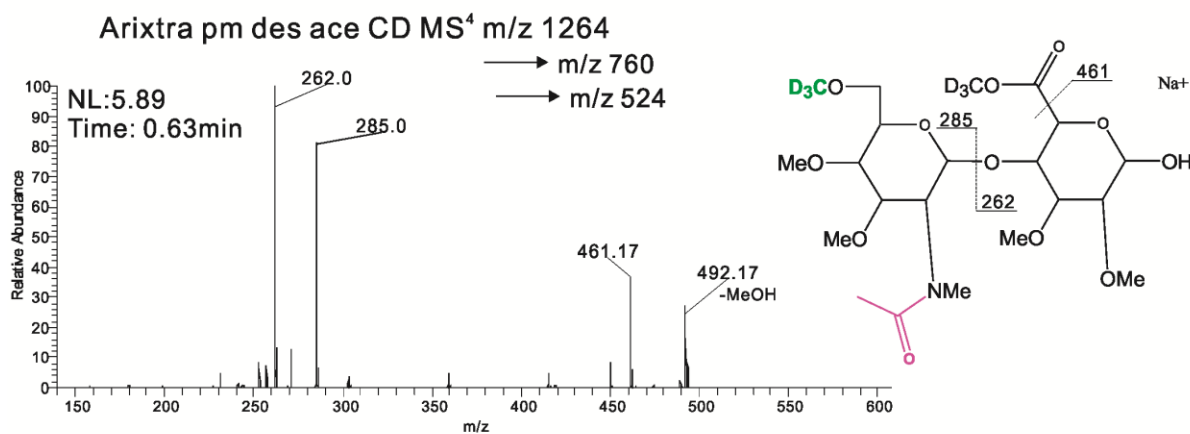
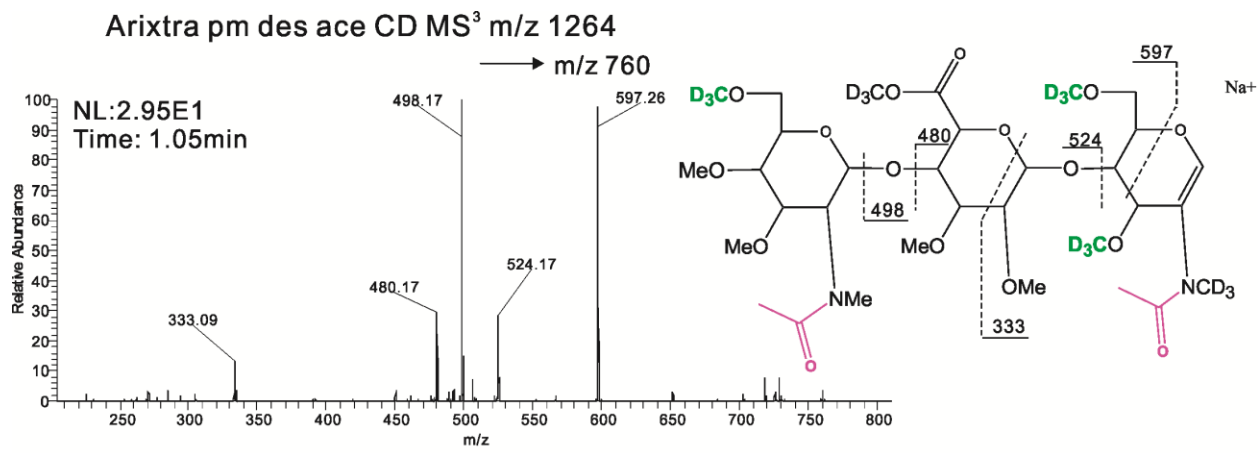


Figure 4-29 MSⁿ analysis of fully derivatized Arixtra, m/z 1264.

At MS³ level (Figure 4-29) of B₃ ion m/z 760, glycosidic cleavage between glucuronic acid residue #2 and GlcNS residue #1 resulted in fragment m/z 498 and m/z 480. C₃-ion m/z 524 was the glycosidic cleavage between glucuronic acid residue #2 and 3-O-sulfated GlcNS residue #3. Another dominated fragment m/z 597 was the 3,5-cross-ring cleavage at the 3-O-sulfated GlcNS residue #3. The other cross-ring cleavage resulted in fragment m/z 333, which was the 3,5-cross-ring cleavage at glucuronic acid residue #2.

In MS⁴ (Figure 4-29) of C₃-ion m/z 524, fragment m/z 262 and m/z 285 were the glycosidic cleavages between glucuronic acid residue #2 and GlcNS residue #1. Loss of deuterated carboxylic acid group glucuronic acid residue #2 and one MeOH resulted in fragment m/z 461 and m/z 492, respectively.

At MS³ level (Figure 4-29) of Y₃-ion m/z 527, fragment m/z 303 and m/z 265 were the glycosidic cleavages between iduronic acid residue#4 and GlcNS residue #5. Loss of deuterated carboxylic acid group at iduronic acid residue#4 and one MeOH resulted in fragment m/z 464 and m/z 495, respectively.

In MS⁴ spectrum (Figure 4-29) of C₃-ion m/z 524, ion m/z 285 suggested that there was one sulfo group at 6-O-position of GlcNS residue #1. Fragment m/z 333 and m/z 597 at MS³ level of B₃-ion m/z 760 indicates 3-O-sulfation and 6-O-sulfation of the GlcNS residue #3, respectively. Fragment m/z 265 at MS³ level of Y₃-ion m/z 527 suggested that one sulfo group was present at the 2-O-position of the iduronic acid residue #4. In the meantime, fragment m/z 303 suggested that 6-O-sulfation is present at GlcNS residue #1. Furthermore, fragment m/z 262 and m/z 265 were seen when disassembling both m/z 1273 and m/z 1264. This proved presence of uronic acid at saccharide #2 and #4.

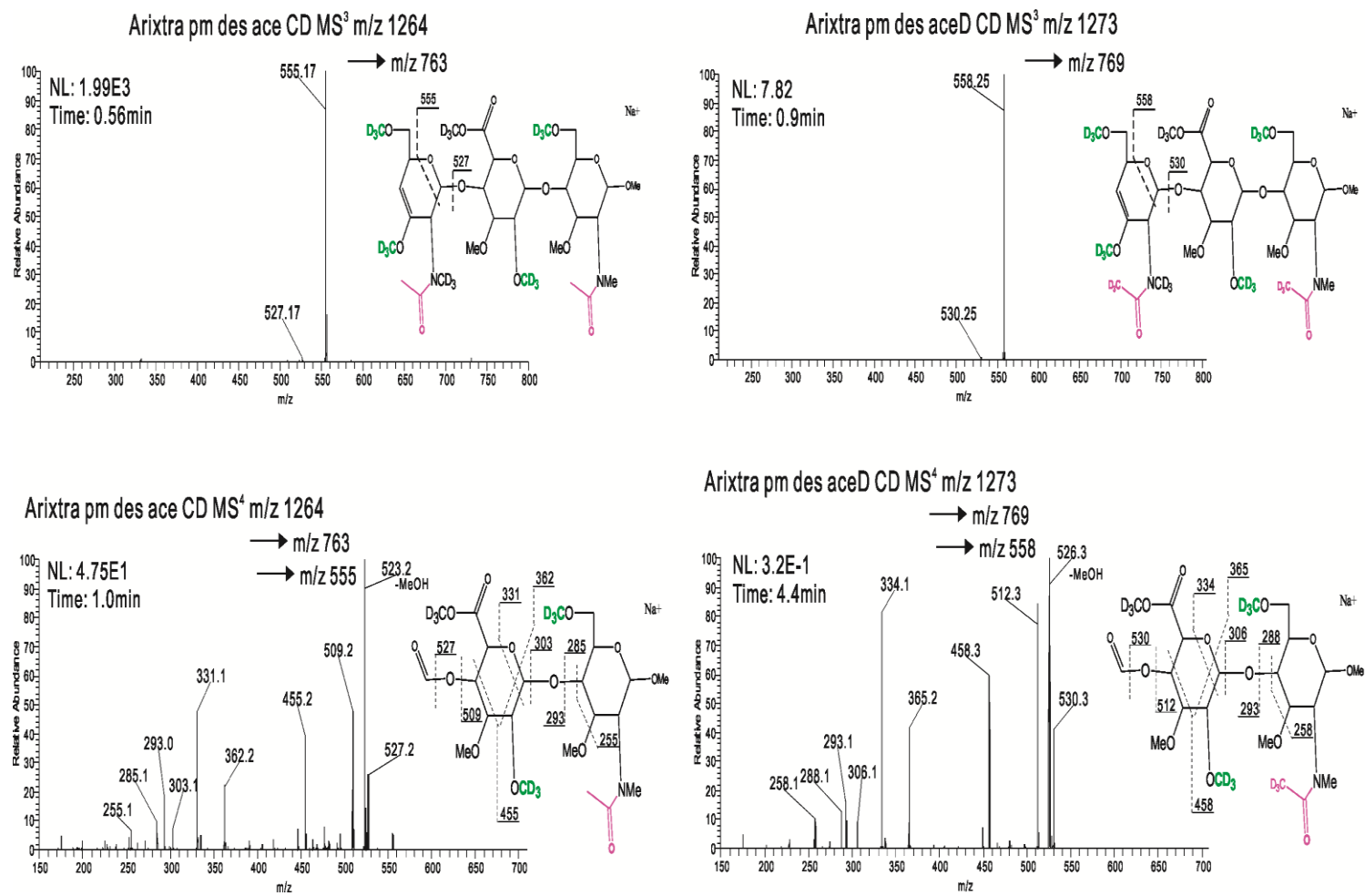


Figure 4-30 MSⁿ comparisons of fully derivatized Arixtra, Z-ions.

As mentioned in discussion of MS² spectra (Figure 4-27), disassembly of Z₂-ions led to Y₃-ions as the dominated peak at MS³ level (Figure 4-30). Fragmentation ions from glycosidic bond cleavage between saccharide #4 and #5 were present at negligible intensity. Hence, this information was lost if Z₂-ion was selected as precursor ion.

In Figure 4-30, at MS³ level of m/z 769, the dominated fragment m/z 558 was the 1,5-cross-ring cleavage at the 3-O-sulfated GlcNS residue #3. In the same way, at MS³ level of m/z 763, the dominated fragment m/z 555 was the 1,5-cross-ring cleavage at the same position.

In MS⁴ (Figure 4-30) of ion m/z 558, fragment m/z 530 and m/z 512 were the glycosidic cleavages between 3-O-sulfated GlcNS residue #3 and iduronic acid residue #4. Fragment m/z 306, m/z 288 and m/z 293 were the glycosidic cleavages between iduronic acid residue #4 and 6-O-sulfated GlcNS residue #5. Fragment m/z 458, m/z 365 and m/z 334 was the 2,4-cross-ring cleavage, 0,2-cross-ring cleavage and 1,5-cross-ring cleavage at iduronic acid residue #4, respectively.

Similarly, in MS⁴ (Figure 4-30) of ion m/z 555, fragment m/z 527 and m/z 509 were the glycosidic cleavages between 3-O-sulfated GlcNS residue #3 and iduronic acid residue #4. Fragment m/z 303, m/z 285 and m/z 293 were the glycosidic cleavages between iduronic acid residue #4 and 6-O-sulfated GlcNS residue #5. Fragment m/z 455, m/z 362 and m/z 331 was the 2,4-cross-ring cleavage, 0,2-cross-ring cleavage and 1,5-cross-ring cleavage at iduronic acid residue #4, respectively.

4.3 Summary

The protocol has been tested and modified using highly sulfated heparin pentasaccharide (Arixtra). Monitoring the derivatization steps of the octasulfated Arixtra is not as direct as heparin disaccharides, especially before removal of sulfo groups. Thus, liquid chromatography technique has been coupled with mass spectrometry to fulfill this purpose. Either MS profile/LCMS chromatogram or MSⁿ spectra, or both, have been used to follow up the sequential derivatizations.

The sample loss is contributed by elimination of 3-O-sulfo group during the first permethylation and incomplete desulfation. Another side reaction is transesterification at carboxyl position where it used to be a methyl ester group during the deuterio permethylation step. Based on working with heparin disaccharide standards, the methyl ester group is always converted to deuterio methyl ester group by adjusting pH with 10% acetic acid after reaction.

In conclusion, the modified protocol has been applied to Arixtra successfully. Comparisons of mass shifts among derivatized Arixtra with differential isotopic labeling provide information to determine the numbers of N-sulfo groups and O-sulfo groups. MSⁿ analysis of selected precursor ions supports structural confirmation of sulfonation patterns. Once a universal protocol was established, it can be used for unknown heparin oligosaccharides and their analogs.

CHAPTER 5

CONCLUSIONS AND PERSPECTIVES

To summarize, the dual permethylation has been successfully applied to heparin disaccharides as well as Arixtra.

The goal of this sophisticated derivatization protocol is to utilize the advantages of permethylation and mass spectrometry to provide a novel approach for heparin structural analysis. After derivatization, O-sulfo groups are converted to O-CD₃ groups and N-sulfo groups are converted to N-deutero acetyl groups. The sulfonation pattern can be traced through changes of m/z values and fragmentation spectra. Comparisons of mass shifts among derivatized Arixtra with differential isotopic labeling provide information to determine the numbers of N-sulfo groups and O-sulfo groups. Although acetylation may not be a necessary step, as a general approach of identifying sulfation position, acetylation should be included considering presence of N-sulfo groups. MSⁿ analysis of selected precursor ions supports structural confirmation of sulfonation patterns.

There is an additional attachment of deutero methyl group at uronic acid residue after deutero permethylation. Under strong basic condition, transesterification happens at carboxyl position where used to be a methyl ester group. Based on working with heparin disaccharide standards, the methyl ester group is always converted to deutero methyl ester group. By only adjusting pH after deutero permethylation, this reaction goes to completion. This additional

deutero methyl group may interfere with identification of sulfonation pattern. This difference can be distinguished by MS^n analysis of selected precursor ions in MS^2 spectra.

The protocol has been tested and modified using highly sulfated heparin pentasaccharide (Arixtra). The sample loss during derivatization of Arixtra is contributed by elimination of 3-O-sulfo group during the first permethylation and incomplete desulfation. Monitoring the derivatization steps of the octasulfated Arixtra is not as direct as heparin disaccharides, especially before removal of sulfo groups. Thus liquid chromatography technique has been coupled with mass spectrometry to fulfill this purpose. Either MS profile/LCMS chromatogram or MS^n spectra or both has been used to follow up the sequential derivatizations.

To reduce the complexity, intact heparin is often depolymerized chemically or enzymatically to smaller oligosaccharides in advance to structural analysis. After that, these oligosaccharides are isolated by liquid chromatographic methods. Preliminary information in terms of size, charge or polarity is generated at this point. In addition, native MS profiles can provide basic information at molecular level. So far, a general predication of possible structure is achievable. However, subtle variations in structure such as uronic acid epimerizations, sulfonation patterns and positional isomers can only be determined through step-wise disassembly of dual permethylated species.

For the purpose of *de novo* structural analysis, a long term goal of this project is to build an MS^n spectral library of dual-permethylated heparin disaccharides and oligosaccharides starting with Arixtra. The library will contain dual-permethylated heparin oligosaccharides as well as their MS^n fragmentation products. For instance, it's able to

identify Arixtra from unknown samples by doing spectral matching. We judge this effort to be an effective approach for detailing heparin structures for both routine and high-throughput applications.

REFERENCES

- Alpert, A. J. (1990). "Hydrophilic-interaction chromatography for the separation of peptides, nucleic acids and other polar compounds." J. Chromatogr. **499**: 177-196.
- Anumula, K. R. and P. B. Taylor (1992). "A comprehensive procedure for preparation of partially methylated alditol acetates from glycoprotein carbohydrates." Anal. Biochem. **203**(1): 101-108.
- Armstrong, D. W., L.-K. Zhang, L. He and M. L. Gross (2001). "Ionic liquids as matrixes for matrix-assisted laser desorption/ionization mass spectrometry." Anal. Chem. **73**(15): 3679-3686.
- Ashline, D. J., A. J. S. Hanneman, H. Zhang and V. N. Reinhold (2014). "Structural Documentation of Glycan Epitopes: Sequential Mass Spectrometry and Spectral Matching." J. Am. Soc. Mass Spectrom. **25**(3): 444-453.
- Ashline, D. J., Y. Yu, Y. Lasanajak, X. Song, L. Hu, S. Ramani, V. Prasad, M. K. Estes, R. D. Cummings, D. F. Smith and V. N. Reinhold (2014). "Structural Characterization by Multistage Mass Spectrometry (MSn) of Human Milk Glycans Recognized by Human Rotaviruses." Mol. Cell. Proteomics **13**(11): 2961-2974.
- Aspberg, A. (2012). "The different roles of aggrecan interaction domains." J. Histochem. Cytochem. **60**(12): 987-996, 910 pp.
- Atha, D. H., J. C. Lormeau, M. Petitou, R. D. Rosenberg and J. Choay (1985). "Contribution of monosaccharide residues in heparin binding to antithrombin III." Biochemistry **24**(23): 6723-6729.
- Banerjee, S. and S. Mazumdar (2012). "Electrospray Ionization Mass Spectrometry: A Technique to Access the Information beyond the Molecular Weight of the Analyte." International Journal of Analytical Chemistry **2012**: 40.
- Barrowcliffe, T. W. (2012). "History of heparin." Handb. Exp. Pharmacol. **207**(Heparin): 3-22.
- Baumann, H., H. Scheen, B. Huppertz and R. Keller (1998). "Novel regio- and stereoselective O-6-desulfation of the glucosamine moiety of heparin with N-methylpyrrolidinone–water or N,N-dimethylformamide–water mixtures." Carbohydrate Research **308**(3–4): 381-388.
- Beirne, J., H. Truchan and L. Rao (2011). "Development and qualification of a size exclusion chromatography coupled with multiangle light scattering method for molecular weight

determination of unfractionated heparin." Analytical and Bioanalytical Chemistry **399**(2): 717-725.

Bhaskar, U., E. Sterner, A. M. Hickey, A. Onishi, F. Zhang, J. S. Dordick and R. J. Linhardt (2011). "Engineering of routes to heparin and related polysaccharides." Appl. Microbiol. Biotechnol. **93**(1): 1-16.

Bisio, A., A. Mantegazza, E. Urso, A. Naggi, G. Torri, C. Viskov and B. Casu (2007). "High-performance liquid chromatographic/mass spectrometric studies on the susceptibility of heparin species to cleavage by heparanase." Semin. Thromb. Hemostasis **33**(5): 488-495.

Bourne, E. J., M. Stacey, J. C. Tatlow and J. M. Tedder (1949). "628. Studies on trifluoroacetic acid. Part I. Trifluoroacetic anhydride as a promoter of ester formation between hydroxy-compounds and carboxylic acids." Journal of the Chemical Society (Resumed)(0): 2976-2979.

Bruggink, C., R. Maurer, H. Herrmann, S. Cavalli and F. Hoefler (2005). "Analysis of carbohydrates by anion exchange chromatography and mass spectrometry." J. Chromatogr. A **1085**(1): 104-109.

Bruggink, C., M. Wuhrer, C. A. M. Koeleman, V. Barreto, Y. Liu, C. Pohl, A. Ingendoh, C. H. Hokke and A. M. Deelder (2005). "Oligosaccharide analysis by capillary-scale high-pH anion-exchange chromatography with on-line ion-trap mass spectrometry." J. Chromatogr. B: Anal. Technol. Biomed. Life Sci. **829**(1-2): 136-143.

Buszewski, B. and S. Noga (2012). "Hydrophilic interaction liquid chromatography (HILIC)-a powerful separation technique." Anal. Bioanal. Chem. **402**(1): 231-247.

Buzzega, D., F. Maccari and N. Volpi (2008). "Fluorophore-assisted carbohydrate electrophoresis for the determination of molecular mass of heparins and low-molecular-weight (LMW) heparins." Electrophoresis **29**(20): 4192-4202.

Calabro, A., R. Midura, A. Wang, L. West, A. Plaas and V. C. Hascall (2001). "Fluorophore-assisted carbohydrate electrophoresis (FACE) of glycosaminoglycans." Osteoarthritis Cartilage **9 Suppl A**: S16-22.

Campo, G. M., S. Campo, A. M. Ferlazzo, R. Vinci and A. Calatroni (2001). "Improved high-performance liquid chromatographic method to estimate aminosugars and its application to glycosaminoglycan determination in plasma and serum." J. Chromatogr. B: Biomed. Sci. Appl. **765**(2): 151-160.

Capila, I. and R. J. Linhardt (2002). "Heparin - protein interactions." Angew. Chem., Int. Ed. **41**(3): 390-412.

Carlsson, P. and L. Kjellen (2012). "Heparin Biosynthesis." Handb. Exp. Pharmacol. **207**(Heparin): 23-41.

Castellot, J. J., Jr., R. L. Hoover, P. A. Harper and M. J. Karnovsky (1985). "Heparin and glomerular epithelial cell-secreted heparinlike species inhibit mesangial-cell proliferation." Am. J. Pathol. **120**(3): 427-435.

Cattaruzza, S. and R. Perris (2006). "Approaching the proteoglycome: molecular interactions of proteoglycans and their functional output." Macromol. Biosci. **6**(8): 667-680.

Chai, W., J. Luo, C.-K. Lim and A. M. Lawson (1998). "Characterization of Heparin Oligosaccharide Mixtures as Ammonium Salts Using Electrospray Mass Spectrometry." Anal. Chem. **70**(10): 2060-2066.

Chang, Y., B. Yang, X. Zhao and R. J. Linhardt (2012). "Analysis of glycosaminoglycan-derived disaccharides by capillary electrophoresis using laser-induced fluorescence detection." Anal. Biochem. **427**(1): 91-98.

Cheng, C. F., G. M. Oosta, A. Bensadoun and R. D. Rosenberg (1981). "Binding of lipoprotein lipase to endothelial cells in culture." J Biol Chem **256**(24): 12893-12898.

Chiari, M. N., M.; Righetti, P.G. (1996). Capillary Electrophoresis in Analytical Biotechnology. P. G. Righetti. Boca Raton, FL, CRC Press: 1-36.

Ciucanu, I. and F. Kerek (1984). "A simple and rapid method for the permethylation of carbohydrates." Carbohydr. Res. **131**(2): 209-217.

Couchman, J. R. and C. A. Pataki (2012). "An introduction to proteoglycans and their localization." J. Histochem. Cytochem. **60**(12): 885-897, 813 pp.

Crank, J. A. and D. W. Armstrong (2009). "Towards a Second Generation of Ionic Liquid Matrices (ILMs) for MALDI-MS of Peptides, Proteins, and Carbohydrates." J. Am. Soc. Mass Spectrom. **20**(10): 1790-1800.

Crum, R., S. Szabo and J. Folkman (1985). "A new class of steroids inhibits angiogenesis in the presence of heparin or a heparin fragment." Science (Washington, D. C., 1883-) **230**(4732): 1375-1378.

Danishefsky, I., H. B. Eiber and J. J. Carr (1960). "Investigations on the chemistry of heparin. I. Desulfation and acetylation." Arch. Biochem. Biophys. **90**: 114-121.

Dell, A., M. E. Rogers, J. E. Thomas-Oates, T. N. Huckerby, P. N. Sanderson and I. A. Nieduszynski (1988). "Fast-atom-bombardment mass-spectrometric strategies for sequencing sulfated oligosaccharides." Carbohydr. Res. **179**: 7-19.

Dicker, K. T., L. A. Gurski, S. Pradhan-Bhatt, R. L. Witt, M. C. Farach-Carson and X. Jia (2014). "Hyaluronan: A simple polysaccharide with diverse biological functions." Acta Biomater. **10**(4): 1558-1570.

- Doneanu, C. E., W. Chen and J. C. Gebler (2009). "Analysis of Oligosaccharides Derived from Heparin by Ion-Pair Reversed-Phase Chromatography/Mass Spectrometry." Anal. Chem. (Washington, DC, U. S.) **81**(9): 3485-3499.
- Dowd, C. J., C. L. Cooney and M. A. Nugent (1999). "Heparan sulfate mediates bFGF transport through basement membrane by diffusion with rapid reversible binding." J. Biol. Chem. **274**(8): 5236-5244.
- Duteil, S., P. Gareil, S. Girault, A. Mallet, C. Feve and L. Siret (1999). "Identification of heparin oligosaccharides by direct coupling of capillary electrophoresis/ionspray-mass spectrometry." Rapid Commun. Mass Spectrom. **13**(19): 1889-1898.
- Esko, J. D. and U. Lindahl (2001). "Molecular diversity of heparan sulfate." J. Clin. Invest. **108**(2): 169-173.
- Esko, J. D. and L. Zhang (1996). "Influence of core protein sequence on glycosaminoglycan assembly." Curr. Opin. Struct. Biol. **6**(5): 663-670.
- Estrella, R. P., J. M. Whitelock, N. H. Packer and N. G. Karlsson (2007). "Graphitized Carbon LC-MS Characterization of the Chondroitin Sulfate Oligosaccharides of Aggrecan." Anal. Chem. (Washington, DC, U. S.) **79**(10): 3597-3606.
- Fermas, S., F. Gonnet, A. Varenne, P. Gareil and R. Daniel (2007). "Frontal Analysis Capillary Electrophoresis Hyphenated to Electrospray Ionization Mass Spectrometry for the Characterization of the Antithrombin/Heparin Pentasaccharide Complex." Anal. Chem. (Washington, DC, U. S.) **79**(13): 4987-4993.
- Folkman, J., R. Langer, R. J. Linhardt, C. Haudenschild and S. Taylor (1983). "Angiogenesis inhibition and tumor regression caused by heparin or a heparin fragment in the presence of cortisone." Science (Washington, D. C., 1883-) **221**(4612): 719-725.
- Forsberg, E., G. Pejler, M. Ringvall, C. Lunderius, B. Tomasini-Johansson, M. Kusche-Gullberg, I. Eriksson, J. Ledin, L. Hellman and L. Kjellen (1999). "Abnormal mast cells in mice deficient in a heparin-synthesizing enzyme." Nature **400**(6746): 773-776.
- Foster, A. B., E. F. Martlew, M. Stacey, P. J. M. Taylor and J. M. Webber (1961). "Amino sugars and related compounds. VIII. Some properties of 2-deoxy-2-sulfonamido-D-glucose, heparin, and related substances." J. Chem. Soc.: 1204-1208.
- Fu, L., L. Li, C. Cai, G. Li, F. Zhang and R. J. Linhardt (2014). "Heparin stability by determining unsubstituted amino groups using hydrophilic interaction chromatography mass spectrometry." Anal. Biochem. **461**: 46-48.
- Funderburgh, J. L. (2000). "Keratan sulfate: structure, biosynthesis, and function." Glycobiology **10**(10): 951-958.

- Galeotti, F. and N. Volpi (2013). "Novel reverse-phase ion pair-high performance liquid chromatography separation of heparin, heparan sulfate and low molecular weight-heparins disaccharides and oligosaccharides." J. Chromatogr. A **1284**: 141-147.
- Gill, V. L., Q. Wang, X. Shi and J. Zaia (2012). "Mass Spectrometric Method for Determining the Uronic Acid Epimerization in Heparan Sulfate Disaccharides Generated Using Nitrous Acid." Anal. Chem. (Washington, DC, U. S.) **84**(17): 7539-7546.
- Gritti, F., A. dos Santos Pereira, P. Sandra and G. Guiochon (2009). "Comparison of the adsorption mechanisms of pyridine in hydrophilic interaction chromatography and in reversed-phase aqueous liquid chromatography." J. Chromatogr. A **1216**(48): 8496-8504.
- Gunay, N. S. and R. J. Linhardt (2003). "Capillary electrophoretic separation of heparin oligosaccharides under conditions amenable to mass spectrometric detection." J. Chromatogr. A **1014**(1-2): 225-233.
- Guo, X., M. Condra, K. Kimura, G. Berth, H. Dautzenberg and P. L. Dubin (2003). "Determination of molecular weight of heparin by size exclusion chromatography with universal calibration." Analytical Biochemistry **312**(1): 33-39.
- Guo, Y. and S. Gaiki (2005). "Retention behavior of small polar compounds on polar stationary phases in hydrophilic interaction chromatography." J. Chromatogr. A **1074**(1-2): 71-80.
- Heiss, C., Z. Wang and P. Azadi (2011). "Sodium hydroxide permethylation of heparin disaccharides." Rapid Commun. Mass Spectrom. **25**(6): 774-778.
- Henriksen, J., L. H. Ringborg and P. Roepstorff (2004). "On-line size-exclusion chromatography/mass spectrometry of low molecular mass heparin." J. Mass Spectrom. **39**(11): 1305-1312.
- Hitchcock, A. M., K. E. Yates, C. E. Costello and J. Zaia (2008). "Comparative glycomics of connective tissue glycosaminoglycans." Proteomics **8**(7): 1384-1397.
- Huang, R., J. Liu and J. S. Sharp (2013). "An Approach for Separation and Complete Structural Sequencing of Heparin/Heparan Sulfate-like Oligosaccharides." Anal. Chem. (Washington, DC, U. S.) **85**(12): 5787-5795.
- Huang, R., V. H. Pomin and J. S. Sharp (2011). "LC-MS(n) analysis of isomeric chondroitin sulfate oligosaccharides using a chemical derivatization strategy." J Am Soc Mass Spectrom **22**(9): 1577-1587.
- Huber, C. G. and A. Krajete (2000). "Comparison of direct infusion and on-line liquid chromatography/electrospray ionization mass spectrometry for the analysis of nucleic acids." J. Mass Spectrom. **35**(7): 870-877.
- Humphries, D. E., G. W. Wong, D. S. Friend, M. F. Gurish, W.-T. Qiu, C. Huang, A. H. Sharpe and R. L. Stevens (1999). "Heparin is essential for the storage of specific granule proteases in mast cells." Nature **400**(6746): 769-772.

Iler, K. R. (1979). The Chemistry of Silica. New York, John Wiley & Sons.

Inoue, Y. and K. Nagasawa (1976). "Selective N-desulfation of heparin with dimethyl sulfoxide containing water or methanol." Carbohydr. Res. **46**(1): 87-95.

Juhasz, P. and K. Biemann (1994). "Mass spectrometric molecular-weight determination of highly acidic compounds of biological significance via their complexes with basic polypeptides." Proc. Natl. Acad. Sci. U. S. A. **91**(10): 4333-4337.

Juhasz, P. and K. Biemann (1995). "Utility of non-covalent complexes in the matrix-assisted laser desorption ionization mass spectrometry of heparin-derived oligosaccharides." Carbohydr. Res. **270**(2): 131-147.

Kailemia, M. J., L. Li, M. Ly, R. J. Linhardt and I. J. Amster (2012). "Complete Mass Spectral Characterization of a Synthetic Ultralow-Molecular-Weight Heparin Using Collision-Induced Dissociation." Anal. Chem. (Washington, DC, U. S.) **84**(13): 5475-5478.

Kantor, T. G. and M. Schubert (1957). "A method for the desulfation of chondroitin sulfate." J. Am. Chem. Soc. **79**: 152-153.

Karlsson, N. G., B. L. Schulz, N. H. Packer and J. M. Whitelock (2005). "Use of graphitised carbon negative ion LC-MS to analyse enzymatically digested glycosaminoglycans." J. Chromatogr. B: Anal. Technol. Biomed. Life Sci. **824**(1-2): 139-147.

Kazatchkine, M. D., D. T. Fearon, D. D. Metcalfe, R. D. Rosenberg and K. F. Austen (1981). "Structural determinants of the capacity of heparin to inhibit the formation of the human amplification C3 convertase." J. Clin. Invest. **67**(1): 223-228.

Kinoshita, A. and K. Sugahara (1999). "Microanalysis of Glycosaminoglycan-Derived Oligosaccharides Labeled with a Fluorophore 2-Aminobenzamide by High-Performance Liquid Chromatography: Application to Disaccharide Composition Analysis and Exosequencing of Oligosaccharides." Anal. Biochem. **269**(2): 367-378.

Koizumi, K. (1996). "High-performance liquid chromatographic separation of carbohydrates on graphitized carbon columns." J. Chromatogr. A **720**(1 + 2): 119-126.

Korir, A. K. and C. K. Larive (2009). "Advances in the separation, sensitive detection, and characterization of heparin and heparan sulfate." Anal. Bioanal. Chem. **393**(1): 155-169.

Kuberan, B., M. Lech, L. Zhang, Z. L. Wu, D. L. Beeler and R. D. Rosenberg (2002). "Analysis of heparan sulfate oligosaccharides with ion pair-reverse phase capillary high performance liquid chromatography-microelectrospray ionization time-of-flight mass spectrometry." J. Am. Chem. Soc. **124**(29): 8707-8718.

Langeslay, D. J., C. J. Jones, S. Beni and C. K. Larive (2012). "Glycosaminoglycans: oligosaccharide analysis by liquid chromatography, capillary electrophoresis, and specific labeling." Methods Mol. Biol. (N. Y., NY, U. S.) **836**(Proteoglycans): 131-144.

- Langeslay, D. J., E. Urso, C. Gardini, A. Naggi, G. Torri and C. K. Larive (2013). "Reversed-phase ion-pair ultra-high-performance-liquid chromatography-mass spectrometry for fingerprinting low-molecular-weight heparins." J. Chromatogr. A **1292**: 201-210.
- Laremore, T. N., S. Murugesan, T.-J. Park, F. Y. Avci, D. V. Zagorevski and R. J. Linhardt (2006). "Matrix-Assisted Laser Desorption/Ionization Mass Spectrometric Analysis of Uncomplexed Highly Sulfated Oligosaccharides Using Ionic Liquid Matrices." Anal. Chem. **78**(6): 1774-1779.
- Laremore, T. N., F. Zhang and R. J. Linhardt (2007). "Ionic liquid matrix for direct UV-MALDI-TOF-MS analysis of dermatan sulfate and chondroitin sulfate oligosaccharides." Anal. Chem. **79**(4): 1604-1610.
- Li, G., J. Steppich, Z. Wang, Y. Sun, C. Xue, R. J. Linhardt and L. Li (2014). "Bottom-Up Low Molecular Weight Heparin Analysis Using Liquid Chromatography-Fourier Transform Mass Spectrometry for Extensive Characterization." Analytical Chemistry **86**(13): 6626-6632.
- Li, L., F. Zhang, J. Zaia and R. J. Linhardt (2012). "Top-Down Approach for the Direct Characterization of Low Molecular Weight Heparins Using LC-FT-MS." Analytical Chemistry **84**(20): 8822-8829.
- Li, Y. L. and M. L. Gross (2004). "Ionic-liquid matrices for quantitative analysis by MALDI-TOF mass spectrometry." J. Am. Soc. Mass Spectrom. **15**(12): 1833-1837.
- Lindahl, U., K. Lidholt, D. Spillmann and L. Kjellen (1994). "More to "heparin" than anticoagulation." Thromb. Res. **75**(1): 1-32.
- Linhardt, R. J. and N. S. Gunay (1999). "Production and chemical processing of low molecular weight heparins." Semin. Thromb. Hemostasis **25**(Suppl. 3): 5-16.
- Linhardt, R. J., K. G. Rice, Z. M. Merchant, Y. S. Kim and D. L. Lohse (1986). "Structure and activity of a unique heparin-derived hexasaccharide." J. Biol. Chem. **261**(31): 14448-14454.
- Linhardt, R. J. and T. Toida (1997). Heparin oligosaccharides: new analogs development and applications, Dekker.
- Liu, G., M. Hultin, P. Oestergaard and T. Olivecrona (1992). "Interaction of size-fractionated heparins with lipoprotein lipase and hepatic lipase in the rat." Biochem. J. **285**(3): 731-736.
- Liu, H., Z. Zhang and R. J. Linhardt (2009). "Lessons learned from the contamination of heparin." Nat. Prod. Rep. **26**(3): 313-321.
- Ly, M., T. N. Laremore and R. J. Linhardt (2010). "Proteoglycomics: recent progress and future challenges." OMICS **14**(4): 389-399.
- Marcum, J. A., J. B. McKenney, S. J. Galli, R. W. Jackman and R. D. Rosenberg (1986). "Anticoagulant active heparin-like molecules from mast cell-deficient mice." Am. J. Physiol. **250**(5, Pt. 2): H879-H888.

- Matsuo, M., R. Takano, K. Kamei-Hayashi and S. Hara (1993). "A novel regioselective desulfation of polysaccharide sulfates: Specific 6-O-desulfation with N,O-bis(trimethylsilyl)acetamide." Carbohydr Res **241**: 209-215.
- McCalley, D. V. and U. D. Neue (2008). "Estimation of the extent of the water-rich layer associated with the silica surface in hydrophilic interaction chromatography." J. Chromatogr. A **1192**(2): 225-229.
- Mikami, T. and H. Kitagawa (2013). "Biosynthesis and function of chondroitin sulfate." Biochim. Biophys. Acta, Gen. Subj. **1830**(10): 4719-4733.
- Mikhailov, D., R. J. Linhardt and K. H. Mayo (1997). "NMR solution conformation of heparin-derived hexasaccharide." Biochem. J. **328**(1): 51-61.
- Miller, I. J. and J. W. Blunt (1998). "Desulfation of algal galactans." Carbohydr. Res. **309**(1): 39-43.
- Mozen, M. M. and T. D. Evans (1962). Process for purifying heparin. US. **3058884**.
- Nagasawa, K. and Y. Inoue (1974). "Solvolytic desulfation of 2-deoxy-2-sulfoamino-D-glucose and D-glucose 6-sulfate." Carbohydr. Res. **36**(2): 265-271.
- Nagasawa, K., Y. Inoue and T. Kamata (1977). "Solvolytic desulfation of glycosaminoglycuronan sulfates with dimethyl sulfoxide containing water or methanol." Carbohydr. Res. **58**(1): 47-55.
- Nagasawa, K., Y. Inoue and T. Tokuyasu (1979). "An improved method for the preparation of chondroitin by solvolytic desulfation of chondroitin sulfates." J. Biochem. **86**(5): 1323-1329.
- Nagasawa, K. and H. Yoshidome (1969). "Solvent catalytic degradation of sulfamic acid and its N-substituted derivatives." Chem. Pharm. Bull. **17**(7): 1316-1323.
- Naggar, E. F., C. E. Costello and J. Zaia (2004). "Competing fragmentation processes in tandem mass spectra of heparin-like glycosaminoglycans." J. Am. Soc. Mass Spectrom. **15**(11): 1534-1544.
- Naimy, H., N. Leymarie, M. J. Bowman and J. Zaia (2008). "Characterization of Heparin Oligosaccharides Binding Specifically to Antithrombin III Using Mass Spectrometry." Biochemistry **47**(10): 3155-3161.
- Navarro, D. A., M. L. Flores and C. A. Stortz (2007). "Microwave-assisted desulfation of sulfated polysaccharides." Carbohydr. Polym. **69**(4): 742-747.
- Nomine, G., L. Penasse and P. Barthelemy (1961). Heparin purification, U C L A F .
- Olsen, B. A. (2001). "Hydrophilic interaction chromatography using amino and silica columns for the determination of polar pharmaceuticals and impurities." J. Chromatogr. A **913**(1-2): 113-122.

Oonuki, Y., Y. Yoshida, Y. Uchiyama and A. Asari (2005). "Application of fluorophore-assisted carbohydrate electrophoresis to analysis of disaccharides and oligosaccharides derived from glycosaminoglycans." Analytical Biochemistry **343**(2): 212-222.

Panasyuk, A. F. (2007). Method for producing sulfated glycosaminoglycans from biological tissues, Savaschuk, Dmitry Alekseevich, Russia . 18pp.

Perrimon, N. and M. Bernfield (2000). "Specificities of heparan sulphate proteoglycans in developmental processes." Nature (London) **404**(6779): 725-728.

Pervin, A., C. Gallo, K. A. Jandik, X.-J. Han and R. J. Linhardt (1995). "Preparation and structural characterization of large heparin-derived oligosaccharides." Glycobiology **5**(1): 83-95.

Przybylski, C., F. Gonnet, D. Bonnaffe, Y. Hersant, H. Lortat-Jacob and R. Daniel (2010). "HABA-based ionic liquid matrices for UV-MALDI-MS analysis of heparin and heparan sulfate oligosaccharides." Glycobiology **20**(2): 224-234.

Rees, D. A. (1961). "Estimation of the relative amounts of isomeric sulfate esters in some sulfated polysaccharides." J. Chem. Soc.: 5168.

Rees, D. A. (1963). "A note on the characterizaiton of carbohydrate sulphates by acid hydrolysis " Biochem J **88**: 343-345.

Rees, D. A. and E. Conway (1962). "Structure and biosynthesis of porphyran: a comparison of some samples." Biochem. J. **84**: 411-416.

Regnier, F. E. and R. Noel (1976). "Glycerolpropylsilane bonded phases in the steric exclusion chromatography of biological macromolecules." J. Chromatogr. Sci. **14**(7): 316-320.

Reiland, J. and A. C. Rapraeger (1993). "Heparan sulfate proteoglycan and FGF receptor target basic FGF to different intracellular destinations." J. Cell Sci. **105**(4): 1085-1093.

Reinhold, V. N., S. A. Carr, B. N. Green, M. Petitou, J. Choay and P. Sinay (1987). "Structural characterization of sulfated glycosaminoglycans by fast atom bombardment mass spectrometry: application to heparin fragments prepared by chemical synthesis." Carbohydr Res **161**(2): 305-313.

Rej, R., M. Jaseja and A. S. Perlin (1989). "Importance for blood anticoagulant activity of a 2-sulfate group on L-iduronic acid residues in heparin." Thromb Haemost **61**(3): 540.

Rhomberg, A. J., S. Ernst, R. Sasisekharan and K. Biemann (1998). "Mass spectrometric and capillary electrophoretic investigation of the enzymic degradation of heparin-like glycosaminoglycans." Proc. Natl. Acad. Sci. U. S. A. **95**(8): 4176-4181.

Roden, L. (1980). Structure and metabolism of connective tissue proteoglycans, Plenum.

Roennberg, E., F. R. Melo and G. Pejler (2012). "Mast cell proteoglycans." J. Histochem. Cytochem. **60**(12): 950-962, 913 pp.

Rubinstein, M. (1979). "Preparative high-performance liquid partition chromatography of proteins." Anal. Biochem. **98**(1): 1-7.

Ruiz-Calero, V., E. Moyano, L. Puignou and M. T. Galceran (2001). "Pressure-assisted capillary electrophoresis-electrospray ion trap mass spectrometry for the analysis of heparin depolymerized disaccharides." J. Chromatogr. A **914**(1-2): 277-291.

Sharath, M. D., Z. M. Merchant, Y. S. Kim, K. G. Rice, R. J. Linhardt and J. M. Weiler (1985). "Small heparin fragments regulate the amplification pathway of complement." Immunopharmacology **9**(2): 73-80.

Shimada, K., P. J. Gill, J. E. Silbert, W. H. Douglas and B. L. Fanburg (1981). "Involvement of cell surface heparin sulfate in the binding of lipoprotein lipase to cultured bovine endothelial cells." J. Clin. Invest. **68**(4): 995-1002.

Sinay, P., J. C. Jacquinet, M. Petitou, P. Duchaussoy, I. Lederman, J. Choay and G. Torri (1984). "Total synthesis of a heparin pentasaccharide fragment having high affinity for antithrombin III." Carbohydr. Res. **132**(2): C5-C9.

Skidmore, M., A. Atrih, E. Yates and J. E. Turnbull (2009). "Labelling heparan sulphate saccharides with chromophore, fluorescence and mass tags for HPLC and MS separations." Methods Mol. Biol. (Totowa, NJ, U. S.) **534**(Glycomics): 157-169.

Skidmore, M. A., S. E. Guimond, A. F. Dumax-Vorzet, A. Atrih, E. A. Yates and J. E. Turnbull (2006). "High sensitivity separation and detection of heparan sulfate disaccharides." J. Chromatogr. A **1135**(1): 52-56.

Skidmore, M. A., S. E. Guimond, A. F. Dumax-Vorzet, E. A. Yates and J. E. Turnbull (2010). "Disaccharide compositional analysis of heparan sulfate and heparin polysaccharides using UV or high-sensitivity fluorescence (BODIPY) detection." Nat. Protoc. **5**(12): 1983-1992.

Sommers, C., H. Ye, R. Kolinski, M. Nasr, L. Buhse, A. Al-Hakim and D. Keire (2011). "Characterization of currently marketed heparin products: analysis of molecular weight and heparinase-I digest patterns." Analytical and Bioanalytical Chemistry **401**(8): 2445-2454.

Staples, G. O., M. J. Bowman, C. E. Costello, A. M. Hitchcock, J. M. Lau, N. Leymarie, C. Miller, H. Naimy, X. Shi and J. Zaia (2009). "A chip-based amide-HILIC LC/MS platform for glycosaminoglycan glycomics profiling." Proteomics **9**(3): 686-695.

Staples, G. O., H. Naimy, H. Yin, K. Kileen, K. Kraiczek, C. E. Costello and J. Zaia (2010). "Improved Hydrophilic Interaction Chromatography LC/MS of Heparinoids using a Chip with Postcolumn Makeup Flow." Anal. Chem. (Washington, DC, U. S.) **82**(2): 516-522.

Stevenson, T. T. and R. H. Furneaux (1991). "Chemical methods for the analysis of sulphated galactans from red algae." Carbohydr Res **210**: 277-298.

Taipale, J. and J. Keski-Oja (1997). "Growth factors in the extracellular matrix." FASEB J. **11**(1): 51-59.

Takano, R., T. Kanda, K. Hayashi, K. Yoshida and S. Hara (1995). "Desulfation of sulfated carbohydrates mediated by silylating reagents." J. Carbohydr. Chem. **14**(6): 885-888.

Takano, R., Z. Ye, T.-V. Ta, K. Hayashi, Y. Kariya and S. Hara (1998). "Specific 6-O-desulfation of heparin." Carbohydr. Lett. **3**(1): 71-77.

Thanawiroon, C. and R. J. Linhardt (2003). "Separation of a complex mixture of heparin-derived oligosaccharides using reversed-phase high-performance liquid chromatography." J. Chromatogr. A **1014**(1-2): 215-223.

Thanawiroon, C., K. G. Rice, T. Toida and R. J. Linhardt (2004). "Liquid chromatography/mass spectrometry sequencing approach for highly sulfated heparin-derived oligosaccharides." J. Biol. Chem. **279**(4): 2608-2615.

Thayer, J. R., J. S. Rohrer, N. Avdalovic and R. P. Gearing (1998). "Improvements to in-Line Desalting of Oligosaccharides Separated by High-pH Anion Exchange Chromatography with Pulsed Amperometric Detection." Analytical Biochemistry **256**(2): 207-216.

Tissot, B., N. Gasiunas, A. K. Powell, Y. Ahmed, Z.-I. Zhi, S. M. Haslam, H. R. Morris, J. E. Turnbull, J. T. Gallagher and A. Dell (2007). "Towards GAG glycomics: Analysis of highly sulfated heparins by MALDI-TOF mass spectrometry." Glycobiology **17**(9): 972-982.

Tumova, S., A. Woods and J. R. Couchman (2000). "Heparan sulfate proteoglycans on the cell surface: versatile coordinators of cellular functions." Int. J. Biochem. Cell Biol. **32**(3): 269-288.

Usov, A. I. (2011). Chapter 4 - Polysaccharides of the red algae. Advances in Carbohydrate Chemistry and Biochemistry. H. Derek, Academic Press. **Volume 65**: 115-217.

Usov, A. I., K. S. Adamyants, L. I. Miroshnikova, A. A. Shaposhnikova and N. K. Kochetkov (1971). "Solvolytic desulfation of sulfated carbohydrates." Carbohydr. Res. **18**(2): 336-338.

Venkataraman, G., Z. Shriver, R. Raman and R. Sasisekharan (1999). "Sequencing complex polysaccharides." Science (Washington, D. C.) **286**(5439): 537-542.

Vidic, H. J. (1978). Heparin, Schering A.-G., Fed. Rep. Ger. . 3 pp.

Wei, W., M. R. Ninonuevo, A. Sharma, L. M. Danan-Leon and J. A. Leary (2011). "A Comprehensive Compositional Analysis of Heparin/Heparan Sulfate-Derived Disaccharides from Human Serum." Anal. Chem. (Washington, DC, U. S.) **83**(10): 3703-3708.

Whistler, R. L., A. H. King, G. Ruffini and F. A. Lucas (1967). "Sulfation of cellulose with sulfur trioxide-dimethyl sulfoxide." Arch. Biochem. Biophys. **121**(2): 358-363.

Wolf from, M. L., J. R. Vercellotti and G. H. S. Thomas (1964). "Carboxyl-reduced heparin. Monosaccharide components." J. Org. Chem. **29**(3): 536-539.

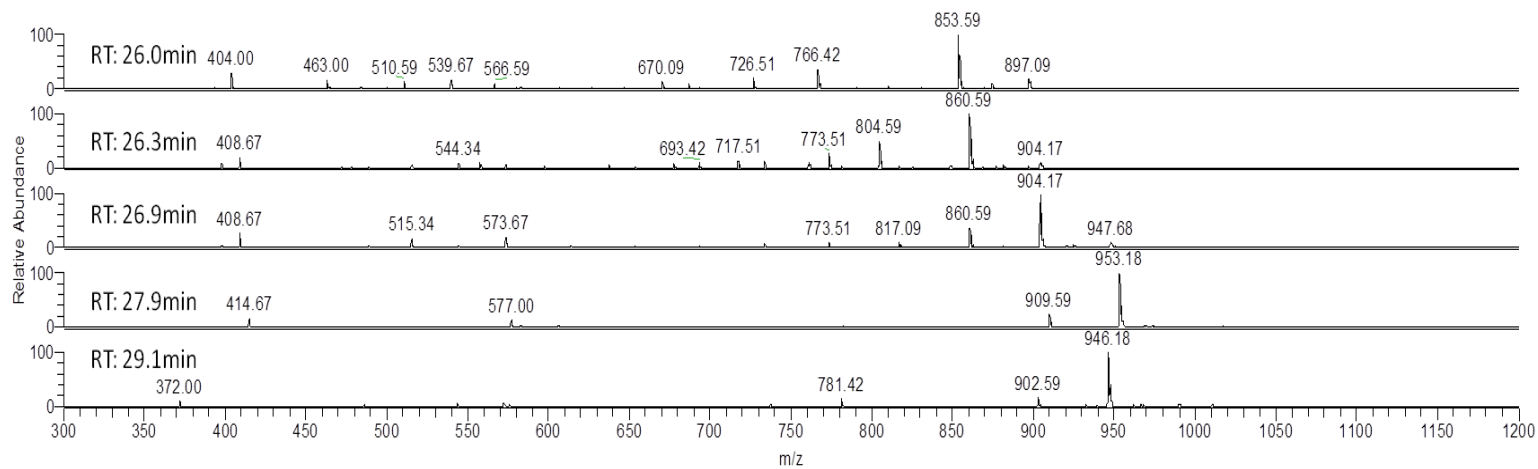
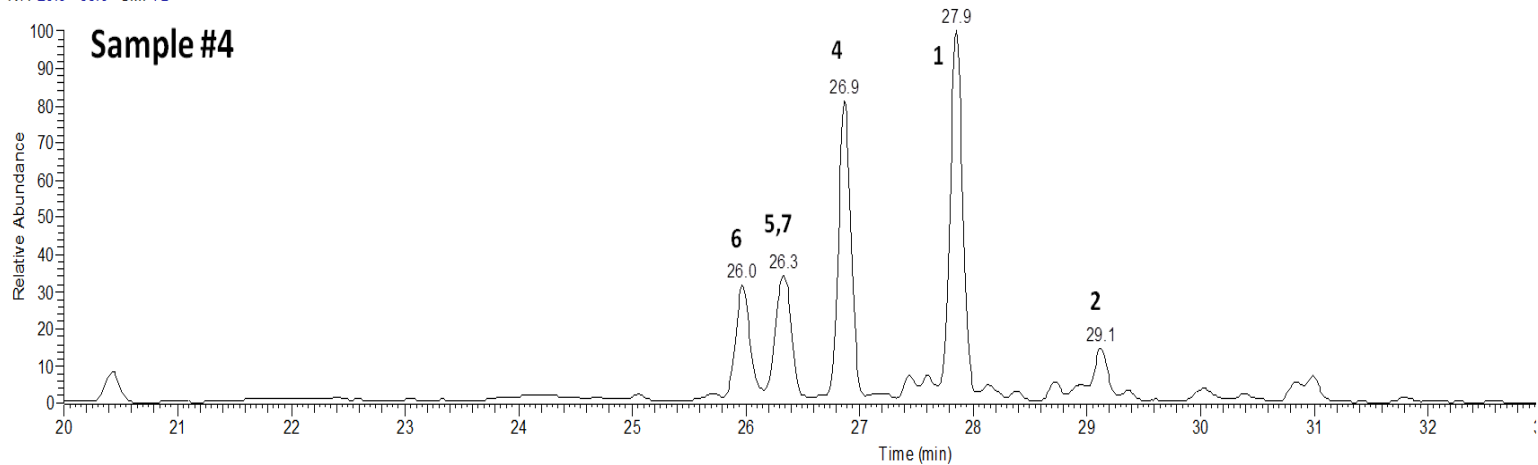
Zak, B. M. (2005). Hereditary multiple exostoses and heparan sulfate polymerization. Copyright (C) 2014 American Chemical Society (ACS). All Rights Reserved.

Zhang, F., B. Yang, M. Ly, K. Solakyildirim, Z. Xiao, Z. Wang, J. M. Beaudet, A. Y. Torelli, J. S. Dordick and R. J. Linhardt (2011). "Structural characterization of heparins from different commercial sources." Anal. Bioanal. Chem. **401**(9): 2793-2803.

Ziegler, A. and J. Zaia (2006). "Size-exclusion chromatography of heparin oligosaccharides at high and low pressure." Journal of Chromatography B **837**(1-2): 76-86.

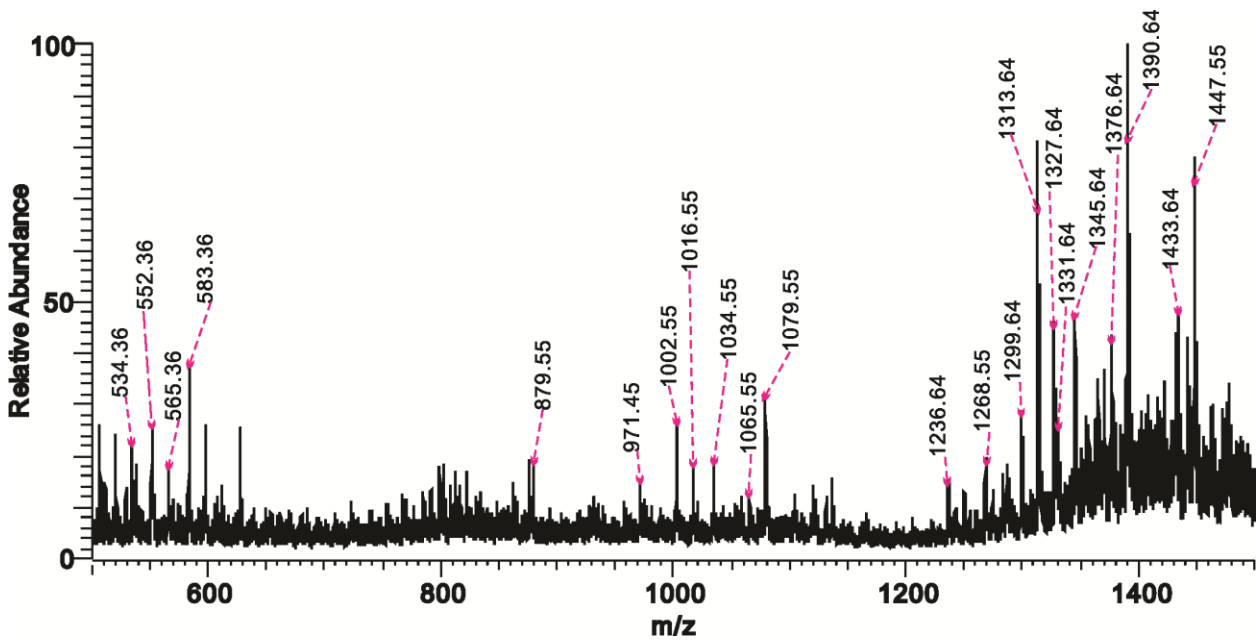
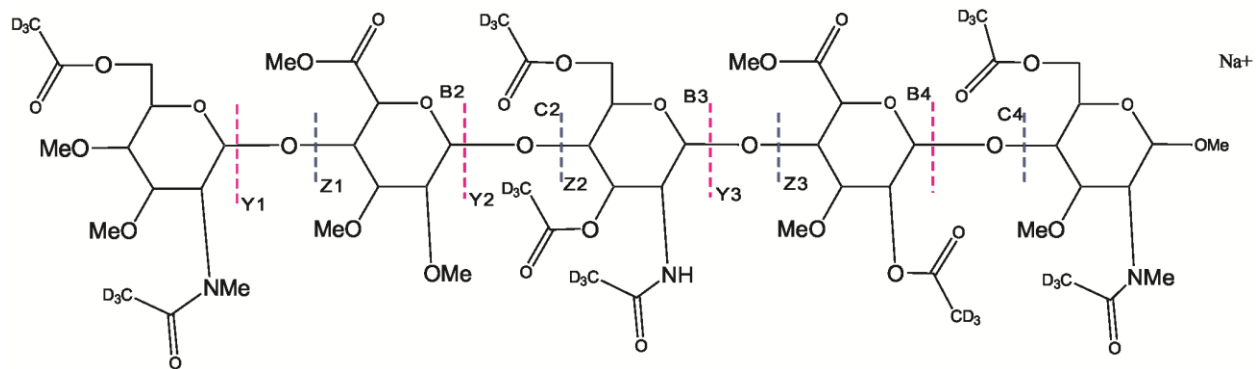
APPENDICES

RT: 20.0 - 35.0 SM: 7B



APPENDIX A: LC/MS profiles of permethylated Arixtra.

APPENDIX B: Spectra ion assignments of derivatized Arixtra following N-acetylation step.



Name	M.W.	Composition
Y ₁	1097	Y ₁
Y ₂	879	Y ₂
Y ₃	583	Y ₃
	1034	[Y ₁ -OAcD-H]
	971	[Y ₁ -2OAcD-2H]
	957	[Y ₁ -Me+H-2OAcD-2H]
Z ₁	1079	Z ₁
	1065	[Z ₁ -Me+H]
	1016	[Z ₁ -OAcD-H]
	1002	[Z ₁ -Me+H-OAcD-H]
Z ₂	861	Z ₂
Z ₃	565	Z ₃
B ₂	534	B ₂
B ₃	830	B ₃
B ₄	1079	B ₄
C ₂	552	C ₂
C ₃	848	C ₃
C ₄	1097	C ₄
^{0,3} X ₁	1239	^{0,3} X ₁
	1176	[^{0,3} X ₁ -OAcD-H]
^{0,2} X ₂	935	^{0,2} X ₂
	872	[^{0,2} X ₂ -OAcD-H]
[M _{AcD} +Na] ⁺	1390	[M _{AcD} +Na] ⁺
	1376	[M _{AcD} -Me+H+Na] ⁺
	1345	[M_{AcD}-AcD+H+Na]⁺
	1327	[M_{AcD}-OAcD-H+Na]⁺
	1331	[M _{AcD} -Me+H-AcD+H+Na] ⁺
	1313	[M _{AcD} -Me+H-OAcD-H+Na] ⁺
	1299	[M _{AcD} -2Me+2H-OAcD-H+Na] ⁺
	1268	[M _{AcD} -Me+H-AcD+H-OAcD-H+Na] ⁺
	1250	[M _{AcD} -Me+H-2OAcD-2H+Na] ⁺
	1236	[M _{AcD} -2Me+2H-2OAcD-2H+Na] ⁺
[(M+S) _{AcD} +Na] ⁺	1447	[(M+S) _{AcD} +Na] ⁺
	1433	[(M+S) _{AcD} -Me+H+Na] ⁺
	1345	[(M+S) _{AcD} -SO ₃ Na+Na] ⁺
	1327	[(M+S) _{AcD} -OSO ₃ Na+Na] ⁺